MOLECULAR DESIGN OF SOME POTENTIAL EXPLOSIVES

A THESIS SUBMITTED TO
THE GRADUATE SCHOOL OF NATURAL AND APPLIED SCIENCES
OF
MIDDLE EAST TECHNICAL UNIVERSITY

BY

TANER ATALAR

IN PARTIAL FULFILLMENT OF THE REQUIREMENTS
FOR
THE DEGREE OF DOCTOR OF PHILOSOPHY

IN

CHEMISTRY

JANUARY 2009

Approval of the thesis:

MOLECULAR DESIGN OF SOME POTENTIAL EXPLOSIVES

submitted by **TANER ATALAR** in partial fulfillment of the requirements for the degree of **Doctor of Philosophy in Chemistry Department, Middle East Technical University** by,

Prof. Dr. Canan Özgen
Dean, Graduate School of **Natural and Applied Sciences**

Prof. Dr. M. Ahmet Önal
Head of Department, **Chemistry**

Prof. Dr. Lemi Türker
Supervisor, **Chemistry Dept.**, **METU**

Examining Committee Members:

Prof. Dr. Fatma Sevin Düz
Chemistry Dept., Hacettepe University

Prof. Dr. Lemi Türker
Chemistry Dept., METU

Prof. Dr. Metin Zora
Chemistry Dept., METU

Prof. Dr. Yılmaz Yıldırır
Chemistry Dept., Gazi University

Assist. Prof. Dr. M. Fatih Danışman
Chemistry Dept., METU

Date: 27.01.2009

I hereby declare that all information in this document has been obtained and presented in accordance with academic rules and ethical conduct. I also declare that, as required by these rules and conduct, I have fully cited and referenced all material and results that are not original to this work.

Name, Last name: Taner ATALAR

Signature:

ABSTRACT

MOLECULAR DESIGN OF SOME POTENTIAL EXPLOSIVES

Atalar, Taner
Ph.D., Department of Chemistry
Supervisor: Prof. Dr. Lemi TÜRKER

January 2009, 195 Pages.

With existing energetic materials, the on going demand from the user for increased performance with reduced vulnerability induces the synthesis of novel explosives. The need to control costs ensured that theoretical methods can help to eliminate any poor candidates due to performance and safety problems. Thus, this study is aimed to design of some potential high explosive molecules which have high detonation properties and are also insensitive. Presently 65 molecules were studied and 54 of them were handled for the first time in the literature. The detonation properties have been evaluated within the limitations of the Kamlet-Jacobs equations, based on the quantum chemically calculated densities and heat of formation values. It is found that there might be some candidates of relatively insensitive and high energy density materials among these 54 studied molecules so far not mentioned in the literature.

Keywords: Nitrocompounds, Kamlet-Jacobs equations, detonation parameters.

ÖZ

BAZI POTANSİYEL PATLAYICILARIN MOLEKÜLER TASARIMI

Atalar, Taner
Doktora, Kimya Bölümü
Tez Yöneticisi: Prof. Dr. Lemi TÜRKER

Ocak 2009, 195 Sayfa

Kullanıcılardan talep edilen yüksek güç ve düşük duyarlılık, var olan patlayıcılar tarafından sağlanamaması, yeni patlayıcıların sentezlerine sevk etmektedir. Ayrıca ihtiyaçlara cevap veren patlayıcı geliştirmesindeki maliyetleri azaltmak için zayıf güçte yahut yüksek duyarlılıktaki patlayıcı adaylarını elemekte teorik yöntemler kullanılmaktadır. Bu çalışmada amaç, talep edilen özelliklere sahip patlayıcıların moleküler düzeyde tasarımıdır. 54 tanesi şimdiye kadar literatürde bahsedilmeyen toplam 65 molekül incelenmiştir. Kuantum kimyasal yöntemleriyle hesaplanmış yoğunluk ve oluşum ısılarına dayanarak ve Kamlet-Jacobs eşitliklerinden faydalanarak (bu yöntemlerin sınırları dâhilinde) moleküllerin patlama parametreleri tahmin edilmiştir. Bu incelenen 54 molekül arasında, kısmen duyarsız ve yüksek yoğunluklu enerjik molekül adaylarının olabileceği öngörülmüştür.

Anahtar kelimeler: Nitro bileşikleri, Kamlet-Jacobs eşitlikleri, patlama parametreleri.

To My family

ACKNOWLEDGEMENTS

I would like to express my sincere feelings of gratitude and appreciation to my supervisor Prof. Dr. Lemi TÜRKER for directing me in this interesting study and for his skillful guidance, endless support, encoragement and patience throughout this tedious work. It has been a great honour for me to work with him. His continuous advice, criticism, supports and guidance throughout the study deserves special appreciation.

I wish to express my deepful thanks to Prof. Dr. Svatopluk ZEMAN for their endless help and close interest as a friend during my short term research at the Institute of Energetic Materials in University of Pardubice in Czech Republic. Also I would like to express my thanks to TUBİTAK for financial support of this abroad study.

I also give my thanks to all the members of D-250 Research Group: Selçuk GÜMÜŞ, Yakup ÇAMUR, Çağlar ÇELİK and Hamza TURHAN.

I also wish to express my deepful thanks to Murat IŞIK, Emre Yusuf YAZICIOĞLU, Mustafa EMRULLAHOĞLU, Serdar SEZER and Mustafa Fatih GENİŞEL for their endless help and close interest as friends.

Finally, my special appreciation and gratitude is devoted to my family for their endless encouragement and moral support, which makes everything possible.

TABLE OF CONTENTS

CHAPTER

1. INTRODUCTION

2. MOLECULAR MODELING: COMPUTATIONAL CHEMSITRY

3. RESULTS AND DISCUSSION

LIST OF TABLES

TABLES

LIST OF FIGURES

LIST OF ABBREVIATIONS

Å	Angstrom
AO	Atomic Orbital
AM1	Austin Model 1
B3LYP	Becke's three parameter exchange hybrid functional with Lee, Yang, Parr (LYP) correlation functional
BDE	Bond Dissociation Energy
CBS	Complete Basis Set
CC	Coupled Cluster Theory
CCSD	Coupled cluster theory with single and double excitations
CCSD(T)	Coupled cluster theory with single and double excitations and noniterative inclusion of triples
CCSDT	Coupled cluster theory with single and double excitations and inclusion of connected triples excitations
CI	Configuration Interaction
CIS	Configuration Interaction Single-Excitation
CISD	Configuration Interaction Single-and-Double-Excitation
CPU	Central Processing Unit
DFT	Density Functional Theory
GIAO	Gauge Invariant Atomic Orbital
GTO	Gaussian Type Orbital
GVB	Generalized Valence Bond
HEDM	High Energy Density Material
HF	Hartree-Fock Theory
HOF	Heat of Formation

HOMO	Highest Occupied Molecular Orbital
LDA	Local Density Approximation
LDSA	Local Density-Spin Approximation
LSDA	Local Spin-Density Approximation
LUMO	Lowest Unoccupied Molecular Orbital
MCSCF	Multi-Configurational Self-Consistent Field Theory
MM	Molecular Mechanics
MNDO	Modified Neglect of Diatomic Overlap
MPn	Møller-Plesset nth-order Perturbation Theory
MO	Molecular Orbital
NICS	Nucleus Independent Chemical Shift
NMR	Nuclear Magnetic Resonance
PM3	Parameterization Method 3
RHF	Restricted Hartree-Fock Theory
Ψ	Wave function (state function)
ROHF	Restricted Open-Shell Hartree-Fock Theory
SE	Semiemprical
SCF	Self-Consistent Field
STO	Slater Type Orbital
UHF	Unrestricted Hartree-Fock
ZPVE	Zero point vibrational energy

CHAPTER 1

INTRODUCTION

1.1 A Brief History of Explosives

Blackpowder, also known as gunpowder, was most likely the first explosive composition. In 220 BC an accident was reported involving blackpowder when some Chinese alchemists accidentally made blackpowder while separating gold from silver during a low-temperature reaction [1]. Blackpowder was not introduced into Europe until the 13th century when an English monk called Roger Bacon in 1249 experimented with potassium nitrate and produced blackpowder, and in 1320 a German monk called Berthold Schwartz studied the writings of Bacon and began to make blackpowder and study its properties [1]. The results of Schwartz's research probably speeded up the adoption of blackpowder in central Europe. By the end of the 13th century many countries were using blackpowder as a military aid to breach the walls of castles and cities. Blackpowder contains a fuel and an oxidizer. The fuel is a powdered mixture of charcoal and sulfur which is mixed with potassium nitrate (oxidizer).

By the middle of the 19th century the limitations of blackpowder as a blasting explosive were becoming apparent. Difficult mining and tunneling operations required a 'better' explosive. In 1846 the Italian, Professor Ascanio Sobrero discovered liquid nitroglycerine [1]. He soon became aware of the explosive nature of nitroglycerine and discontinued his investigations. A few years later the Swedish inventor, Immanuel Nobel developed a process for manufacturing nitroglycerine, and in 1863 he erected a small manufacturing plant in Helenborg near Stockholm with his son, Alfred. Nobel began to license the construction of nitroglycerine plants which were generally built very close to the site of intended use, as transportation of liquid nitroglycerine tended to generate loss of life and property. The Nobel family suffered many set backs in marketing nitroglycerine because it was prone to accidental initiation, and its initiation in bore holes by blackpowder was unreliable. There were many accidental explosions, one of which destroyed the Nobel factory in 1864 and killed Alfred's brother, Emil. Alfred Nobel in 1864 invented the metal 'blasting cap' detonator which greatly improved the initiation of blackpowder. The detonator contained mercury fulminate [$Hg(CNO)_2$] and was able to replace blackpowder for the initiation of nitroglycerine in bore holes. After another major explosion in 1866 which completely demolished the nitroglycerine factory, Alfred turned his attentions into the safety problems of transporting nitroglycerine. To reduce the sensitivity of nitroglycerine Alfred mixed it with absorbent clay, 'Kieselguhr'. This mixture became known as ghur dynamite and was patented in 1867. Nitroglycerine has a great advantage over blackpowder since it contains both fuel and oxidizer elements in the same molecule. At the same time as nitroglycerine was being prepared, the nitration of cellulose to produce nitrocellulose (also known as guncotton) was also being undertaken. Many accidents occurred during the preparation of nitrocellulose, and manufacturing plants were destroyed in France, England and Austria. During these years, Sir Frederick Abel was working on the instability problem of nitrocellulose for the British Government at Woolwich and Waltham Abbey, and in 1865 he published his solution to this problem by converting nitrocellulose into a pulp. Abel showed through his process of pulping, boiling and washing that the stability of nitrocellulose could be greatly improved. Nitrocellulose was not used in military and commercial explosives until 1868 when Abel's assistant, E.A. Brown discovered that dry, compressed, highly-nitrated nitrocellulose could be detonated using a mercury fulminate detonator, and wet, compressed nitrocellulose could be exploded by a small quantity of dry nitrocellulose (the principle of a Booster). Thus, large blocks of wet nitrocellulose could be used with comparative safety.

Alfred Nobel discovered that on mixing nitrocellulose with nitroglycerine a gel was formed. This gel was developed to produce blasting gelatine, gelatine dynamite and later in 1888, ballistite, the first smokeless powder. Ballistite was a mixture of nitrocellulose, nitroglycerine, benzene and camphor. Since the discovery of blackpowder, nitroglycerine is the very important cornerstone in this field, because both oxidizer and fuel part present in the same molecule so maybe this is the first modern explosive.

1.2 General Information on Explosives

1.2.1 Definitions of Important Terms Related with Explosives

An explosive defined according to the Dictionary of Explosions & Explosives [2] is an intrinsically energetic solid or liquid chemical compound, mixture, or device, which, on being heated, struck or detonated, is capable by chemical reaction of producing an explosion by its own energy without the participation of external reactants such as atmospheric oxygen, with substantially instantaneous production of heat and gas. In general, an explosive has three basic characteristics:

i) It is an intrinsically energetic unstable chemical compound or mixture ignited by detonation, friction, heat, impact, shock, or a combination of these conditions.

ii) Upon ignition it decomposes very rapidly in a detonation (as opposed to a deflagration, which is a slower decomposition as with ignition of gunpowder).

iii) Upon detonation there is a rapid release of heat and large quantities of high-pressure gases, which expand rapidly with sufficient force to overcome confining forces, e.g., the confining forces of surrounding rock formation.

Only intrinsically, an energetic, unstable chemical substance where generally the fuel and oxidizer are combined in the same material, and which takes part in a chemical explosion is an explosive. For example, in spite of the wood has higher energy content than most explosives, wood is not an explosive because its energy of activation is much greater, and its energy is released over much longer period.

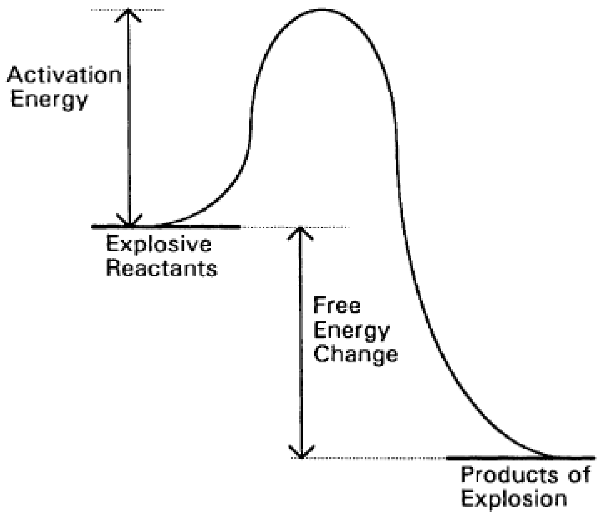

Figure 1.1 Schematic diagram of the reaction profile for chemical explosives
Reprinted from “The Chemistry of Explosives” J. Akhavan, The Royal Society of Chemistry, 2004, pp 125.

An explosive does not occur naturally but it is entirely man-made. Cuprous acetylide is an explosive which explodes by decomposing into copper and carbon and heat, no gas is evolved but the sudden heat causes a sudden expansion of the air in the neighborhood, and the result is an unequivocal explosion [3].

Explosion is defined [2] as an act of bursting or exploding. It is a violent expansion or bursting that is caused by sudden release of energy, from a very rapid chemical reaction, or from an escape of gases under pressure as in a gas cylinder, which is accompanied by loud noise. Thus, an explosion may be defined generally as a phenomenon of the sudden a noisy release of the previously confining energy, affecting the surroundings. So explosion is sudden and rapid conversion of potential energy into kinetic energy with the release or production and release of gases under pressure accompanied by heat, shock and a loud noise.

In an explosion, production and release of gases under pressure accompanied by heat, shock and loud noise causes a significant blast wave capable of causing damage to surrounding property. On the other hand, the resultant high-pressure gases of an explosion are utilized in some cases to perform the physical work. So some explosions are desired and controlled, as in blasting in quarries and mines or in the cylinder of an internal combustion engine. Peaceful use of explosives is not limited in mining, quarrying and engineering enterprises but in making fireworks, signal lights, rockets. Unfortunately, the destructive effects of explosives are much more spectacular than peaceful uses.

1.2.2 Classification of Explosives

Classification of explosive materials is based on various criteria. They may be classified both from the chemical point of view and according to their uses [4]. From the chemical viewpoint, explosives can be distinguished as individual chemical explosives and mixtures. The main subclasses of the former are divided into:

1) Nitro compounds
2) Nitric esters
3) Nitramines
4) Derivatives of chloric and perchloric acids
5) Azides
6) various compounds capable of producing an explosion, for example fulminates, acetylides, nitrogen rich compounds such as tetrazene, peroxides and ozonides, etc.

Individual substances are explosive if their molecules contain groups which confer upon them explosive properties. The first attempt at a systematic approach to the relation between the explosive properties of a molecule and its structure was made by van't Hoff [5]. He pointed out, that the explosive molecules generally contain the following groups.

1) O-O linkage in peroxides, ozone and ozonides

2) O-Cl in chlorides and perchlorates

3) N-Cl in nitrogen chloride

4) N=O in nitro compounds, nitric acid esters andsalts

5) N=N in diazo compounds, hydrazoic acid, its salts and esters

6) N=C in fulminates and cyanogen

7) C≡C in acetylene and acetylides

A further effort to establish a relationship between explosive properties and structure was made by Pletz [6]. He proposed the theory of "explosophores" and "auxoploses" in a way analogous to Witt's suggestion of chromophores and auxochromes in the dyes, and Ehrlich's toxophores and autotoxes in chemotherapeutics. According to Pletz the explosive properties of any substance depend upon the presence of definite structural groupings, called explosophores. The auxoploses fortify or modify the explosive properties conferred by the explosophore. Pletz divided all explosives into eight classes containing the following groups as explosophores:

(1) $–NO_2$ and $–ONO_2$ in both organic and inorganic substances

(2) –N=N- and -N=N=N- in inorganic and organic azides

(3) –N=C in fulminates

(4) $–NX_3$, for example in NCl_3 (X: a halogen)

(5) –O-O- and –O-O-O- in inorganic and organic peroxides and ozonides

(6) $–OClO_2$ and $–OClO_3$ in inorganic and organic chlorates and perchlorates

(7) -C≡C- in acetylene and metal acetylides

(8) M-C metal bonded with carbon in some organometallic compounds.

Although this classification is in principle correct, the distinction between the terms “explosophore” and “auxoplose” is very vague and of little practical value. A further step in the classification of explosives was made by Lothrop and Handrick [7], who collected and classified all the available information on the performance of explosives and related it to four factors. Those are the oxygen balance, “plosophoric” groups, “auxoplosive” groups and heat of explosion. A plosophore has been defined as a group of atoms which is capable of forming an explosive compound on introduction into a hydrocarbon. According to these authors there exist two classes of plosophores differing sharply in effectiveness and consistency in producing power. Hence, it is suggested that these be called “primary” and “secondary” plosophores. Primary plosophores include aromatic and aliphatic nitro groups, nitrate esters, and the nitramine group. The secondary plosophores include groups such as azo, azide, nitroso, peroxide, ozonide, perchlorate, etc. If more than one type of these groups is present, such a molecule may be named a hybrid according to Lothrop and Handrick [7]. Groups which do not themselves produce explosive properties, but may influence them (in the same way that auxochromic groups vary the color intensity and shade of a dye), are called auxoplosives by these authors. As example of such groups, we may quote hydroxyl, carboxyl, chlorine, sulfur, ether, oxygen, amine, etc. Although the classification of groups existing in explosive molecules suggested by Lothrop and Handrick [7] may generally be accepted, their far-reaching postulations concerning a close relation between the oxygen balance and performance of explosives aroused strong criticism [8, 9], because the oxygen present (for example, in carbonyl or hydroxyl groups) has little effect on the performance of an explosive. This is due to the high heat of formation of C-O and C-O-H bonds. The ease of detonation of picric and styphnic acids as compared with trinitrobenzene is well known. Smolenski and Czuba pointed out that dinitrophenol detonate more readily than dinitrobenzene [10]. From the classic work of Wöhler and Wenzelberg, it is also well known that the sensitivity to impact of aromatic nitro compounds increases with increase in the number of substituents for a given member of the nitro groups [11].

According to their uses explosives are divided into:

i) Primary explosives or initiators

ii) High explosives

iii) Propellants (low explosives).

Primary explosives and their mixtures are divided into those used for filling ignition caps and those used in detonators [12]. High explosives may be classified according to their physical properties as powdery, meltable, semi-meltable and plastic. On the other hand, propellants may be grouped on the basis of chemical composition into gun powder and similar mixtures, nitrocellulose (single base) and nitroglycerine (double base) powders. With respect to their uses and some properties they are divided into black powder, smokeless and flashless powders, and rocket propellants. Explosives, as mentioned this section, are classified in terms of their carious properties such as chemical structure, sensitivity, and stability. However, the most satisfying classification seems to be primary (initiating) explosives, high (secondary) explosives, propellants and pyrotechnics [13].

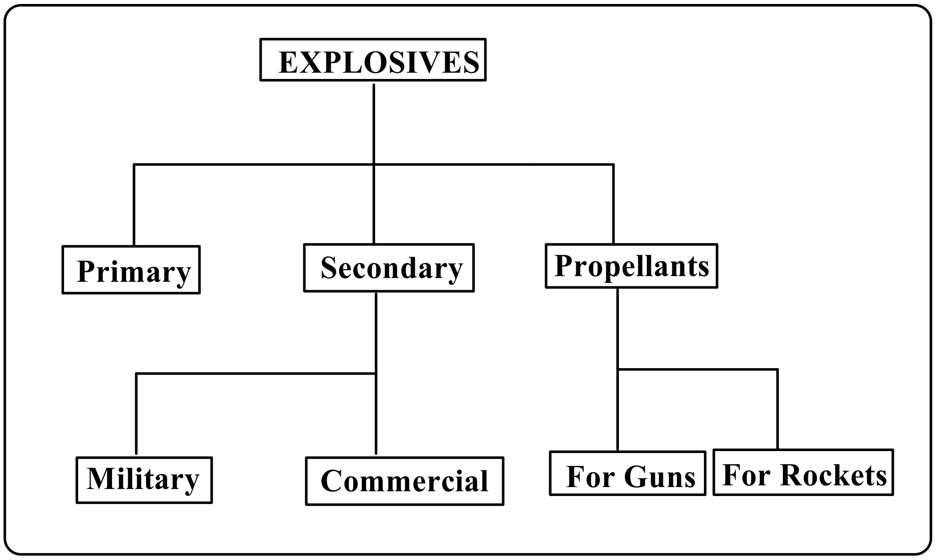

Figure 1.2 Schematic diagram of the classification of explosives

1.3 Important Parameters Related to Performance of Explosives:

1.3.1 Detonation and Deflagration

The term “detonation” is used to describe an explosion phenomenon. It is an exothermic chemical reaction that propagates through the reaction zone toward the unreacted material at a supersonic velocity forming a propagating shock wave. Normally a detonation is brought about by shock wave traveling at supersonic velocity through material. This shock wave initially compresses the material, heating it and causing it to break down into its constituent molecular materials. This causes the liberation of the fuel and oxidizer that heretofore were chemically bonded and they recombine to form gases. Almost instantaneous reaction produces a blast of rapidly expanding hot gases. Some unique events take place in the brief instant of a detonation such as the detonation wave travels as fast as 9 kilometers per second, the shock wave produces pressure up to 500000 times that of Earth’s atmosphere, and temperature can soar to 5500 K [2]. General concept of an explosive compound’s initiation is seen in Figure 1.3. Over a finite time period, these three functions begin in the bulk material; proceed into lower compositional levels possibly continuing on through the atomic realm to produce final, mostly gaseous products which are detected back at the bulk level.

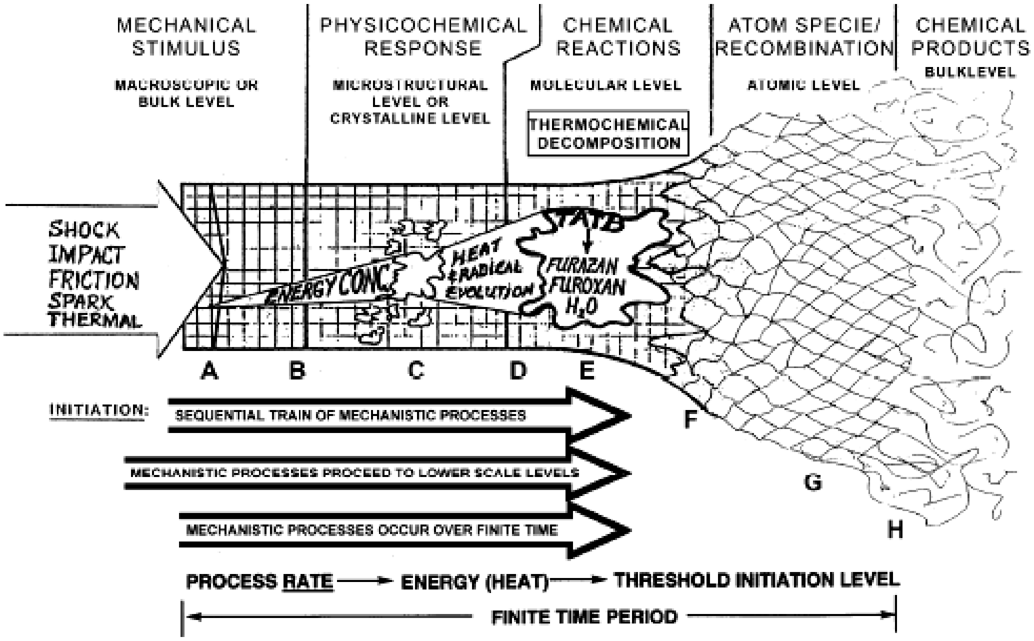

Figure 1.3 A general concept concerning explosives initiation

Reprinted from S. A. Shackelford, J. de Physique IV 4 (1995) C4-485.

Generally, primary and secondary explosives detonate and low explosives deflagrate. However, under certain conditions, low explosives can detonate and primary or secondary explosives can deflagrate. As mentioned before, the detonation of an explosive is the propagation of a shock wave through the explosive material where the rates of reaction are controlled by thermodynamic conditions; the deflagration rate of an explosive consists of the chemical burning of the material wherein its propagation rates are dependant on chemical kinetics [2]. Deflagrating explosives burn faster and more violently than ordinary combustible materials. They burn with a flame or sparks, or hissing or cracking noise. Detonation occurs almost simultaneously through the whole mass of the high explosive, whereas deflagration is a progressive rapid burning of the low explosive. Detonation velocities lie in the approximate range of 1500 to 9000 meters per second however the rate of deflagration is necessarily below that of the detonation velocity. Additionally, the rate of reaction in a detonation is supersonic, but the rate of reaction in a deflagration is subsonic.

1.3.2 Detonation Velocity

Another very important term is the velocity of detonation or detonation velocity. The rate at which the detonation wave through a high explosive. The term “velocity of detonation relates only to high explosives whereas “velocity of explosion refers to both high and low explosives. Primary explosives detonate in the range of 3500-5500 ms^{-1}, on the other hand values of detnation velocities in secondary explosives are in the range of 5500 ms^{-1} and above.

1.3.3 Detonation Pressure

The detonation of an explosive is the result of a complicated interplay between chemistry and hydrodynamics, which produces the extreme pressure and temperature immediately behind the detonation wave. Chapman-Jouguet (C-J) thermodynamic detonation theory has traditionally been used to study detonation of Explosives [14-20]. The detonation energy is released in the form of kinetic energy and heat over a very short time, i.e. microseconds. In a detonating explosive a supersonic wave is established near to the initiation point and travels through the medium of the explosive, sustained by the exothermic decomposition of the explosive material behind it. On reaching the periphery of the explosive material the detonation wave passes into the surrounding medium, and exerts on it a sudden, intense pressure, equivalent to a violent mechanical blow. If the medium is a solid, i.e. rock or stone, the violent mechanical blow will cause multiple cracks to form in the rock. This effect is known as ‘brisance’ which is directly related to the detonation pressure in the shockwave front. After the shockwave has moved away from the explosive composition the gaseous products begin to expand and act upon the surrounding medium. A crater will be formed if the medium is earth, in water a gas bubble is formed and in air a blast wave develops. The intensity of the gaseous expansion will depend upon the power of the explosive, and one of the important factors determines the power of explosive is detonation pressure.

1.3.4 Oxygen Balance (Ω)

If the amount of oxygen present in the explosive molecule is insufficient for the complete oxidation a negative oxygen balance (Ω) results; this can be seen in the molecule of TNT (trinitrotoluene). Nitroglycerine, however, has a high portion of oxygen, more than required for complete oxidation of its fuel elements and therefore has a positive oxygen balance. This oxygen balance can be defined as the amount of oxygen, expressed in weight percent, liberated as a result of the complete conversion of the explosive material to carbon dioxide, water, sulfur dioxide, aluminum oxide, etc. It can be seen from Table 1.1 that explosive substances may have a positive or negative oxygen balance. The oxygen balance provides information on the types of gases liberated. If the oxygen balance is large and negative then there is not enough oxygen for carbon dioxide to be formed. Consequently, toxic gases such as carbon monoxide will be liberated. This is very important for commercial explosives as the amount of toxic gases liberated must be kept to a minimum.

Table 1.1 Oxygen balance (Ω) values of some well-known explosives.

Explosives	Emprical Fromula	Ω
Ammonium nitrate	NH_4NO_3	19.90
Nitroglycerine	$C_3H_5N_3O_9$	3.50
EGDN	$C_2H_4N_2O_6$	0.00
PETN	$C_5H_8N_4O_{12}$	-10.13
RDX	$C_3H_6N_6O_6$	-21.60
HMX	$C_4H_8N_8O_8$	-21.62
Nitroguanidine	$CH_4N_4O_2$	-30.70
Picric acid	$C_6H_3N_3O_7$	-45.40
Tetryl	$C_7H_5N_5O_8$	-47.39
TATB	$C_6H_6N_6O_6$	-55.80
HNS	$C_{14}H_6N_6O_{12}$	-67.60
TNT	$C_7H_5N_3O_6$	-74.00

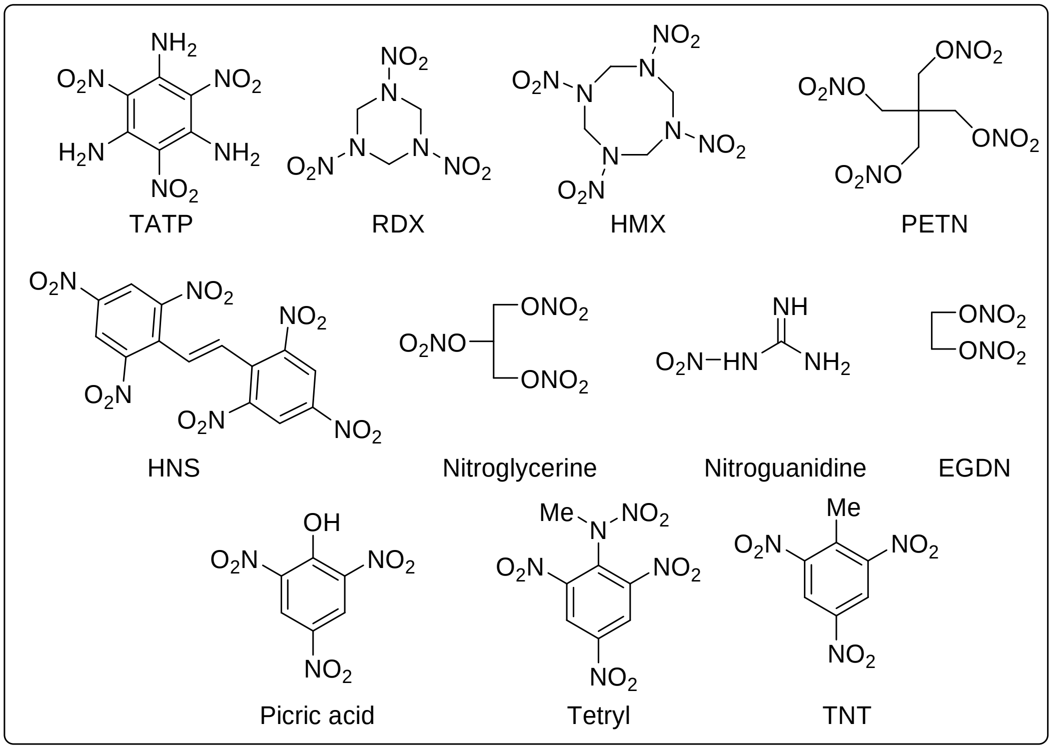

Figure 1.4 Chemical structures of the some well-known explosives

The oxygen balance does not provide information on the energy changes which take place during an explosion. This information can be obtained by calculating the heat liberated during decomposition of explosive substances, known as the 'heat of explosion'. In order to calculate the heat of explosion, the decomposition products of the explosive must be determined, since the magnitude of the heat of explosion is dependent upon the thermodynamic state of its products. The decomposition process will be by detonation in the case of primary and secondary explosives, and burning in the case of gunpowders and propellants.

1.3.5 Heat of Detonation

Detonation pressure and detonation velocity as well as detonation energy or heat of detonation have been regarded as the principle measures of performance of detonating explosives for many years. Heat of detonation can be used as the energy available to do mechanical work and estimating potential damage to surroundings [21]. In order to calculate heat of detonation we use the heat of formation values. Heat of formation is also one of the most important thermochemical properties of energetic materials because it is related directly with detonation parameters. In a chemical reaction involving explosives, energy is initially required to break the bonds of explosive into its constituent elements as shown in Reaction 1.1 for hexahydro-1,3,5-trinitro-1,3,5-triazine, RDX.

$$C_3H_6N_6O_6 \rightarrow 3C + 6H + 6N + 6O \qquad (1.1)$$

These elements quickly form new bonds with the release of a greater quantity of energy as shown in Reaction 1.2.

$$3C + 6H + 6N + 6O \rightarrow 3CO + 3H_2O + 3N_2 \qquad (1.2)$$

The molecules of an explosive are first raised to a higher energy level through input of the 'heats of atomization' in order to break their interatomic bonds. Then the atoms rearrange themselves into new molecules, releasing a larger quantity of heat and dropping to an energy level lower than the original as shown in elements, then energy is released when new bonds are formed. For instance, the reaction may take place in several stages involving complex systems of reaction chains, etc. Nevertheless, the energy evolved depends only on the initial and final states and not on the intermediate ones. Once the reaction is completed, the net heat evolved is exactly the same as if the reactant molecules were first dissociated into their atoms, and then reacted directly to form the final products (Hess's Law).

1.3.6 Density

It is determined that the energy which a detonation wave releases within and behind itself will depend upon the mass of explosive traversed per unit area of the wave. However, detonation velocity appears to be proportional to loading density. Density is an important aspect of performance behavior on the other hand, density of energetic materials have important role in predicting their detonation pressures and velocities. In a series of important papers [22-27], Kamlet and coworkers have presented empirical equations for calculating the ideal detonation velocity and pressure of a condensed explosive in terms of certain parameters of the explosive. One of the most important parameter is the density in these equations. Higher the density higher the detonation parameters. Thus, designing of new energetic materials strongly follow the density criteria. See the Table 1.2 for distinct effect of density on performance values of explosives.

Table 1.2 Some new explosives and their density and detonation velocities

	ρ (gcm^{-3})	**D (ms^{-1})**	**ΔH°$_f$ (kJ/mol)**
TNAD	1.84	8400	56.2
TN650	1.97	8800	71.1
HHTDD	2.07	9600	273.5
BCHMX	1.87	9050	80.2
TN550	1.91	9100	23.0
TENGU	2.01	9150	206.3

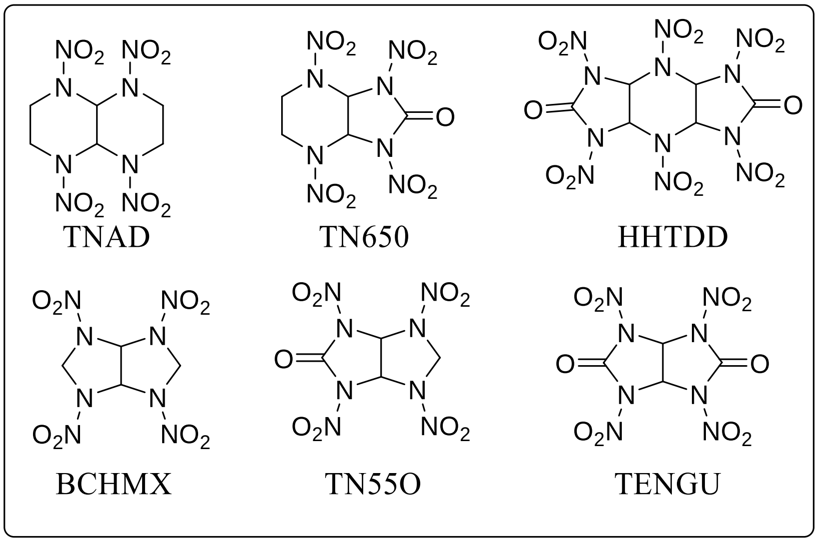

Figure 1.5 Chemical structures of the some new explosives.

1.4 Motivation to the Study on Molecular Design of Explosive

Energetic materials (explosives, propellants and pyrotechnics) are used extensively for Civil as well as Military Applications. Today the variety and number of high energy materials for various applications have become innumerable of which chemistry; synthesis, properties and other salient features are available in the literature. In the past, common explosives hexahydro-1,3,5-trinitro-1,3,5-triazine (RDX), octahydro-1,3,5,7-tetranitro-1,3,5,7-tetrazocine (HMX) and 2,4,6 trinitrotoluene (TNT) were considered adequate for all weapon applications. Because of many catastrophic explosions resulting from unintentional initiation of munitions by either impact or shock, aboard ships, aircraft carriers, and munitions trains, these explosives have become less attractive. Of course, higher performance has always been a prime requirement in the field of research and development of explosives and the quest for the most powerful high explosives still continues and this search seems to be never ending. The demand from the user for increased performance with reduced or low vulnerability could not be met with existing materials, and the need to control costs ensured that the processes for producing compositions were also subject to rapid change. Thus, in modern ordnance there are strong requirements for explosives having good thermal stability, impact and shock insensitivity and better performance. However, these requirements are somewhat mutually exclusive. The explosives having good thermal stability and impact insensitivity usually exhibit poorer explosive performance and vice versa. Therefore, the foremost objective at the stage of synthesis of new explosives consists of finding the molecule having both a good energy capability and optimal safety (reduced vulnerability, shock and impact insensitivity) to those in current use [28].

In this study, firstly well-known explosives were investigated in order to better understand what makes new energetic compounds useable. The tautomers and charged forms of well-known explosives were investigated and then some potential candidates of new energetic materials were proposed.

1.4.1 Tautomerism in Explosive Initiation Mechanisms

The driving force behind the development (or at least the funding for development) of any new materials for defense use is, and almost certainly always will be, performance. This readily apparent from almost all recent papers proposing or describing new energetic compounds. An example is found in Olah and Squire [29].

One of the important processes occurring during detonation of high energetic nitro compounds is tautomerism, which involves the transfer of a hydrogen either by an unimolecular 1,3- or 1,5-shift or by a bimolecular process where the transfer occurs intermolecularly. This hydrogen shift leads to the formation of *aci*-nitro compounds, which dissociate by release of energy to give smaller fragments. Tautomerism is competitive to many other processes that occur during detonation.

Hydrogen transfer reactions invoving a 1,3-H shift are very common in organic and biological systems. Investigations into tautomerism have lead to greater understanding of such concepts as acid-base relationships, structure-reactivity correlations, hydrogen bonding, etc. and have provided valuable insights into the nature of chemical processe. More prevalent tautomeric processes are keto-enol, imine-enamine, nitroso-oxime, thiol-thione, amide-iminol, nitro-aci-nitro, hydrazo-azo, phenol-keto etc [30-40]. Keto-enol tautomerism is the most commonly observed and most widely studiedprocess, and is very important in many chemical applications. Theoretical studies provide much insight into the details of the tautomeric processes including electronic and energetic aspects. Table 1.3 gives a list of important tautomeric processes with selected data. Cooperatively between two or more tautomeric processes is also known to occur and they can influence one another significantly.

Table 1.3 Parent tautomeric processes and energetic data (kcal/mol) [30].

Tautomeric Process	**Compounds**	**ΔE**	**PA**
Keto-enol	CH_3CHO	10.8	365.9
Imıne-enamine	CH_3-CH=NH	3.9	377.1
Amide-imide	NH_2-CH=0	11.5	359.5
Oxime-nitroso	CH_2=N-OH	12	362.5
Nitro-*aci*-nitro	CH_3-NO_2	14.1	355.9
Nitramide-*aci*-nitramide	NH_2-NO_2	8.8	339.7

ΔE is the tautomeric energy difference; PA is the proton affinity of the most stable anion.

As an example for the role of tautomerism in explosives, tautomeric processes were important in nitromethane (NM) initiation mechanism [41-43]. This process produces *aci*-forms of these compounds, which are also called nitronic acids. According to Manelis [41], the existence of *aci*-form of NM represents a more probable cause of lowering of the activation energy of thermal decomposition of liquid NM as compared with the gas-phase thermolysis (i.e. in relation to the theories of bimolecular mechanism of this decomposition [41]). Recently, Zeman and coworkers studied on NM initation [43], a well-known effect of amines, and also of water, on detonation characteristics of nitromethane (NM) is discussed from the point of view of the published knowledge about the study of initiation reactivity of this nitro paraffin. The most widespread concepts of the primary steps of this initiation, i. e. formation of *aci*-NM anion $[CH_2{=}NO_2]^-$ by intermolecular proton transfer in the neat NM submitted to shock and formation of this anion by action of an amine, have been scrutinized by the DFT method and evaluated as thermodynamically disadvantageous. Also the 1,3-intramolecular proton shift in the NM molecule was characterized as a higher-barrier process. Two favorable primary mechanisms of fission in the NM initiation and development of its detonation were investigated: homolysis of $C–NO_2$ bond in the neat NM and homolysis of N–OH bond in its *aci*-form. The second mentioned pathway (*aci*-form) was found to be thermodynamically the most preferable mechanism of fission.

1.4.2 Electrostatic Charging of Explosives in Terms of Safety and Mechanism of Initiations

Another very important aspect of initiation of explosives is the charge development on explosive molecules. For many years it has been detected that free electrons exist in combustion flames and gaseous detonations [44, 45]. The influence of applied fields on gaseous systems detonating at their threshold conditions has been observed years ago, e.g. detonations are capable of generating large electromotive forces in external systems [44]. Also it has been reported that electromagnetic radiation having ‘video’ frequencies to ‘centimeter waves’ accompany detonations [46, 47]. The evidence for free electrons in the detonation wave of solid explosives and that described previously for free electrons in flames and detonation waves in gases seem therefore to justify the conclusion that the electrical current in the reaction zone of solids is carried preponderantly by free electrons. However, of course there must also be many positive charges as free electrons in the reaction zone of solid explosives. All these experimental facts indicate abundance of ions and electrons in the explosion mixture. Consequently, positively or negatively charged ions of explosive material just before explosive decomposition of the molecule might have transient existence. Also, molecules of explosive materials might be exposed to some electrical fields and get polarized or ionized which may lead to explosion. Hence, it would be interesting to study the influence of ionization at the molecular levels by means of quantum chemical methods. For this purpose, some well-known explosive molecules have been considered presently and its univalent anionic and cationic forms quantum chemically investigated in order to better understand the explosion phenomenon. .

1.5 Overviews of Recent Research on Explosives

Although explosives have been known for over a thousands years, the science of explosives is still very new. Scientists are only beginning to understand the nonlinear interaction between chemistry and fluid mechanics that produces the rapid energy release known as detonation [48]. A major focus of work during the past twenty years has been the *design,* characterization and evaluation of new and proposed energetic compounds [49-59]. The goal is to help further the development of materials that combine improved performance with diminished vulnerability (sensitivity) to unintended external stimuli, such as impact and shock. The specific objectives have included a) assessment of stability and sensitivity, b) determination of thermodynamic data relevant to combustion and decomposition, and c) analysis of mechanisms and activation barriers of key steps in synthesis, combustion and decomposition processes.

There are some very good studies on review of advanced high performance stable energetic materials [60-63]. One of the principal target molecules, particularly of US researchers, is octanitrocubane (ONC). Recently, Zhang et al. [64] made successfully heptanitrocubane and the long sought ONC in 45–50% isolated yield over the last 18 years of synthesis efforts continued on the molecule. Both hepta- and octa-nitrocubane (HpNC and ONC) have decomposition temperatures well above 200 ºC. Samples were not detonated by hammer taps. HpNC is currently easier to make than ONC, an impressively high density (2.028 g/cm^3) was measured for HpNC. It may prove to be a more powerful explosive and/or monopropellant since it is more dense, has a calculated heat of formation only about 6% less than ONC. It will also produce some lighter gaseous products as it is not perfectly oxygen balanced [65, 66]. The most recently published calculated value for heat of formation of solid ONC [$(CNO_2)_8$] is 594 kJ/mol, corresponding to 74 kJ/mol per (CNO_2) mole. The highest calculated ΔH_f of solid hexanitrobenzene [$(CNO_2)_6$], one of the most energetic explosive known [66] is about 200 kJ/mol corresponding to 33 kJ/mol per (CNO_2)-molecule, less than half that of ONC [67]. The energy content of hexanitrobenzene is lowered by the stabilizing resonance energy of the aromatic systems. The energy content of octanitrocubane is increased by the strain energy of its unique carbon skeleton.

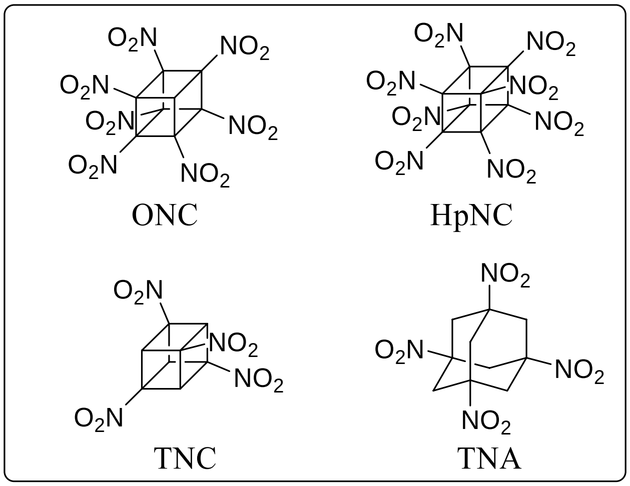

Figure 1.6 Chemical structures of ONC, HpNC, TNC and TNA

Less nitrated cubanes such as tetranitrocubane (TNC) has recently been proved to be an extraordinary material as investigated by Eaton et al. [68]. It is a crystalline solid with high density (1.814 g/cm^3) and is kinetically quite stable, not melting until 270 ◦C. Detonation has been achieved purposefully under controlled condition at US Army Armament Research & Development Command (now ARDEC); the explosive energy release exceeded expectation, but the quantitative results are not yet available publically. Calculations indicate that TNC may well prove to be a better monopropellant than ONC [69]. Another line of research in the field of cage compounds concerned the synthesis of nitroadamantane compounds. At the start, the preparation of 1,3,5,7-tetranitroadmantane (TNA) was reported by Sollott [70]. However, despite much optimism only a few adamantanes have been reported since that time and prove that these show no significant effect of adding nitrogoups in the ring. TNA with its high melting point of ca. 350 ºC is likely to be of value as a heat resistant explosive.

Researchers from United States of America have reported several thermally stable energetic materials. The first compound prepared under this program was 2,4,6-tris(picrylamino)-*s*-triazine or *N*,*N*-nitropicrylmelamine (TPM). The compound 2, 4, 6-tris (picrylamino)-*s*-triazine is reported to exhibit moderate thermal stability, with a performance slightly better than that of trinitrotoluene. Subsequently, the heterocyclic nitrogen atoms of *N*, *N*-nitropicrylmelamine were systematically replaced with the C-nitro function to give nitro substituted tris(picrylamino)pyrimidine, pyridine, and benzene. Tris(picrylamino)pyrimidine is more thermally stable than TPM. Thermal stability is an important characteristic of the energetic materials. Improved thermal stability ensures safer production, increased shelf life of munitions and low vulnerability to accidental initiations. Owing to more favorable elemental composition, hetero aromatic nitro compounds represent class of explosives capable of delivering higher performance compared to analogous aromatic system [71, 72]. The preparation of the energetic pyridines with higher energy potential implies the introduction of more than three nitro groups into the rings. However, it may lead to unstable vicinal dinitro groups. Another approach may be nitration of amino groups of aminopyridines resulting in primary and secondary nitraminopyridines.

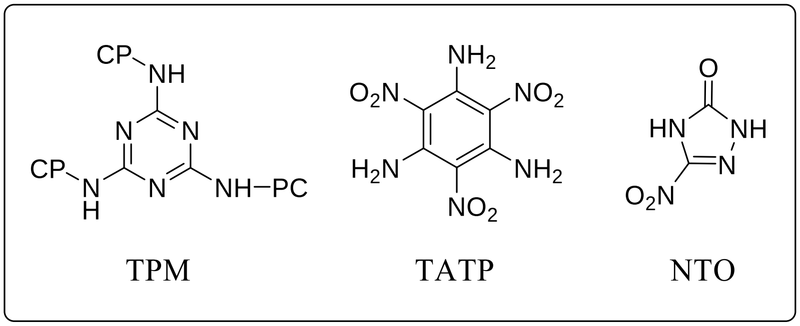

Figure 1.7 Some examples of thermally stable explosives.

Coburn and Singleton [73] have described the explosive properties of the nitropyridine derivatives namely, 2,4,6-trinitropyridine (TNPy), 2,4,6-trinitropyridine-1-oxide (TNPyOx), and 2,6-diazido-4-nitropyridine-1-oxide (DazNPyOx). However, analogous nitro compounds of the series of *N*-

heterocyclic aromatics (pyridine, diazine, triazine) have not become popular. 3, 5-dinitro-2, 6-bispicrylamino pyridine (PYX) [74] is also reported as an attractive thermally stable high explosive with decomposition temperature 460 ºC. It can offer higher velocity of detonation (7497 m/s) and detonation pressure (308 kbar) compared to tetranitro dibenzotetraazapentalene. Extraordinary thermal stability and insensitivity to mechanical stimuli has paved way for applications of 3, 5-dinitro-2, 6-bispicrylamino pyridine in the area of sheet explosives as well as civil applications such as oil-well perforation [75, 76].

Recent developments of novel explosive materials have concentrated on reducing the sensitivity of the explosive materials to prevent accidental initiation by shock, impact and thermal effects. The explosive materials, which have this reduced sensitivity, are calling Insensitive Munitions, (IM). Although these explosive materials are insensitive to accidental initiation they still perform very well when suitably initiated. Whatever impact future technologies may have on the design of rocket motors and ordnance, chemical propellants and explosives will always have a place in the science of controlled kinetic energy release.

CHAPTER 2

MOLECULAR MODELING: COMPUTATIONAL CHEMISTRY

2.1. Introduction

Modeling in chemistry is a tool for better understanding of chemistry. Models are central for understanding of chemistry. Molecular modeling allows one to do and teach chemistry better by providing better tools for investigating, interpreting explaining or discovering new phenomena. Nadendla [77] said that like experimental chemistry, it is a skill- demanding and must be learnt by doing and not just reading. Molecular modeling is easy to perform with currently available software, but the difficulty lies in getting the right model and proper interpretation.

Computational chemistry (also called molecular modeling; the two terms mean about the same thing) is a set of techniques for investigating chemical problems on a computer. Questions commonly investigated computationally are:

- *Molecular geometry:* The shapes of molecules – bond lengths, angles, and dihedrals.
- *Energies of molecules and transition states:* This tells us which isomer is favored at equilibrium, and (from transition state and reactant energies) how fast a reaction should go.

- *Chemical reactivity:* For example, knowing where the electrons are concentrated (nucleophilic sites) and where they want to go (electrophilic sites) enables us to predict where various kinds of reagents will attack to a molecule.
- *IR, UV, and NMR spectra:* These can be calculated easily.
- *The interaction of a substrate with an enzyme:* Seeing how a molecule fits into the active site of an enzyme is one approach to designing better drugs.
- *The physical properties of substances:* These depend on the properties of individual molecules and on how the molecules interact in the bulk material. For example, the strength and melting point of a polymer (e.g. a plastic) depend on how well the molecules fit together and on how strong the forces between them are. People investigate various physical and chemical properties like this work in the field of materials science.

The first step to making the theory more closely mimic the experiment is to consider not just one structure for a given a chemical formula, but all possible structures. Many aspects of chemistry can be reduced to questions about potential energy surfaces (PES) [78]. A PES displays the energy of a molecule as a function of its geometry. It can resemble a hilly landscape, with valleys and mountain peaks. Real PESs have many dimensions, but key feature can be represented by a 3 dimensional PES, as depicted in Figure 2.1.

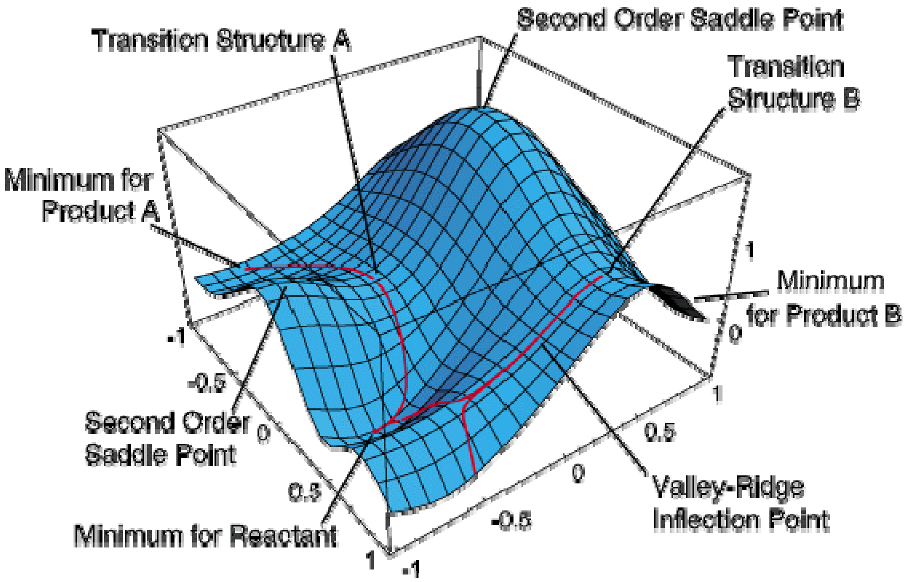

Figure 2.1 A simplified PES in three dimensions

Reprinted from "An Introduction to Theoretical Chemistry" Jack Simons, Cambridge University Press, 2003.

The form of a potential energy surface for a specific number of nuclei and electrons, can be calculated by solving the Schrödinger equation for every possible set of atomic coordinates. The transition state of a reaction corresponds to a maximum in the reaction coordinate and a minimum in all other coordinates, i.e. the highest point on the lowest energy path being a first-order saddle point. A reaction path connects reactants and products through a mountain pass. Energetic of reactions can be calculated from the energies or altitudes of the minima for reactants and products. The structure, energetics, properties, reactivity, spectra and dynamics of molecules can be readily understood in terms of potential energy surfaces. Except in very simple cases, the potential energy surface cannot be obtained from experiment.

Everything in today's world, from the simplest to the very complex, is firstly designed by computer simulations. There is no reason why chemistry should not be part of such a world. Evolution of quantum chemistry after some major steps allowed us to practice chemical research by such simulations. First *ab initio* (Latin phrase meaning, “From the beginning”) computations, which predated computers, sought qualitative agreement between experiment and semi-empirical calculations. Computers launched a second age extending the applications to a larger portion of the chemist’s interest. Computational chemistry can now be used as an analytical tool in the same sense that an NMR or X-ray crystallography. Its true place, however, is as a predictive tool, to be considered before the experiment. Nowadays, depending on the desired accuracy, one can computationally acquire a wealth of information from systems containing several thousands of atoms (by using supercomputers). A really important problem, and the line which current developments in theoretical/computational chemistry will follow is, the achievement of putting facilities with rapidly increasing performance [79-82]. Nowadays the number and extent of theoretical/computational chemistry resources publicly available increased continuously and reached a tremendous amount.

The following are some of the most commonly used computational methods:

- Semiempirical (SE) methods
- *Ab initio* methods
- Density functional theory

2.2 Semiemprical Methods

Semiempirical calculations are set up with the same general structure as a HF calculation in that they have a Hamiltonian and a wave function. Within this framework, certain pieces of information are approximated or completely omitted. Usually, the core electrons are not included in the calculation and only a minimal basis set is used. Also, some of the two-electron integrals are omitted. In order to correct for the errors introduced by omitting part of the calculation, the method is parameterized. Parameters to estimate the omitted values are obtained by fitting the results to experimental data or *ab initio* calculations. Often, these parameters replace some of the integrals that are excluded.

2.2.1 Parameterization Method 3 (PM3)

Parameterization method 3 (PM3) [83] employed partly in the present study uses nearly the same equations as the AM1 [84] method along with an improved set of parameters. The PM3 method is also currently extremely popular for organic systems. It is more accurate than AM1 for hydrogen bond angles, but AM1 is more accurate for hydrogen bond energies. The PM3 and AM1 methods are also more popular than other semiempirical methods due to the availability of algorithms for including solvation effects in these calculations.

There are also some known strengths and limitations of PM3. Overall heats of formation are more accurate than with AM1. Hypervalent molecules are also predicted more accurately. PM3 tends to predict that the barrier to rotation around the C-N bond in peptides is too low. Bonds between Si and the halide atoms are too short. PM3 also tends to predict incorrect electronic states for germanium compounds. It tends to predict sp^3 nitrogen as always being pyramidal. Some spurious minima are predicted. Proton affinities are not accurate. Some polycyclic rings are not flat. The predicted charge on nitrogen is incorrect. Nonbonded distances are too short. Hydrogen bonds are too short by about 0.1Å, but the orientation is usually correct. On average, PM3 predicts energies and bond lengths more accurately than AM1.

2.3 *Ab initio* Methods

This name is given to computations that are derived directly from theoretical principles with no inclusion of experimental data. Various approximations are involved in *ab initio*. The approximations made are usually mathematical approximations, such as using a simpler functional form for a function or finding an approximate solution to a differential equation.

2.3.1 The Hartree-Fock Theory

The most common type of *ab initio* calculation is called a Hartree-Fock calculation (abbreviated HF) [85, 86], in which the primary approximation is the central field approximation. This means that the Coulombic electron-electron repulsion is taken into account by integrating the repulsion term. This gives the average effect of repulsion, but not the explicit repulsion interaction. This is a variational calculation, meaning that the approximate energies calculated are all equal to or greater than the exact energy. Because of the central field approximation, energies from HF calculations are always greater than the exact energy and tend to a limiting value called the Hartree-Fock limit as the basis set is improved (see Figure 2.2).

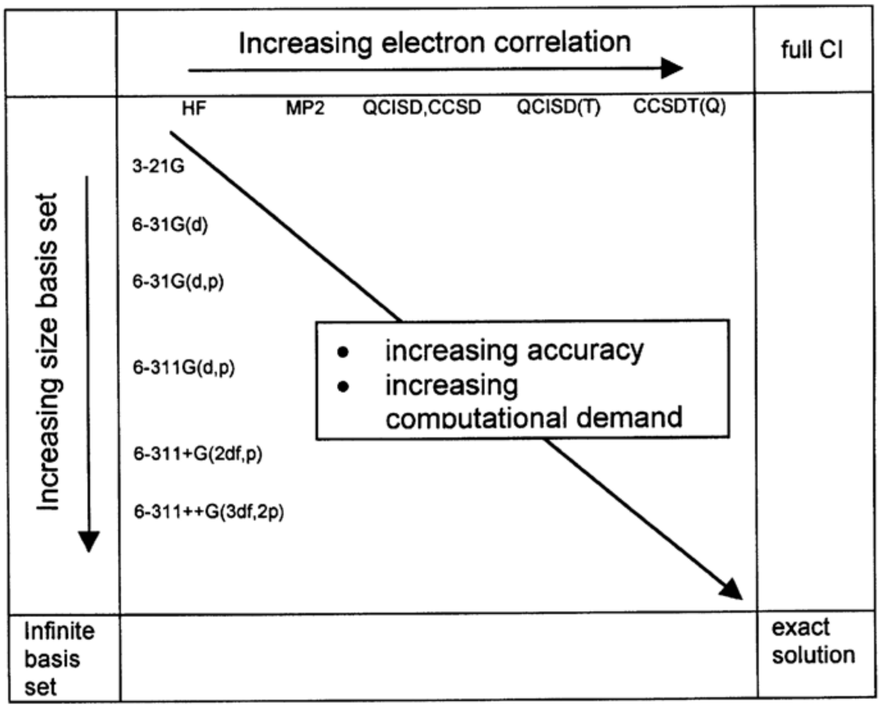

Figure 2.2 Pople diagram showing the dependence of the performance of an *ab initio* method on the basis set and the amount of electron correlation.

Reprinted from "Ab Initio Molecular Orbital Theory" W. J. Hehre, L. Radom, P. v. R. Schleyer, and J. A. Pople, Wiley,New York, 1986.

One of the advantages of this method is that it breaks the many-electron Schrödinger equation [87] into many simpler one-electron equations. Each one-electron equation is solved to yield a single-electron wave function, called an orbital, and energy, called an orbital energy. The orbital describes the behavior of an electron in the net field of all the other electrons.

These orbitals are then combined into a determinant. This is done to satisfy two requirements of quantum mechanics. One is that the electrons must be indistinguishable. By having a linear combination of orbitals in which each electron appears in each orbital, it is only possible to say that an electron was put in a particular orbital but not which electron it is. The second requirement is that the wave function for fermions (an electron is a fermion) must be antisymmetric with respect to interchanging two particles. Thus, if electron 1 and electron 2 are switched, the sign of the total wave function must change and only the sign can change. This is satisfied by a determinant because switching two electrons is equivalent to interchanging two columns of the determinant, which changes its sign.

The steps in a Hartree-Fock calculation start with an initial guess for the orbital coefficients, usually using a semiempirical method. This function is used to calculate energy and a new set of orbital coefficients, which can then be used to obtain a new set, and so on. This procedure continues iteratively until the energies and orbital coefficients remain constant from one iteration to the next. This is called having the calculation converge. There is no guarantee the calculation will converge. In cases where it does not, some technical expertise is required to fix the problem. This iterative procedure is called a self-consistent field procedure (SCF). Some researchers refer to these as SCF calculations to distinguish them from the earlier method created by Hartree, but HF is used more widely.

A variation on the HF procedure is the way that orbitals are constructed to reflect paired or unpaired electrons. If the molecule has a singlet spin, then the same orbital spatial function can be used for both α and β spin electrons in each pair. This is called the restricted Hartree-Fock method (RHF) [88].

There are two techniques for constructing HF wave functions of molecules with unpaired electrons. One technique is to use two completely separate sets of orbitals for α and β electrons. This is called an unrestricted Hartree-Fock wave function (UHF) [89]. This means that paired electrons will not have the same spatial distribution. This introduces an error into the calculation, called spin contamination. Spin contamination might introduce an insignificant error or the error could be large enough to make the results unusable depending on the chemical system involved. UHF calculation is popular because they are easy to implement and run fairly efficiently.

Another way of constructing wave functions for open-shell molecules is the restricted open shell Hartree-Fock method (ROHF) [90]. In this method, the paired electrons share the same spatial orbital; thus, there is no spin contamination. The ROHF technique is more difficult to implement than UHF and may require slightly more CPU time to execute. ROHF is primarily used for cases, in which usage of UHF yields high spin contamination.

The RHF scheme results in forcing electrons to remain paired. This means that the calculation will fail to reflect cases where the electrons should uncouple. For example, a series of RHF calculations for H_2 with successively longer bond lengths will show that H_2 dissociates into H^+ and H^-, rather than two H atoms. This limitation must be considered whenever processes involving pairing and unpairing of electrons are modeled. This is responsible for certain systematic errors in HF results, such as activation energies that are too high, bond lengths slightly too short, vibrational frequencies too high, and dipole moments and atomic charges that are too large. UHF wave functions usually dissociate correctly.

2.3.2 Correlation

One of the limitations of HF calculations is that they do not include electron correlation. This means that HF takes into account the average effect of electron repulsion, but not the explicit electron-electron interaction. Within HF theory the probability of finding an electron at some location around an atom is determined by the distance from the nucleus but not the distance to the other electrons as shown in Figure 2.3. This is not physically true, but it is the consequence of the central field approximation, which defines the HF method.

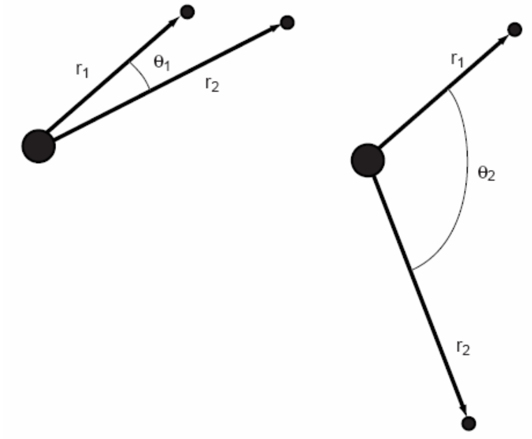

Figure 2.3 Two arrangements of electrons around the nucleus of an atom having the same probability within HF theory, but not in correlated calculations
Reprinted from “Computational Chemistry”D. Young, Wiley-Intercsience, New York, 2001.

A number of types of calculations begin with a HF calculation and then correct for correlation. Some of these methods are Møller-Plesset [91] perturbation theory (MPn, where n is the order of correction), the generalized valence bond (GVB) method, multi-configurational self-consistent field (MCSCF), configuration interaction (CI), and coupled cluster theory (CC) [92-94]. As a group, these methods are referred to as correlated calculations. Correlation is important for many different reasons. Including correlation generally improves the accuracy of computed energies and molecular geometries. For organic molecules, correlation is an extra correction for very-high-accuracy work, but is not generally needed to obtain quantitative results. In general, *ab initio* calculations give very good qualitative results and can yield increasingly accurate quantitative results as the molecules in question become smaller. The advantage of *ab initio* methods is that they eventually converge to the exact solution once all the approximations are made sufficiently small in magnitude. In general, the relative accuracy of results is

$$\text{HF} \ll \text{MP2} < \text{CISD} \approx \text{MP4} \approx \text{CCSD} < \text{CCSD(T)} < \text{CCSDT} < \text{Full CI}$$

However, this convergence is not monotonic. Sometimes, the smallest calculation gives a very accurate result for a given property. There are four sources of error in *ab initio* calculations:

1. The Born-Oppenheimer approximation
2. The use of an incomplete basis set
3. Incomplete correlation
4. The omission of relativistic effects

The disadvantage of *ab initio* methods is that they are expensive. These methods often take enormous amounts of computer CPU time, memory, and disk space. The HF method scales as N^4, where N is the number of basis functions. Correlated calculations often scale much worse than this. In practice, extremely accurate solutions are only obtainable when the molecule contains a dozen electrons or less. However, results with an accuracy rivaling that of many experimental techniques can be obtained for moderate-size organic molecules. The minimally correlated methods, such as MP2 is often used when correlation is important to the description of large molecules.

2.4 Density Functional Theory

The density functional theory (DFT) has emerged during the past decades as a powerful methodology for the simulation of chemical systems [95]. DFT is built around the premise that the energy of an electronic system can be defined in terms of its electron probability density, ρ. For a system comprising *n* electrons, ρ(*r*) represents the total electron density at a particular point in space *r*. According to the DFT formalism, the electronic energy *E* is regarded as a functional of the electron density *E* [ρ]. The advantage of DFT treatment over a more pure approach based on the notion of wavefunction can be best illustrated considering the following: for a system comprising *n* electrons, its wavefunction would have three coordinates for each electron and one more per electron if the spin is included, i.e., a total of 4*n* coordinates, whereas the electron density depends only on three coordinates, independently of the number of electrons that constitute the system. Hence, while the complexity of the wavefunction increases with the number of electrons, the electron density maintains the same number of variables, independently of the system size.

2.4.1 Basic Principles: The Hohenberg-Kohn Theorem

The concept of density functional emerged for the first time in the late 1920s, implicit in the work developed by E. Fermi [96] and L. H. Thomas, [97] which introduced the idea of expressing the energy of a system as a function of total electron density. Even though these theories were able to relate (albeit with several limitations) the energy and other properties of the system with the electron density, a formal proof of this notion came only in the 1960s, when P. Hohenberg and W. Kohn published a theorem [98] demonstrating that the ground-state energy of a nondegenerate electronic system and the correspondent electronic properties are uniquely defined by its electron density. However, although the Hohenberg-Kohn theorem confirms the existence of a functional relating the electron density and the energy of a system, it does not tell us the form of such functional. The search for functionals able to connect these two quantities remains one of the goals of DFT methods.

2.4.2 The Kohn-Sham Formalism

W. Kohn and L. Sham [99] developed a formalism that is the foundation for the current application of DFT in the computational chemistry field. This formalism yields a practical way to solve the Hohenberg-Kohn theorem for a set of interacting electrons, starting from a virtual system of noninteracting electrons having an overall ground-state density equal to the density to some real system of chemical interest where electrons do interact. The main problem behind initial DFT formalisms was the difficulty in representing the kinetic energy of the system. The central premise in the Kohn-Sham approach is that the kinetic energy functional of a system can be split into two parts: one part that can be calculated exactly and that considers electrons as noninteracting particles and a small correction term accounting for electron-electron interaction.

The Kohn-Sham orbitals in each iteration are normally expressed in terms of a set of basis functions. In this sense, solving the Kohn-Sham equations corresponds to determining the coefficients in a linear combination of basis functions, in a similar way to what is done in Hartree-Fock calculations. The choice of the basis set is therefore of great importance also in DFT calculations, but whereas in Hartree-Fock calculations the computational time associated scales as the fourth power of the number of basis functions, in DFT calculations it scales only as the third power (see Table 2.1). The exchange-correlation energy is generally divided into two separate terms, an exchange term and a correlation term, although the legitimacy of such separation has been the subject of some doubt. The exchange term is normally associated with the interactions between electrons of the same spin, whereas the correlation term essentially represents those between electrons of opposite spin.

Table 2.1 Formal scaling behavior, as a function of basis function N, of various electronic structure methods

Scaling behavior	**Method(s)**
N^3	DFT
N^4	HF
N^5	MP2
N^6	MP3, CISD, CCSD, QCISD
N^7	MP4, CCSD(T), QCISD(T)
N^8	MP5, CISDT, CCSDT
N^9	MP6
N^{10}	MP7, CISDTQ, CCSDTQ

These two terms are themselves also functionals of the electron density. The corresponding functionals are known as the exchange functional and the correlation functional, respectively. Both components can be of two distinct types: local functionals, depending only on the electron density ρ, and gradient corrected, which depend on both ρ and its gradient Δρ. Despite the progress in the field, it is important to retain that the main source of inaccuracy in DFT is normally a result of the approximate nature of the exchange-correlation functional.

2.4.3 Hybrid Density Functional Methods

Hybrid density functional generalized gradient approximation (H-GGA) methods combine the exchange-correlation of a conventional GGA method with a percentage of Hartree-Fock exchange. A certain degree of empiricism is used in optimizing the weight factor for each component and the functionals that are mixed. In fact, the exact amount of Hartree-Fock exchange cannot be assigned from first-principles and therefore is fitted semiempirically. One way to do so is to fit these coefficients to experimental atomization energies, ionization potentials, proton affinities, total atomic energies, and other data, for a representative set of small molecules [100]. Hybrid functionals have allowed a significant improvement over GGAs for many molecular properties. For this, they have become a very popular choice in quantum chemistry and are now widely used. However, in solid-state physics this type of functional was much less successful due to difficulties in computing the exact-exchange part within a plane-wave basis set. Examples of hybrid density functionals include B3LYP [101], B3P86 [102], B3PW91 [103], BH&HLYP [104] and mPW3LYP [105].

2.4.4 General Performance of Density Functionals

In Perdew’s vision of Jacob’s ladder [95, 106], the users take the place of the angels, climbing or descending the ladder, according to their needs for precision or computational efficiency. Figure 2.4 represents Jacob’s ladder, as proposed by J. Perdew, with the five rungs representing the hierarchy of density approximations: the local density approximation or local density approximation LDA (first rung), the generalized gradient approximation or GGA (second rung), the meta generalized gradient approximation M-GGA (third rung), the hybrid generalized gradient approximation (or H-GGA) and the hybrid meta generalized gradient approximation (or MH-GGA) (fourth rung), and finally the fully nonlocal description (the fifth rung). Although each rung has particular strengths and weaknesses, as outlined in the literature [95], the global outcome for most properties is a steady improvement in the quality of the results and an increase in the computational cost associated, when moving from the lower to the higher rungs.

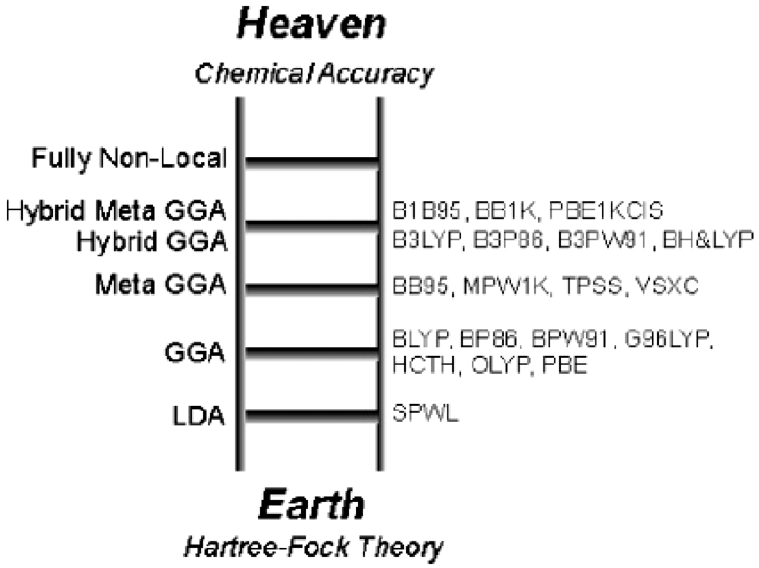

Figure 2.4 Jacob's ladder for the five generation of DFT functionals, according to the vision of J. Perdew [95], with indication of some of the most common DFT functionals with each rung.

Reprinted from J. Phys. Chem. A. 111 (2007) 10439.

2.5 Basis Sets

A basis set [85, 107-110] is a set of functions used to describe the shape of the orbitals in an atom. Molecular orbitals and entire wave functions are created by taking linear combinations of basis functions and angular functions. Most semiempirical methods use a predefined basis set. When *ab initio* or density functional theory calculations are done, a basis set must be specified. Although it is possible to create a basis set from scratch, most calculations are done using existing basis sets. The type of calculation performed and basis set chosen are the two biggest factors in determining the accuracy of results.

Most calculations today are done by choosing existing segmented Gaussian type orbitals (GTO) basis set [111, 112]. These basis sets are identified by one of a number of notation schemes. These abbreviations are often used as the designator for the basis set in the input to *ab initio* computational chemistry programs. Another family of basis sets, commonly referred to as the Pople basis sets, are indicated by such a notation 6-31G [111]. The Pople basis set notation can be modified by adding one or two asterisks, such as 6-31G* (meaning of 6-31G (d)) or 6-31G** (meaning of 6-31G (d, p)). A single asterisk means that a set of d primitives has been added to atoms other than hydrogen. Two asterisks mean that a set of p primitives has been added to hydrogen as well. These are called polarization functions because they give the wave function more flexibility to change shape.

One or two plus signs can also be added, such as 6-31+G* (alternative representation, 6-31+G (d)) or 6-31++G* (alternative representation, 6-31++G (d)). A single plus sign indicates that diffuse functions have been added to atoms other than hydrogen. The second plus sign indicates that diffuse functions are being used for all atoms. These diffuse functions are primitives with small exponents, thus describing the shape of the wave function far from the nucleus. Diffuse functions are used for anions, which have larger electron density distributions. They are also used for describing interactions at long distances, such as van der Waals interactions. The effect of adding diffuse functions is usually to change the relative energies of the various geometries associated with these systems.

2.6 Computational Chemistry in Explosive Field

Computational chemistry (molecular modeling) is focused on obtaining results relevant to chemical problems as well as explosives engineering. Intensive search is on all over the world to develop new high energy materials (HEMs) to meet the futuristic needs. Rapid development of computer technology and theoretical chemistry provide us with a more rigid and accurate approach to explosive phenomena. Of particular importance in designing new explosives, is the ability to predict performance of compounds before the laborious and expensive task of synthesizing them [113-115]. Rigorous mathematical approaches developed at present, allow one to formalize the knowledge of specialists in synthesis [115]. The search of energetic materials is best carried out presently using thermodynamics and molecular engineering approaches, which help in designing efficient materials. In recent past, theoretical calculations to predict detonation behavior of explosives have evinced great interest [116, 117]. Theoretical screening of notional materials allows for identification of promising candidates for additional study and elimination of poor candidates from further consideration, and thus, reducing costs associated with synthesis, and evaluation of the materials [118]. This capability leads to better designs and shorter design cycles. One of the most important parameters used during performance parameters calculation is the density. The widely used versatile codes to calculate detonation properties are TIGER, CHEETAH, LOTUSES and EXPLO 5 [119-122]. In this study, we have proposed some novel candidates for high explosives without using very expensive codes.

2.7 The Computational Chemistry Suites Employed

The calculations in this work have been performed by using Gaussian 98W, Gaussian 03W [123], Spartan 06W [124], Hyperchem 6.03W and Hyperchem 7.51W [125] suite programs. The details of the calculations will be given in the results and discussion part before each separate study. A graphical interface program, which allows integration of various packages have been used for the processes of giving input and assessing output to windows platforms as well as all kind of visualization jobs. Our in-house PCs of the D-250 Laboratory were the primary computer resources in this work.

CHAPTER 3

RESULTS AND DISCUSSION

3.1 Parameters Investigated in This Study Related to Explosives

3.1.1 Geometry and Energy Consideration

In the literature, it is well-known fact that there is sufficiently strong dependence of detonation parameters on the chemical structure (chemical composition as well) of an explosive, including detonation pressure that directly determines brisance. The measure of brisance is the amount of detonation products to perform work near the charge. Zeman [126, 127] mentioned that a separation of charges within the molecule, increasing size of the molecule by addition of whole building blocks, and the presence of intra- and intermolecular hydrogen bonds all increase the physical thermal stability of bulk material (which is the primary condition for fast thermolysis of polynitro compounds in solid state) but decrease the chemical thermal stability. On the other hand, the study on the correlation between impact sensitivity of energetic materials (and other sensitivities) and molecular structures has recently been an ongoing area of research in explosive theory [128-130]. Primary fragmentation in thermal decomposition of organic polynitro compounds were initiated by homolysis of C-NO_2, N-NO_2, and O-NO_2 bonds [131-133]. Gilman proposed that the compression in detonation fronts causes local pseudo metallization in the unreacted material when either the density, or the bending of covalent bonds, reaches a critical level [134]. According to Gilman, in covalently bonded materials, when bonds are stretched and bent, there are regions in the nuclear configuration space where the energies of the highest occupied molecular orbital (HOMO) and that of the lowest unoccupied molecular orbital (LUMO) become degenerate. In periodic solids, the HOMO-LUMO gaps develop into band gaps, hence, a band gap closure and the delocalization of the valence band electrons (metallization) would be achieved as molecules are confined to the intersection regions.The HUMO-LUMO energy band closure due to bond-bending allows the electrons in the bonding states to expand at constant volume, and thus the occurrence of fast reactions [135]. Knowledge of these merges one to consider the optimized geometries, homolytic bond dissociation energies (BDE), frontier orbitals (HOMO, LUMO), total energies, and heat of formation energies even if dipole moments while studying explosives. In the molecular design of energetic materials, all these computed parameters have the prime importance to be considered.

3.1.2 Detonation Parameters and Equations to Calculate Detonation Pressure and Velocity

For an organic chemist, concerning the synthesis of new high explosive molecules, to compute detonation properties (detonation pressure, energy, and velocity and product composition) from a given molecular structure and know (the measured or computed) the crystal density is a matter of vital importance. Quantitative estimation of the properties of compounds, such as heats of formation, density, detonation parameters and sensitivity would permit the selection of the most promising high energy density material (HEDM) candidates for laboratory synthesis and further considerations [136].

Detonation velocity (*D*), and detonation pressure (*P*) are the important parameters to evaluate the explosive performances of energetic materials and can be predicted by the empirical Kamlet-Jacobs [22-27] equations as follows:

$$D = 1.01 \, (N \, M^{1/2} \, Q^{1/2} \,)^{1/2} \, (1+130 \, \rho) \qquad (1)$$

$$P = 1.558 \, \rho^2 N \, M^{1/2} \, Q^{1/2} \qquad (2)$$

where each term in eqs 1 and 2 is defined as follows: D, detonation velocity (km/s); P, detonation pressure (GPa); ρ, density of a compound (g/cm^3); N, moles of gaseous detonation products per gram of explosive; M , average molecular weight of gaseous products; Q, chemical energy of detonation (kJ/g). The parameters N, M, and Q are calculated according to the chemical composition of each explosive as listed in Table 3.1.

Table 3.1 Formulas for calculating the N, M and Q parameters of the $C_aH_bO_cN_d$ explosives.

	Stoichiometric ratio		
parameters	$c \geq 2a+b/2$	$2a+b/2 > c \geq b/2$	$b/2 > c$
N	$(b+2c+2d)/4MW$	$(b+2c+2d)/4MW$	$(b+d)/2MW$
M	$4MW/(b+2c+2d)$	$(56d+88c-8b)$ $/(b+2c+2d)$	$(2b+28d+32c)$ $/(b+d)$
Q	$(28.9b+94.05a+0.239\Delta Hf^{\circ})$ $/MW$	$[28.9b+94.05(c/2-b/4)+$ $0.239\Delta Hf^{\circ}]/MW$	$(57.8c+0.239\Delta Hf^{\circ})$ $/MW$

In the table, $C_aH_bO_cN_d$ denotes the empirical formula of the compound. N is moles of gaseous detonation products per gram of explosive (in mol/g); M is the average molecular weight of the gaseous products (in g/mol); Q is the chemical energy of detonation (in kJ/g); MW in the formula is the molecular weight of the title compounds (in g/mol); ΔH°_{f} is the standard heat of formation of the studied compound (in kJ/mol).

It is clear from the equations (1 and 2) that density has been considered as the primary physical parameter in detonation performance, because detonation velocity and pressure of the explosives increase proportionally with packing density and square of it, respectively. The simplest and earliest method used for the prediction of density is the "group or volume additivity" method, where the molar volume is obtained by summing up the volume of appropriate atoms or functional groups [137]. However, this method has the drawback that it cannot readily account for the molecular conformation, isomerization and crystal packing efficiency. That is, it yields the same density values for different isomers or conformations of the same compound or even for different compounds with the same functional group composition, and ignores the density differences due to crystal polymorphism. So, it is not efficient to predict the density of HEDMs by using the volume additivity method. Keshavarz [138] also develop some simple equations for predicting density of energetic materials, however, these equations work only for some limited elements or functional groups like acyclic and cyclic nitramines, nitrate esters etc. In this study, we utilized a convenient methodology already used in the literature for predicting the crystalline densities of energetic materials not limited only for some classes but valid for nearly all organic explosives and it is based on quantum chemical computations (on the other hand, this method takes so much time, but reliable method). The density of each compound was predicted from the molecular volume divided by molecular weight, while the molecular volume of each molecule was obtained from the statistical average of 100 single-point molar volume calculations for each optimized structure. The molar volume was defined as inside a contour of 0.001 electrons/Bohr^3 density that was evaluated by using a Monte Carlo integration implemented in the Gaussian 98 W program. In the literature, this method has been successfully tested on various molecules and accurately predicts the densities. Using this density and by the help of Kamlet-Jacobs equations, detonation velocities, and detonation pressures of the explosives were accurately determined [139-144].

In order to calculate detonation parameters, heat of formation values in gas phase are needed. According to the K-J equations (see equations 1 and 2) [22-27], the heat of detonation Q has only a small influence on D and P. Q is determined by ΔH_f of the detonation reactant and products, so ΔH_f also has a small influence on D and P. Therefore, it is allowable to estimate ΔH_f approximately using the semiemprical molecular orbital method such as PM3 [83]. On the other hand, it has been reported that PM3 method provide excellent values for simple 23 nitrogen heterocyclic compounds [145]. Also previous studies [146-148] have reported and proved that ΔH_f calculated by the PM3 method could replace the experimental data reasonably well in evaluating the D and P of the energetic compounds due to above mentioned reasons. PM3 is also very fast method so computational cost is so low compared to high level of theories such as DFT and *ab initio* methods.

On the other hand, Walker [149] stated a new detonation theory, based on the concept of physical kinetics,which includes the experimental and calculational observations that nearly all of the covalent bonds of the explosive molecules are broken or rearranged within the detonation shock front (about 20-100Å) by impact, compression and shear forces. The majority of the free atoms and radicals and other highly activated species formed then react in a very short time (10^{-14} to 10^{-12} s) to release chemical energy which maintains the enormous levels of kinetic energy at the detonation front. To rationalize the time interval more clearly, some other duration of seconds are given: electron circulation on the orbit 10^{-16}, excitations molecules by electrons 10^{-16}, excitation molecules by phonons 10^{-18}, lifetime of the higher excited states 10^{-14} and detonation velocity 0.5-1.0 nm per 10^{-13}s (autoignition of semtex 1A (heat convection), plastic bonded explosive made in Czech Republic, is around 0.5 J per 10^{-4}s) [150-152]. Other subsequent “more normal” reactions provide the adiabatic expansion forces and the final products. Since the molecules are essentially broken down to their elements in the shock front, the detonation velocities are determined by the weight-averaged shock velocities of the elements of the empirical formula. According to the Walker [149], thermodynamics, excited atomic and molecular states, the transfer of energy from shock produced phonons to the internal vibrations of the molecules, electronic transitions, and some other often considered factors, although certainly involved at some level, have a relatively minor influence on detonation velocity. On the other hand, this idea is not accepted by the wide community of chemists especially from the point of chemistry.

Presently, homolytic bond dissociation energy calculations of the weakest bond in the proposed energetic molecules were performed for the purpose of assessment of the stability and the sensitivity. Main objective of this study is molecular design of some potential explosive molecules or/and suggest some better candidates of them, beside the study of some properties of already known explosives.

3.2 Studies on Explosives Already in Use

3.2.1 1, 4-Dinitroglycoluril (DINGU) Configurational Isomers: *cis*-DINGU and *trans*-DINGU

This part of the present study has already been published in the Jounal of Hazardous Matreials (2006) [153]. DINGU exhibits to configurational isomers; *cis*- and *trans* forms. The former one is mentioned in the literature but no mention about the *trans*-DINGU.

3.2.1.1 Brief Information about DINGU

cis-1,4-Dinitroglycoluril (*cis*-DINGU) is an important explosive, that has been of interest to the HEMs (high energy materials) community recently. *cis*-DINGU was prepared as early as 1888 by Franchimont and Klobbie [154, 155]. The synthesis of *cis*-DINGU and its derivatives were described in the literature [156–158]. *cis*-DINGU is regarded as one of the potential ingredients for LOVA (low vulnerability ammunition) applications [159]. It has been as an insensitive alternative to RDX (hexahydro-1,3,5-trinitro-*s*-triazine) and TNT (trinitro-toluene) [160]. *cis*-DINGU based PBXs (polymer bonded explosives) possess high explosion energy, good physico-chemical stability and low vulnerability, which is comparable to TATB (triamine-trinitro-bezene)-based PBXs. Toxicological study of *cis*-DINGU was also investigated [161] and according to the classical guidelines, it would be considered only slightly toxic. In the literature, there are many studies on *cis*-DINGU including its synthesis [156–158], structure determination (X-ray diffraction for *cis*-DINGU) [162], evaluation of the solid-state formation enthalpy [163], spectro- thermal decomposition [164], mass-spectral fragmentation pathways [165], modelization by molecular mechanics [166], modelization by using AM1 and PM3 methods [167]. However, to the best of our knowledge, there is no study on *trans*-DINGU (neither about its synthesis any X-ray crystallographic investigation nor computational study for it). In the present work, *ab initio* and the density functional theory (DFT) calculations have been carried out concerning *cis*-DINGU and *trans*-DINGU and the results are compared. The chemical structure of DINGU (for both isomers in two-dimensional drawing space), numbering of atoms and numbering of bond distances (r) are shown in Figure 3.1.

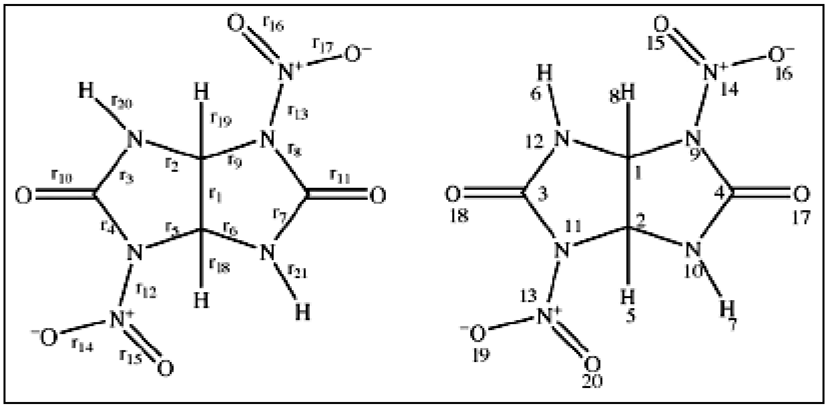

Figure 3.1 Numbering of the atoms and the bonds of DINGU (for both isomers)

3.2.1.2 Computational Details

Geometry optimizations were achieved within the framework of density functional theory (DFT, B3LYP) [101] at the level of 6-31G (d,p) (restricted closed-shell and also unrestricted open-shell). In addition to the DFT calculations, *ab initio* RHF/6-31G (d,p) and UHF/6-31G (d,p) calculations [85, 86] were performed. Furthermore, single point MP2 calculations were carried out (for the *ab initio* RHF and UHF calculations) in order to obtain more accurate energy data. The total electronic energies are corrected for zero point vibration energy

(ZPVE). In order to compare the N–NO_2 bond strengths in the isomers, homolytic bond dissociation energy (BDE) calculations, for the removal of nitrogen dioxide moiety from the structures, were performed (the geometry optimized structures were considered, and in one set of calculations UB3LYP/6-31G(d,p) and in the other set UHF/6-31G(d,p) levels of theories were adopted). The homolytic BDE [168, 169] is defined for the present case as BDE = $E(NO_2) + E(R) - E(R–NO_2)$, where E stands for the respective total electronic energy corrected for the zero-point energy for each parent structure and the fragments of the low-energy NO_2 scission reaction. Furthermore, the basis set superposition error (BSSE) analyses were carried out with the counterpoise method, introduced by Boys and Bernardi [170]. The corresponding BSSE analyses were performed at the same theoretical levels (UB3LYP/6-31G (d,p) and UHF/6-31G (d,p)). The normal mode analysis for each fragment resulted in no imaginary frequencies. This indicates that the structure of each molecule corresponds to at least a local minimum on the potential energy surface. This part is given as an example of our computational approach and other method of calculations for rest of the study are not given in detail, on the other hand, important points of the calculation details are given in the results and discussion sections of them.

3.2.1.3 Results and Discussion

cis-DINGU is a nitramine type organic explosive and its isomer, yet unknown *trans*-DINGU should exhibit explosive properties too. It has been found that polynitro aliphatics containing at least one N–NO_2 (nitramine) linkage are more sensitive than nitro aliphatic explosives containing C–NO_2 linkage. On the other hand, the stabilities and impact/shock sensitivities of energetic materials have frequently been related to the strengths of C–NO_2 and/or N–NO_2 bond strengths [171–173]. In the literature, the structure of *cis*-DINGU was investigated by using X-ray diffraction [162]. In Table 3.2, the presently calculated geometric parameters for *cis*- and *trans*-DINGU molecules as well as the experimental X-ray diffraction data [162] for *cis*-DINGU (bond lengths) are presented. The

B3LYP/6-31G (d, p) bond lengths differ from the crystal averages with rms deviations of 0.022 Å. The rms deviations for the UB3LYP/6-31G (d,p) bond lengths are 0.020 Å. Whereas, RHF/6-31G (d,p) and UHF/6-31G(d,p) type calculations cause, the rms deviations to increase to 0.023 Å. Unrestricted calculations give results qualitatively and quantitatively in agreement with those performed by using the restricted formalism. The differences between the experimentally observed (*cis*-DINGU) and theoretical bond lengths can be attributed to crystal packing effects existing in the experimental data. The geometry optimized structures of the *cis*-DINGU and *trans*-DINGU are shown in Figure 3.2. Note that the configurational isomerism in DINGU arises from the different spatial orientations of the hydrogen atoms at the bridge head positions.

Table 3.2 Calculated bond lengths (in Å) of *cis*-DINGU and *trans*-DINGU at the different theoretical levels and their radicals after cleavage of one of the nitro group from the molecules.

	B3LYP[a]	RHF[a]	X-ray diffraction[b]	UB3LYP[c]	UHF[c]	B3LYP[d]	RHF[d]	UB3LYP[e]	UHF[e]
r_1	1.553	1.539	1.574	1.560	1.544	1.518	1.500	1.528	1.504
r_2	1.431	1.420	1.437	1.445	1.429	1.441	1.427	1.444	1.432
r_3	1.381	1.363	1.354	1.383	1.365	1.403	1.388	1.400	1.385
r_4	1.443	1.419	1.406	1.436	1.416	1.483	1.454	1.482	1.451
r_5	1.470	1.459	1.463	1.468	1.460	1.453	1.441	1.456	1.444
r_6	1.430	1.419	1.435	1.425	1.416	1.441	1.427	1.437	1.426
r_7	1.381	1.364	1.337	1.389	1.368	1.403	1.388	1.415	1.399
r_8	1.443	1.419	1.434	1.429	1.422	1.483	1.454	1.457	1.448
r_9	1.469	1.460	1.469	1.453	1.448	1.453	1.441	1.426	1.428
r_{10}	1.201	1.176	1.205	1.201	1.177	1.196	1.173	1.198	1.173
r_{11}	1.200	1.176	1.199	1.211	1.185	1.196	1.173	1.208	1.181
r_{12}	1.402	1.359	1.387	1.398	1.357	1.426	1.375	1.425	1.375
r_{13}	1.402	1.359	1.361			1.426	1.375		
r_{14}	1.211	1.177	1.220	1.213	1.178	1.229	1.175	1.210	1.176
r_{15}	1.234	1.200	1.219	1.233	1.200	1.210	1.197	1.229	1.197
r_{16}	1.211	1.200	1.229			1.210	1.197		
r_{17}	1.235	1.176	1.205			1.229	1.175		
r_{18}	1.092	1.078	–	1.092	1.078	1.098	1.086	1.099	1.086
r_{19}	1.092	1.078	–	1.098	1.083	1.098	1.086	1.109	1.092
r_{20}	1.011	0.994	–	1.010	0.995	1.014	0.997	1.012	0.998
r_{21}	1.011	0.996	–	1.010	0.994	1.014	0.997	1.013	0.997

[a] cis-DINGU. [b] X-ray diffraction data for cis-DINGU. [c] NO_2 removed *cis*-DINGU radical [d] trans-DINGU. [e] NO_2 removed trans-DINGU radical.

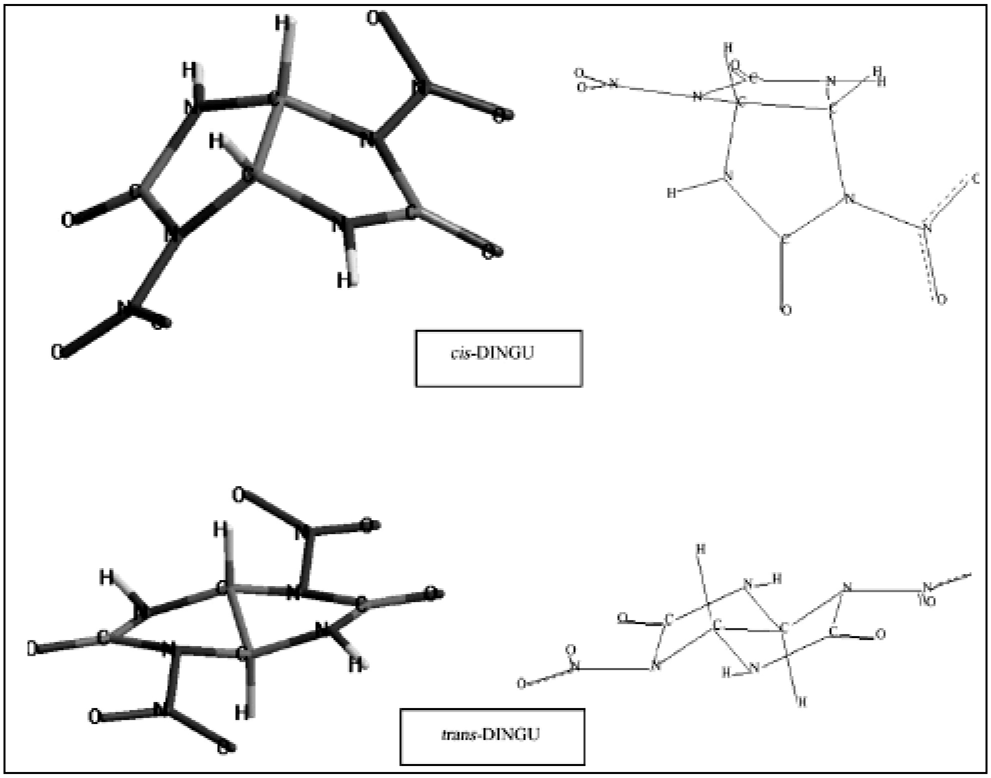

Figure 3.2 The geometry optimized structure of *cis*- and *trans*-DINGU (B3LYP/6 31G (d,p)). The molecules at the left-side are oriented as in Fig. 3.1.

The geometry-optimized structures based on the calculations have C_2 and C_1 type molecular point groups for *cis*-DINGU and *trans*-DINGU, respectively. The presently used calculation methods show a parallelism in reflecting the geometrical differences existing between *cis*- and *trans*-DINGU. Comparing the calculated bond lengths of *cis*-and *trans*-DINGU obtained by using different theoretical methods (shown in Table 3.2), r_1 bond in *cis*-DINGU is found to be somewhat longer than r_1 bond in the *trans*-DINGU about 0.04 Å. Also, r_4 and r_8 bonds (C–N bonds) in *cis*-DINGU are shorter than those bonds in the other isomer about 0.04 Å. A similar character was also exhibited for r_3 and r_6 bonds (C–N bonds of the amido group linked to the NO_2 moiety). It can be seen from Table 3.2 that r_1 (C–C bond) stands for the longest bond length of the both isomers.

As for the N–N bond lengths, the calculated values are 1.402 and 1.426 Å for the *cis*- and *trans*-isomer, respectively. According to the different theoretical levels performed, the nitramine (N–NO_2) bond in the *trans*-isomer is longer than the same bond in the *cis*-isomer about 0.02 Å (see Table 3.2). On the other hand, the geometry optimizations indicate that the *trans*-isomer possesses a puckered structure.

Table 3.3 Calculated total energies for *cis*- and *trans*-DINGU at different calculation levels (Energies in kJ /mol). (Basis set is 6-31G (d,p) for all the calculations).

	RHF^a	**RHF**^{b}	**B3LYP**^{a}	**B3LYP**^{b}
Total Energy	-2440186	-2440051	-2453446	-2453337
Total Energy (with MP2)	-2447136	-2447032		

(**a:** *cis*-DINGU, **b:** *trans*-DINGU)

Table 3.3 shows some of the calculated energies of the compounds (the total electronic energies are corrected for ZPVE). According to the DFT geometry optimization at the level of B3LYP/6-31G (d, p), *cis*-DINGU is more stable than the *trans*-isomer about 109 kJ/mol in terms of the total electronic energy. Furthermore, according to the *ab initio* results the *cis*-isomer is again more stable than the *trans*-one about 135 kJ/mol and after MP2 single point calculation, energy difference between *cis*- and *trans*-isomers was found to be 104 kJ/mol and *cis*-isomer having lower energy. All these results show that the stability order is *cis*-DINGU > *trans*-DINGU. Also the heats of formation in the gas phase for the both isomers were calculated by a semiempirical method, PM3, based on the DFT optimized geometry. *cis*-DINGU has the heat of formation of −26.23 kcal/mol (exothermic), but the respective value for *trans*-DINGU is 6.41 kcal/mol (endothermic). Also, these data confirm that *cis*-DINGU is a more stable molecule than the *trans*-isomer in terms of the heat of formation values. Thermal stability of nitramines is mainly related to the energy required for the initial reaction of decomposition [174]. The common initial step of thermal decomposition of nitramines is the NO_2 fission reaction through breaking of N–NO_2 bond as known in the decomposition of hexahydro- 1,3,5-trinitro-*s*-triazine (RDX) and 1,3,5,7-tetranitro-1,3,5,7- tetraazacyclooctane (HMX) [175]. Khire and co-workers [164] studied spectro-thermal decomposition of *cis*-DINGU and they proposed that the thermal decomposition mechanism of *cis*-DINGU should involve N–NO_2 bond cleavage as the primary step. Keeping these in mind, and the results of presently performed different theoretical methods, which yield longer N–N bonds in *trans*-DINGU as compared to the *cis*-form, one expects the *trans*-isomer should decompose by NO_2 liberation and even should be a more sensitive explosive than the *cis*-isomer (in terms of the bond length data). Furthermore homolytic bond dissociation energy (BDE) of the nitramine group (N–NO_2) for the both isomers was performed at UB3LYP/6-31G (d,p) and UHF/6-31G(d,p) theoretical levels. The BDE (N–NO_2) for *cis*-isomer is slightly higher than the *trans*-one as a result of *ab initio* and DFT (B3LYP) calculations. The BDE (N–NO_2) difference between the *cis*- and *trans*-isomers at *ab initio* and DFT levels were found to be 12 kJ/mol and 5 kJ/mol, respectively. Hence, N–NO_2 bond strength for *cis*-isomer is slightly greater than the corresponding bond strength for the *trans*-isomer at these theoretical levels.

Figure 3.3 shows the charge density maps (as well as the atomic charges) for the species, respectively. The *cis*- and *trans*-isomers generate an electrostatic potential field around them due to the overall effect of positive and negative charge distribution. The darker and lighter regions are negative and positive electrostatic potential fields, respectively. As evident from the figure, the lighter regions (positive field) predominate in both of the isomers. These maps are important because some explosive materials are sensitive to electromagnetic and electrostatic fields they are exposed [176]. The effect is due to interaction of the external field with electron distribution within the molecule thus with the electrostatic potential field, such that in some sensitive explosives this interaction causes the rupture of chemical bonds.

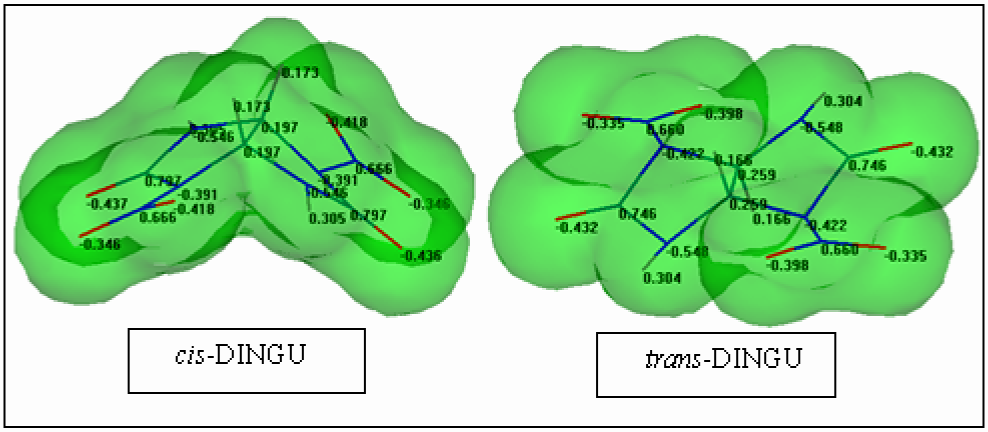

Figure 3.3 3D-charge density maps and charges of atoms of *cis*- and *trans*-DINGU (B3LYP/6-31G (d, p)).

(Colors stand for; grey: carbon, blue: nitrogen, red: oxygen, light grey: hydrogen)

It is clear from Figure 3.3 that why the *cis*-isomer has higher dipole moment than the *trans*-isomer. In the case of the *trans*-isomer, bond dipoles oriented in the molecule so that the net dipole moment is almost zero. Whereas, *cis*-DINGU is a polar compound and has the calculated dipole moment value of 4.089 and 4.828 Debye at employed DFT level (see Table 3.4). The LUMO–HOMO energy differences in the *cis*- and *trans*-isomers were calculated at DFT (B3LYP/6-31G (d,p)) method as 5.886 and 5.896 eV, respectively. The electron pair is localized on the nitrogen atom rather than being shifted to the NO_2 group. Whereas, in the optimized geometry of *trans*-DINGU, the lone pair of the nitramine nitrogen can conjugate better with the nitro group. Thus, the NO_2 groups exert their electron withdrawing effects on the adjacent amino (nitramine) groups more effectively. Thus, the HOMO and LUMO energies of the *trans*-DINGU turns out to be lower than the corresponding energies for the *cis*-isomer for the conducted DFT calculations (see Table 3.4)

Table 3.4 The HOMO and LUMO energies (ε) of *cis*-DINGU and *trans*-DINGU at different calculation levels

	B3LYP[a]	**UB3LYP**[a]	**B3LYP**[b]	**UB3LYP**[b]
HOMO	-8.364	-8.367	-8.488	-8.488
LUMO	-2.481	-2.481	-2.592	-2.592
Δε	5.886	5.886	5.896	5.896
Dipole Moment	4.0894	4.0894	0.000	0.000

a: *cis*-DINGU, **b:** *trans*-DINGU)

Energies in eV. $\Delta\varepsilon = \varepsilon_{LUMO} - \varepsilon_{HOMO}$. Dipole moments in Debye.

Basis set is 6-31G (d,p) for all the calculations.

3.2.1.4 Summary of DINGU Study

The stabilities and impact/shock sensitivities of energetic materials have frequently been related to the strengths of C–NO_2 and/or N–NO_2 and some experimental studies revealed that the thermal decomposition mechanism of *cis*-DINGU should involve N–NO_2 bond cleavage as the primary step. Thus, it is logical to assume that the same mechanism should be operative for *trans*-DINGU, the greater homolytic BDE value of this bond, for the *cis*-isomer than the *trans*-isomer, indicates the possibility of rupture of those bonds in *trans*-DINGU more favorably than *cis*-DINGU. In addition to BDE values, considering the energy data (total electronic energy and heat of formation) *trans*-DINGU should be less stable. Hence, in the light of all these results, *trans*-DINGU so far not mentioned in the literature, may be a more powerful explosive than *cis*-DINGU on the other hand *trans*-DINGU is expected to be more sensitive than the *cis*-isomer.

3.2.2 5-Nitro-2,4-dihydro-3H-1,2,4-triazol-3-one (NTO) and Some of Its Constitutional Isomers

NTO has improved performance over that of trinitrotriaminobenzene (TATB) and is much less sensitive to hazard stimuli then cyclotrimethylene trnitramine (RDX), commonly used benchmarks for insensitive and energetic properties respectively. Some constitutional isomers of NTO are handled as new candidates of insensitive and high energetic materials in this study. This part was published in the Journal of Hazardous Materials (2006) [177].

3.2.2.1 Brief Information about NTO

The synthesis of nitrotriazoles as energetic materials and as intermediates to energetic materials has received a great deal of attention in the past ten years. The most studied nitrotriazole explosives is 5-nitro-2, 4-dihydro-3H-1, 2, 4-triazol-3-one (NTO), because it exhibits good thermal stability [178] and low chemical sensitivity to radiation damage [179] and is relatively insensitive to impact and shock [180]. The numbering scheme and molecular structure of a generic NTO and its tautomers and its isomers were seen in Figure 3.4. NTO was first reported in 1905 [181] incorrectly as its hydroxy tautomer [182]. Its explosive nature was recognized later. A large number of papers related to NTO and its tautomers 1A and 1B have been published [183]. As a result of these properties of NTO, it was first characterized as an insensitive energetic material in 1988 [184]. NTO as an explosive compound was developed at Los Alamos in 1983 as a result of on-going explosives synthesis program [184]. Its explosive performance characteristic is similar to RDX, but it is less sensitive [185].

A useful summary of the structural aspects, chemical and explosives properties and thermal behavior, has been published [186]. Although, there have been many studies about NTO in the literature [187-195], there has been very rare information about the constitutional isomers or tautomers of NTO (**2** and **4,** see Figure 3.4). In the case of compound **2**, there is only one paper published concerning the synthesis of it [196] and **4** was mentioned in the literature as an intermediate as a result of decomposition of NTO [197]. Furthermore, to the best of our knowledge, there has been no information about compounds **3, 5** and **6** which are the constitutional isomers of NTO. In the literature, there is no theoretical study on the constitutional isomers or tautomers of NTO; **2,3,4,5** and **6**. In this study, the position of the NO_2 changes on the ring so derived molecules are mostly nitramine type molecules (see Figure 3.4).

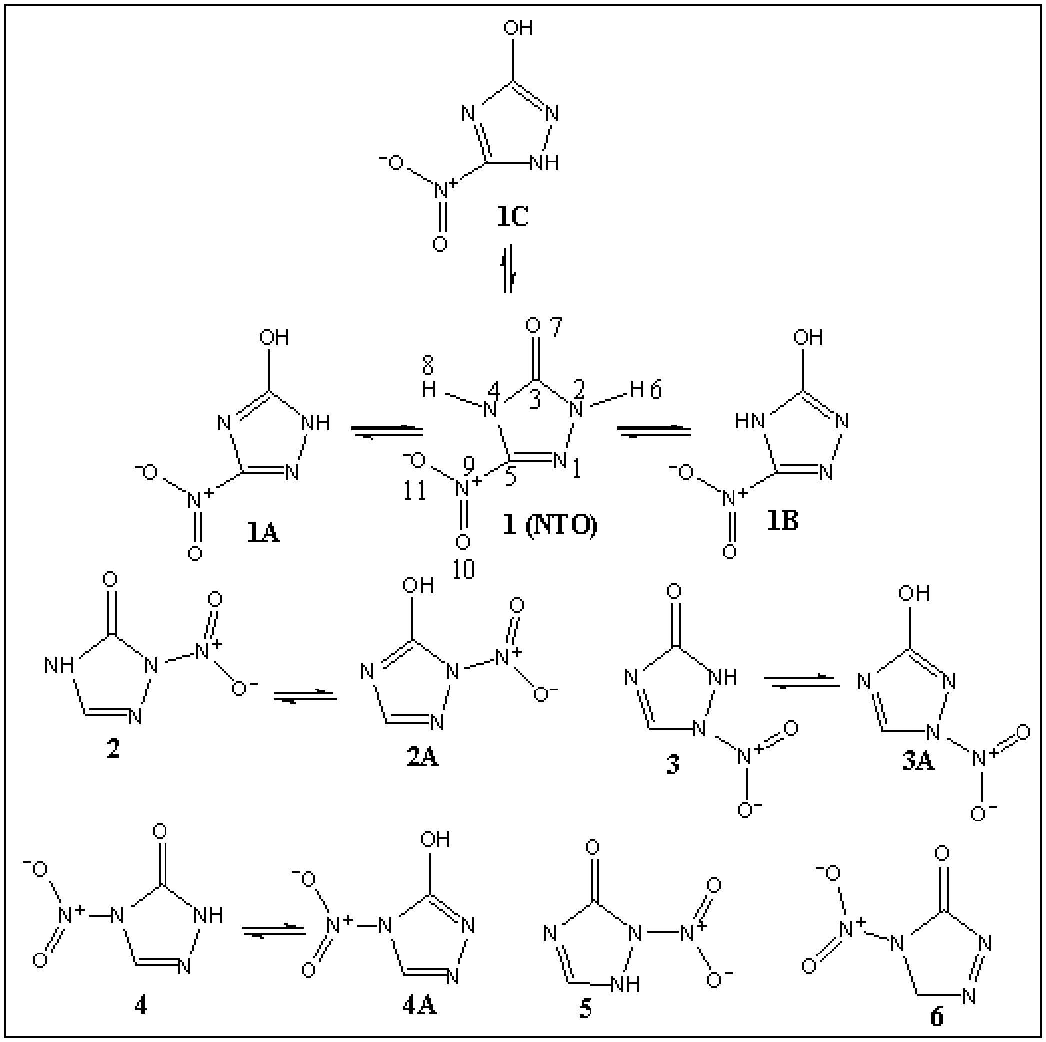

Figure 3.4 Numbering schemes of NTO (1) and its constitutional isomers.

3.2.2.2 Results and Discussion on NTO study

The geometry optimized structures of the considered compounds calculated at the B3LYP/6-31G (d, p) level are presented in Figure 3.5. The bond lengths and angles for the geometry optimized NTO at the different theoretical levels are presented in Table 3.5. The numbering in Table 3.5 is consistent with the numbering scheme employed in Figure 3.4. The corresponding experimental X-ray diffraction values of β-NTO [198, 199] are shown in the table (at both 100K and 273K). The rms deviations in ROB3P86/6-311G (d, p) bond lengths are 0.017 Å (298K) and 0.019Å (100K). For the isolated molecule in the case of B3LYP/6-31G (d,p) results, the rms deviations become 0.019 Å at both 298K and 100K. The corresponding values for the larger basis set B3LYP/6-311++G (d,p) calculation (taken from the literature) are 0.018 Å (298K) and 0.019 Å (100K). Furthermore, the experimental and calculated results indicate that C-O bond length of NTO in the crystal state is longer than that of an isolated molecule in the gas phase because of intermolecular hydrogen bonding. Also there were changes in bond lengths of hydrogen as well as oxygen atoms. Additionally, some ring deformations in the crystalline phase compared to the structure in the gas phase exist (see Table 3.5).

The structures **2**, **3**, **4, 5** and **6** are the nitramine type organic molecules (2,5 and 4,6 are related structures) which are potential candidates as explosives. Note that polynitro aliphatics containing at least one N-NO_2 (nitramine) linkage are generally more sensitive than nitroaliphatic explosives containing C-NO_2 linkage. In the case of compound **1** (NTO), it is an explosive containing one C-NO_2 linkage shown in Figure 3.4. NTO, a planar molecule containing five-membered hetero-cyclic ring with one nitro substituent (see Figure 3.4), is an extra ordinary stable high energy compound.

Figure 3.5 shows the geometry optimized structures (B3LYP/6-31G (d, p) level) of the materials studied. Table 3.6 shows some geometrical features of the NTO and its isomeric structures. Comparing the N1-N2 bond lengths of **1A** and **2A**, one finds that **2A** has the longer bond length. This might be due to electron withdrawing effect of NO_2 group attached to N2 atom in **2A**. Structure **3** has the longest N-NO_2 bond length among the nitramine type isomers. The C5-N9 bond in tautomer **1A** stands for the longest bond length among the NTO and its tautomers. The geometry optimizations indicate that **3** and **5** possess puckered structures. Although, **5** and **6** are similar molecules, unlike to **5**, compound **6** has a planar geometry. Furthermore the N-NO_2 bond length in **5** is longer than the same type of bond in **6**.

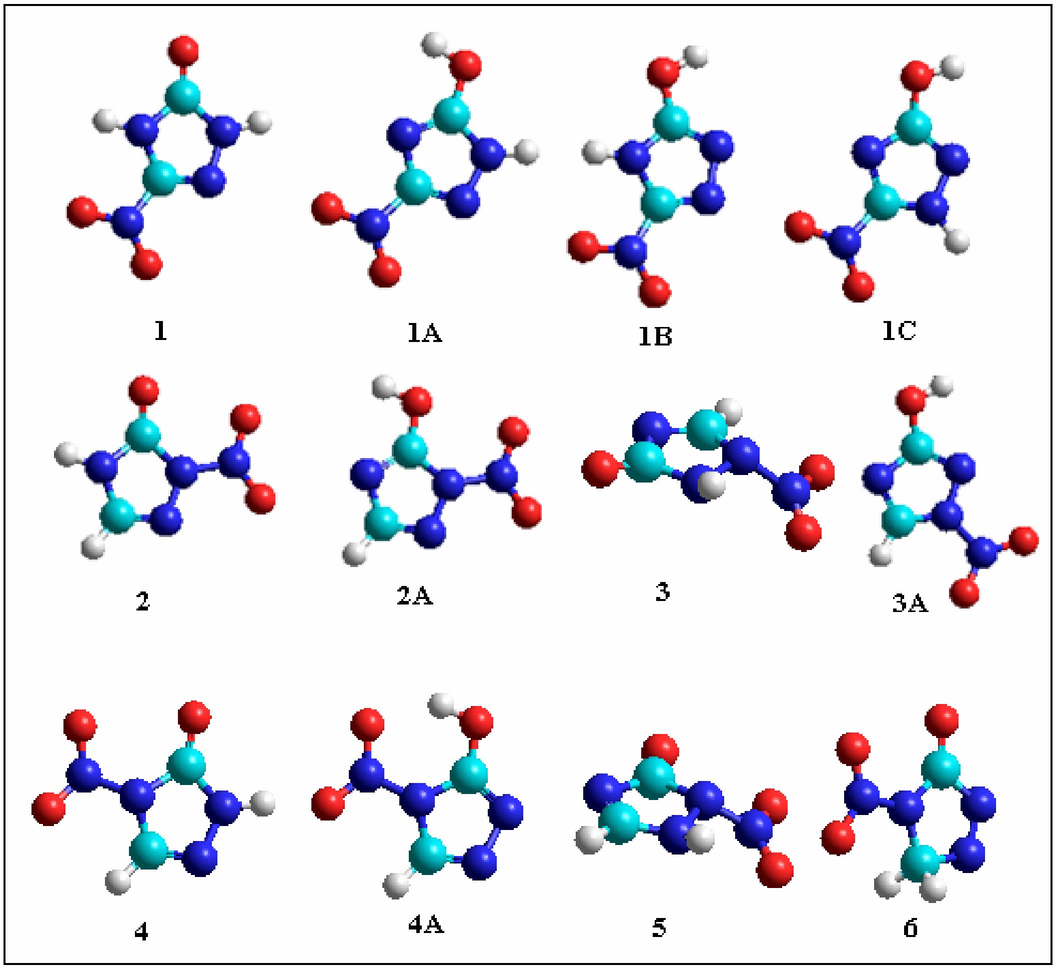

Figure 3.5 Geometry optimized structures of the NTO (1) and its isomers at B3LYP/6-31G (d,p) level of theory.

(Colors stand for; light blue: carbon, blue: nitrogen, red: oxygen, white: hydrogen)

Table 3.5 Calculated and experimental bond lengths (Å) and angles (º) for NTO.

	ROB3P86/ 6-311G(d,p)	B3LYP/ 6-31G(d,p)	B3LYP/ 6-311G(d,p)[a]	Exp[b] (298 K)	Exp[b] (100 K)
N1-N2	1.350	1.360	1.359	1.366	1.370
N2-C3	1.393	1.399	1.398	1.369	1.368
C3-N4	1.398	1.403	1.405	1.373	1.377
N4-C5	1.359	1.366	1.365	1.352	1.352
C5-N1	1.289	1.297	1.290	1.290	1.295
N2-H6	1.007	1.009	1.008		
C3-O7	1.201	1.210	1.203	1.228	1.235
N4-H8	1.008	1.009	1.008		
C5-N9	1.444	1.445	1.451	1.444	1.444
N9-O10	1.209	1.222	1.214	1.226	1.230
N9-O11	1.223	1.236	1.230	1.212	1.222
N1-N2-C3	114.753	114.731	114.570	113.000	112.900
N2-C3-N4	100.503	100.592	100.540	103.500	104.000
C5-N1-N2	103.173	103.046	103.290	102.600	102.300
H6-N2-N1	120.088	120.112	120.090		
O7-C3-N2	129.563	129.417	129.630	127.000	126.900
O7-C3-N4	129.934	129.990	129.840	129.000	129.100
H8-N4-C3	126.199	126.284	126.080		
N9-C5-N4	121.730	121.747	121.740	123.100	123.000
O10-N9-C5	118.208	118.401	118.270	117.200	117.100
O11-N9-C5	114.569	114.668	114.670	117.100	116.700
O10-N9-O11	127.223	126.932	127.050	125.700	126.200

[a] Values are as reported in Ref. [199].
[b] Reported in Ref. [198].

Table 3.6 Comparison of selected bond lengths (Å) for NTO, its tautomers and isomers and their symmetry point groups.

	ROB3P86/6-311G(d,p)			**B3LYP/6-31G(d,p)**			
	N(C)-NO_2	N1-N2	C3-N4	N(or C)-NO_2	N1-N2	C3-N4	sym.
1	1.444	1.350	1.398	1.445	1.360	1.403	Cs
1A	1.462	1.350	1.311	1.462	1.360	1.317	Cs
1B	1.438	1.362	1.350	1.439	1.374	1.355	Cs
1C	1.446	1.343	1.352	1.447	1.353	1.359	Cs
2	1.426	1.377	1.399	1.426	1.377	1.399	Cs
2A	1.399	1.357	1.298	1.440	1.369	1.310	Cs
3	1.458	1.378	1.421	1.468	1.393	1.429	C1
3A	1.428	1.349	1.369	1.426	1.363	1.374	Cs
4	1.409	1.365	1.437	1.414	1.377	1.443	Cs
4A	1.424	1.389	1.382	1.397	1.406	1.410	Cs
5	1.438	1.380	1.389	1.451	1.393	1.398	C1
6	1.399	1.239	1.401	1.404	1.246	1.406	Cs

Table 3.7 shows the total energies calculated at different levels of theory for the compounds. As seen from the table, generally a good agreement of stability order has been found among the calculated total energies of the compounds obtained at different levels. In the limitations of the levels of the theory, the most stable compound in terms of total energy consideration is NTO and the least stable one is isomer **6**. Furthermore, it is obvious that the estimated energy differences between NTO and its tautomers **1A**, **1B**, **1C** and its isomers are sensitive to the theoretical methods employed (see Table 3.7). Smaller energy differences are obtained with the use of correlated methods. The related hydroxy (iminol) tautomers **1A**, **1B** and **1C** are less stable than NTO. On the other hand, these tautomers are evidently stabilized as compared to the other isomers of NTO (nitramine type isomers). This stability may be attributed to the enhanced aromaticity in these structures (also, **2A**, **3A** and **4A** have six π-electrons). Whereas, structures **3**, **5** and **6** do not conform to the aromatic criteria.

Table 3.7 Calculated total energies (in kJ/mol) for NTO (1) its tautomers and isomers at different theoretical levels.

	B3LYP/6-31G(d,p)	ROB3P86/6-311G(d,p)	MP2/6-311G(d,p)[a]
1	-1370275	-1373720	-1367928
1A	-1370240	-1373683	-1367909
1B	-1370218	-1373658	-1367877
1C	-1370251	-1373693	-1367919
2	-1370194	-1373639	-1367871
2A	-1370154	-1373610	-1367817
3	-1370154	-1373596	-1367799
3A	-1370164	-1373608	-1367818
4	-1370193	-1373637	-1367838
4A	-1370127	-1373564	-1367776
5	-1370144	-1373586	-1367786
6	-1370102	-1373533	-1367739

The total energies are corrected for ZPVE. [a] Single point calculation after RHF/6-311G(d,p) geometry optimization: MP2/6-311G(d,p)//RHF/6-311G(d,p).

Also, in the case of structure **4A**, it is destabilized because of the repulsion between the neighboring lone pairs on the ring nitrogens N1 and N2. Neglecting **6** (contains N=N bond which is absent in the others), structures **4A** is found to be the least stable isomer. The stability order in terms of total energy is **1**>**1C**>**1A**>**1B**>**2**>**4**>**2A**>**3A**>**3**>**5**>**4A**>**6** at the ROB3P86/6-311G (d, p) level. According to the MP2/6-311G (d,p) level, the stability order is **1**>**1C**>**1A**>**1B**>**2**>**4**>**3A**>**2A**>**3**>**5**>**4A**>**6** (see Table 3.7).

In the literature, there are many studies on the decomposition of NTO [200, 201], and initial step for several proposed decomposition mechanisms of NTO have been studied theoretically, and all these computations suggest that the C-NO$_2$ bond homolysis is the most probable initial step for unimolecular decomposition of NTO. Furthermore, at high temperatures ca. above 900 ºC, the most important pathway for decomposition of nitro aromatic explosives is by initial cleavage of the C- NO$_2$ bond [202]. Thus, it is logical to assume that the same mechanism should be operative for the nitramine type isomers of NTO.

On the other hand, for designing and evaluating new energetic materials, it is accordingly important to be able to determine computationally the dissociation energies of these bonds. Shao et.al. studied bond dissociation energies for removal of nitrogen dioxide moiety in some nitro aromatic molecules, by using three hybrid density functional theories B3LYP, B3PW91 and B3P86 methods with different basis sets [203]. By comparing the computed energies and experimental results, the B3P86 method was found to give the best agreement with the experimental BDE data, especially with 6-311G (d, p) basis set.

Table 3.8 summarizes the computed homolytic BDE values of N-NO_2 and C-NO_2 for the presently considered species at B3P86/6-311G (d,p) level of theory. For the initial stages in their thermal decompositions, it can be deduced on the basis of the BDE that the relative stability order of these molecules may be in the following sequence **1A**>**1C**>**1B**>**1**>**3A**>**2A**>**2**>**4**>**4A**>**5**>**3**>**6**. Generally speaking, C- NO_2 bond strength is higher than the N-NO_2 bond strength. The positions of nitramine group also have an important effect on the BDE. According to the suggestion of Chung et. al. [204] that a molecule should have more than a 20 kcal/mol (83.68 kJ/mol) barrier to dissociate in order to be considered as a viable candidate for HEDM, thus we can conclude that the molecules in Figure 3.5 (except **3, 5** and **6)** are all viable candidates for HEDMs. As it is already known that NTO is one of the HEDMs, it is worth nothing that bond strength of C- NO_2 in **1A** is much higher than the corresponding bond strength in NTO. This might be explained partially due to the aromaticity of **1A** (contains six π-electrons) compared to NTO (cyclic conjugation via charge separated resonance structures).

Table 3.8 The calculated homolytic bond dissociation energies, in kJ/mol, (BDE) of N-NO_2 and C-NO_2 bonds for the species considered at ROB3P86/6-311G(d,p) theoretical level.

Molecules	BDE
1	276
1A	438
1B	290
1C	389
2	115
2A	136
3	52
3A	174
4	91
4A	89
5	68
6	29

Table 3.9 collects the predicted densities and detonation properties of the NTO and its isomers. The heats of formation (HOF) values were also calculated and listed in the table. When these data in Table 3.9, compared to NTO, which is a well known explosive, gave some clue about the explosive character of the molecules derived from NTO, which are unknown compounds in the literature so far. The positions of nitro group in the five-membered ring skeleton also have an important effect on the explosive properties of energetic materials (see Table 3.9). For example, in the case of compounds **3**, **5** and **6**, only the position of NO_2 differs and all are nitramine type compounds but **5** (a tautomer of **2** and **2A**) has the highest calculated detonation velocity and pressure value among them. The isomers of NTO (preserving the main skeleton of the ring), which are the subject of present study have better detonation performances than NTO or close to it. Therefore, if these stable isomers of NTO, which are nitramine type molecules, can be synthesized, they will have higher or comparable detonation values.

Table 3.9 Computed densities and estimated detonation properties

	ρ (g/cm^3)	HOF^a (kJ/mol)	V^b (cm^3/mol)	D (km/s)	P (Gpa)
1	1.73	35.30	75.21	7.95	27.38
1A	1.79	74.32	72.58	8.27	30.16
1B	1.76	54.47	74.07	8.17	28.74
1C	1.77	72.69	73.69	8.19	29.45
2	1.75	109.3	74.29	8.24	29.52
2A	1.72	163.92	75.57	8.29	29.55
3	1.68	139.58	77.45	8.08	27.76
3A	1.70	161.99	76.64	8.21	31.46
4	1.75	106.69	74.34	8.22	29.47
4A	1.77	159.76	73.45	8.43	31.21
5	1.72	145.19	75.70	8.23	28.86
6	1.71	128.93	76.01	8.15	28.56

[a] Heat of formation values obtained from the PM3 single point calculations over B3LYP/6-31G(d,p) geometry optimized structures. [b] Average volume from 100 single-point volume calculations at the B3LYP/6-311G(d,p) level.

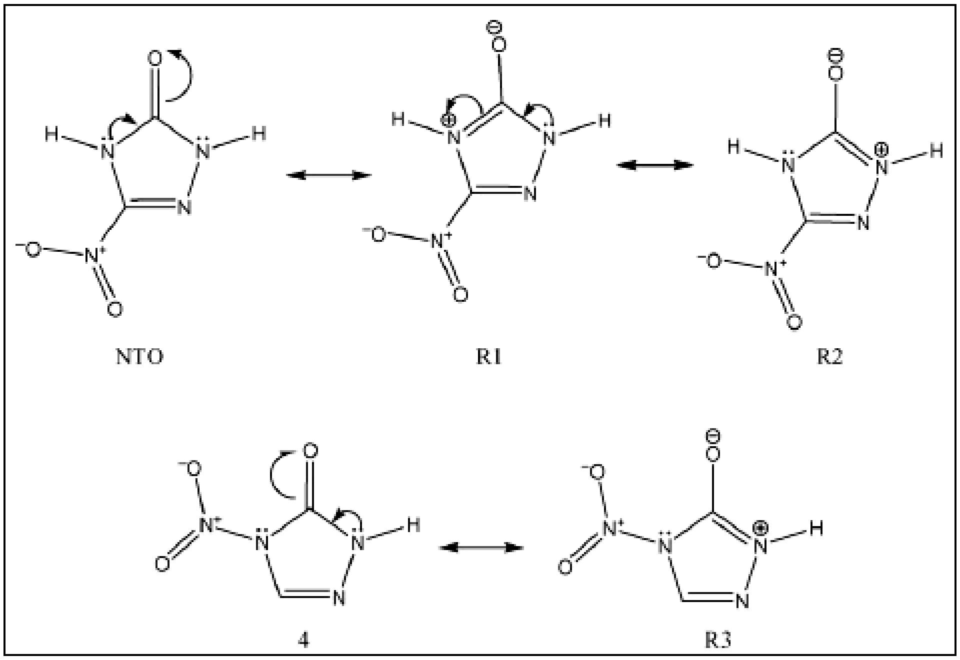

Figure 3.6 Some resonance forms of NTO and its isomeric molecule **4.**

On the basis of valence bond theory, NTO in structure **1** (a monocyclic coplanar system with 7 π-electron over the ring atoms) cannot have the extra stabilization produced by л-electron delocalization. Whereas in the case of tautomeric forms of NTO (**1A**, **1B** and **1C**) π-skeleton contains 6 π-electrons and they all planar systems thus conforming to the criteria of the Hückel's aromaticity. On the other hand, NTO may gain some aromatic character if the charge separated resonance structures **R1, R2**, etc. (Figure 3.6) have some contribution. Note that they are coplanar systems with 6 π-electrons; indeed an analysis based on absolute magnetic shielding [197] confirms that NTO exhibits significant aromatic character. This effect partially accounts for its unusual stability.

Schleyer et. al. [205] examined the aromaticity of a comprehensive set of five -membered ring heterocycles and showed that there was excellent agreement between the magnitudes of the NICS (nucleus independent chemical shift) values and the corresponding aromatic stabilization energies for these type compounds. We have investigated the NICS values for NTO and its isomers and their tautomers to examine their aromaticity. Table 3.10 shows the calculated NICS (ppm) values of them at different levels of theory. Aromaticity order at B3LYP/cc-pVDZ level is **1A>1C>2A>1>3A>1B>4>2>4A>5>3>6**. At the B3LYP/6-31G (d,p) level aromaticity order is **1A>1C>2A>3A>1B>1>4>2>4A>3=5>6**. Also pyrrole and triazole's NICS values were calculated at the same theoretical levels (see Table 3.10) for comparison purpose. The keto forms (more correctly amide forms) of NTO, **2** and **3** are less aromatic than the enol (more correctly iminol) tautomers **1A, 1B, 2A**, and **3A**. Whereas, it is interesting that the keto tautomer of **4** is more aromatic than the enol tautomer **4A**, which suggests the contribution of some aromatic, charge separated resonance structures in to the resonance hybrid of **4**. It is obvious from the NICS values that isomers **3**, **5** and **6** lack of aromatic character. All the NICS values for the presently considered structures should be considered on the relative basis, just to compare relative aromaticities of the isomers and tautomers. Since no experimental values are available for these structures, it is not possible to evaluate the precision of the present NICS data. However, the two calculation methods used for this purpose generally give comparable results for each structure. For comparison purpose NICS data of pyrrole nd triazole are also tabulated in Table 3.10.

Table 3.10 Calculated NICS (ppm) values and dipole moments (Debye) for the considered species .

	NICS[a]	**NICS**[b]	**Dipole moment**[c]
1	-11.4	-11.2	1.558
1A	-13.1	-13.4	6.268
1B	-11.1	-11.3	5.332
1C	-12.5	-12.2	1.454
2	-10.5	-10.3	6.209
2A	-12.0	-12.1	3.272
3	-6.2	-6.2	2.537
3A	-11.3	-11.4	0.882
4	-10.6	-10.6	3.336
4A	-10.0	-10.0	3.065
5	-6.4	-6.2	6.044
6	-0.3	-0.2	3.344
pyrrole	-14.8	-15.9	1.902
triazole	-12.8	-13.1	5.609

[a] Calculated at B3LYP/cc-pVDZ .
[b] Calculated at B3LYP/6-31G(d,p).
[c] For NICS and dipole moment calculations, optimized geometries obtained from B3LYP/6-31G(d,p) theoretical level.

3.2.2.3 Summary of NTO Study

Stabilities of the compounds were investigated in terms of the total electronic energy, BDE values of N-NO_2 and C-NO_2 bonds and NICS values for aromaticity. The detonation properties have been investigated and found that there might be some candidates of HEDMs among the NTO isomers so far not investigated in the literature from this point of view. The initial step for pyrolysis of NTO is the homolysis of the C-NO_2 bonds; based on this information BDEs of isomers have been calculated. In the light of the calculations, it is concluded that C-NO_2 bond is stronger than the nitramine bond. Consequently, if some isomers of NTO presently studied are used as explosive materials they would not be impact insensitive explosives compared to NTO due to their low BDEs of N-NO_2 values.

3.2.3 Nitroglycol (EGDN), Ethylenedinitramine (EDNA) and Their Sulfur Analogs (Thionitrates)

3.2.3.1 General Information about the Molecules Concerned

Nitroglycol's (**1**) properties and performance characteristics are practically the same as those of nitroglycerine. It is 150 times more volatile and about four times more soluble in water, and it is less viscous and gelatinizes nitrocellulose more rapidly than nitroglycerine [206]. Nitroglycol, **1,** is utilized in mixtures with nitroglycerine, because it depresses the freezing temperature of the later compound. On the other hand, like all nitrate esters, nitroglycol, **1,** strongly affects blood circulation; its maximum permitted concentration at the workplace is 1.5mg/m^3 [206]. Ethylenedinitramine **2** possesses considerable brisance, combined with a high chemical stability and relative low mechanical sensitivity [206]. One of the well-known and widely used energetic plasticizers is nitratoethylnitramine (NENA) type structures. NENA (**6**) has an inorganic ester group (nitrate) as well as a nitramine functional group. Presence of these groups and the flexibility of the bonds are responsible for the energetic plasticizer properties of it. Various alkyl-NENAs are known and readily manufactured by nitration of commercially available alkylethanolamines in high yields (80%) [207]. There have been some studies about these mentioned compounds (**1**, **2** and **6**), whereas a few thionitrates were studied to date [208-211]. Additionally, sulphur element in the form of S-NO_2 group is not used before in the energetic materials. On the other hand, Sitzmann et al [212] investigated the effect of the pentafluorosulfonyl group (SF_5) on the properties of explosive nitro compounds. The initial results support that this group can provide explosives with improved properties (increased density, greatly reduced impact, sensitivity and good thermal stability) relative to very similar compounds that contain no SF_5 group. For the first time in the literature, thionates are investigated in terms of the explosive capability by this study.

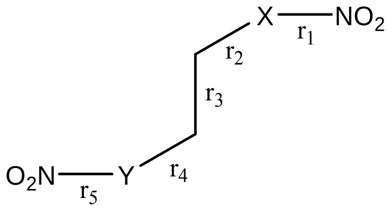

	X	Y
1 (EGDN)	O	O
2 (EDNA)	NH	NH
3	S	S
4	S	NH
5	S	O
6 (NENA)	NH	O

Figure 3.7 Chemical structures and numbering of the bonds and the molecules.

3.2.3.2 Results and Discussions on the Thionates

Figure 3.7 shows the chemical structures of considered species **1**-**6** and numbering of the bonds. Note that these types of explosive materials are more prone to detonation by electrical and magnetic effects. Thus, their response to such kind of effects is very important and vital for their storage and handling. On the other hand, after detonation, free electrons or charged particles are formed and according to the general principle of classical electromagnetic theory, that charged bodies in motion are accompanied by certain electromagnetic waves [44]. Hence, to study the charged forms of explosive materials at the molecular level is very informative for many practical purposes.

The geometry optimized structures of **1**-**6** and their ionic forms at UB3LYP/6-311+G (d, p) level are shown in Figure 3.8. Table 3.11 tabulates the some selected bond lengths of univalent charged and neutral forms of the considered molecules. Firstly neutral species were considered. Comparing the computed bond lengths of C-C (r_3 bonds) in the structures **1-6**, the longest bond value of r_3 belongs to **3** (1.533Å), whereas the shortest one belongs to **1**

(EGDN) which has the value of 1.516Å. This bond elongation can be attributed to sulfur's effect (as a result of size) in **3**, **4** and **5**.

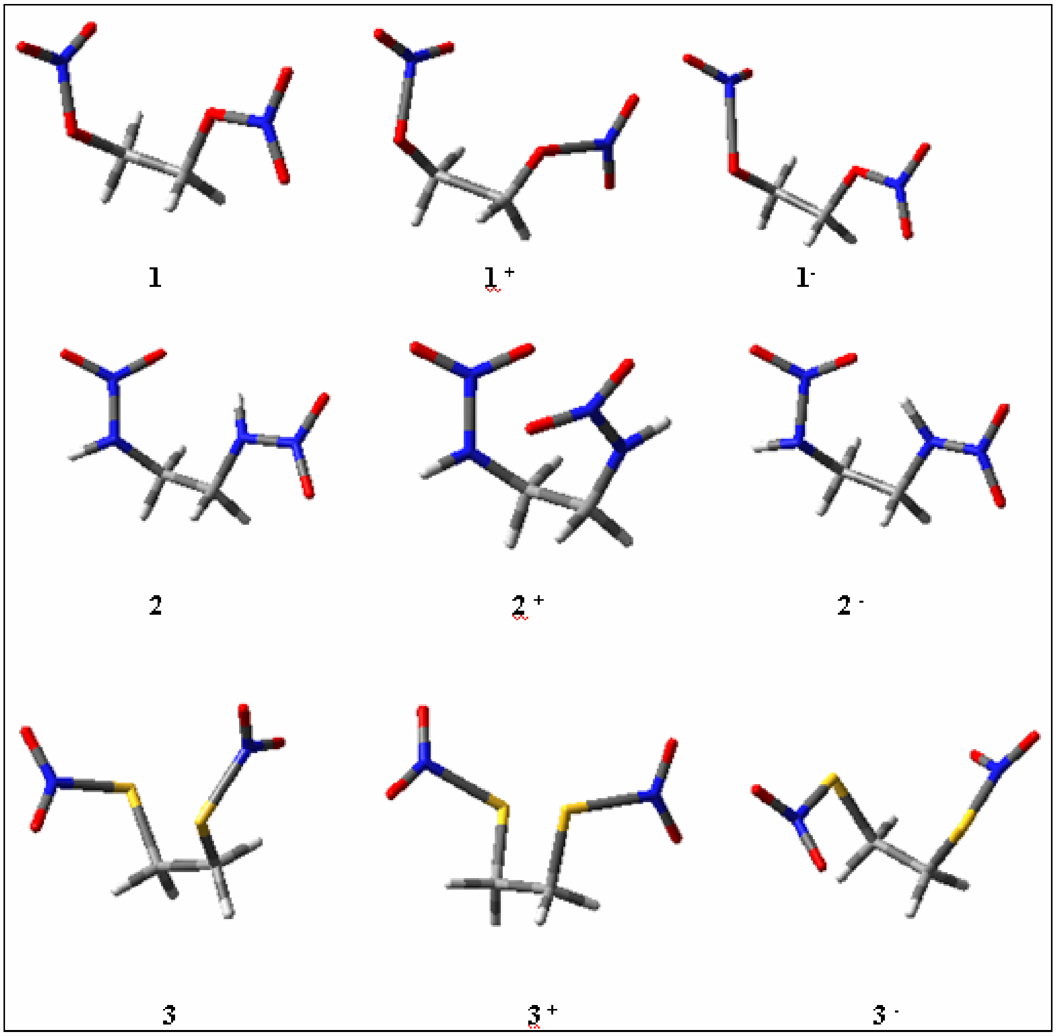

1 $\mathbf{1}^{+}$ $\mathbf{1}^{-}$

2 $\mathbf{2}^{+}$ $\mathbf{2}^{-}$

3 $\mathbf{3}^{+}$ $\mathbf{3}^{-}$

Figure 3.8 Geometry optimized structures of neutral and univalent ions of **1–3** at UB3LYP/6-311+G (d, p) level.

(Colors stand for; grey: carbon, yellow: sulfur, blue: nitrogen, red: oxygen, white: hydrogen)

Big atomic size of sulfur element, compared to oxygen and nitrogen analogs may cause weak orbital overlap with carbon's sp^3 orbital. Hence, this orbital interaction may significantly affect the C-C orbital interaction (weakens the orbital interaction between the carbon atoms). Especially, this effect is more drastic in the case of C-S bond. Comparing the C-S (r_2) and S-NO_2 (r_1) bonds with corresponding C-O (or C-N) and O-NO_2 (N-NO_2) bonds, the bond distances are sharply elongated in the case of sulfur containing molecules (see Table 3.11). C-S (r_1) bond value in **3** is found to be 1.828Å, C-O (r_2) bond value in **1** is found to be 1.438Å.

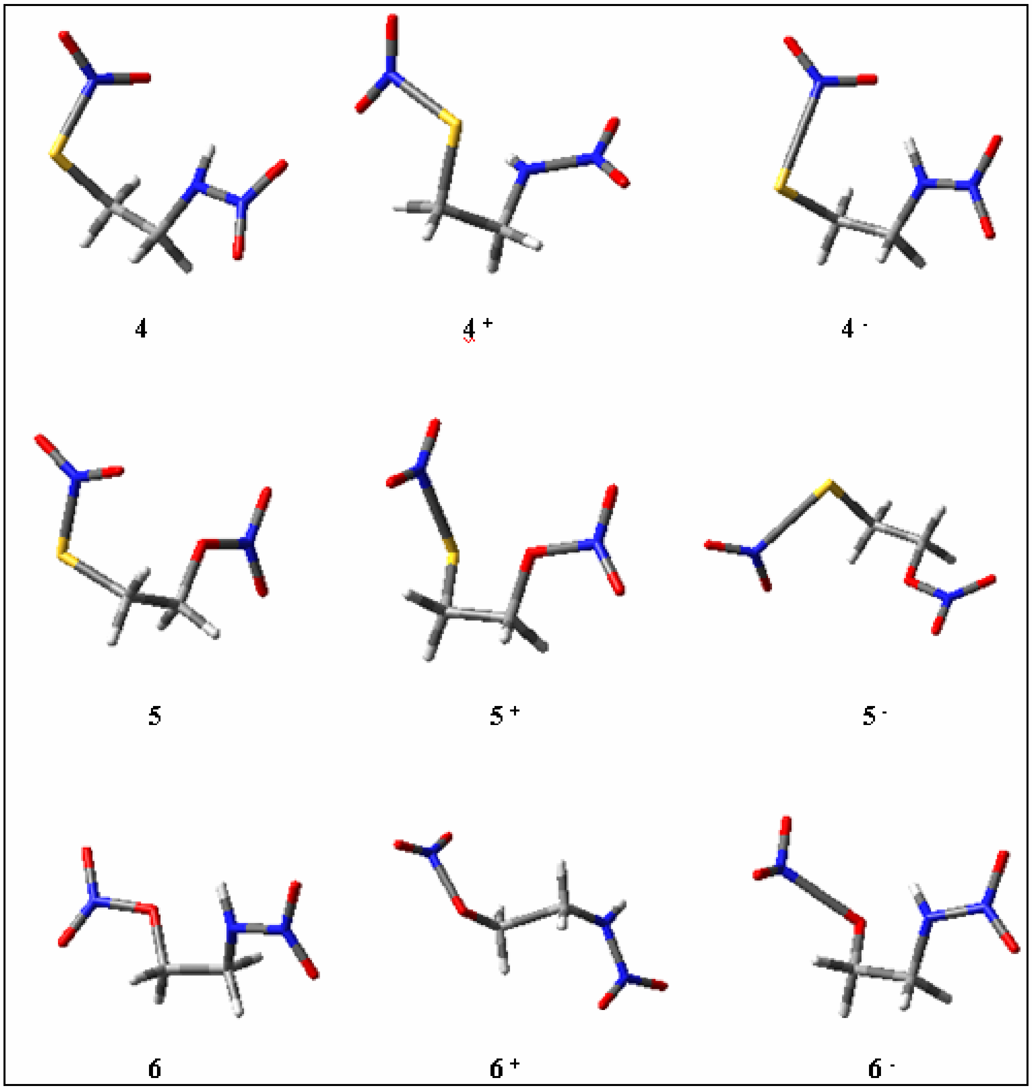

Figure 3.9 Geometry optimized structures of neutral and univalent ions of **3–6** at UB3LYP/6-311+G (d, p) level.

(Colors stand for; grey: carbon, yellow: sulfur, blue: nitrogen, red: oxygen, white: hydrogen)

Furthermore, the same parallelism was observed in the case of S-NO_2 (1.851Å in **3**), N-NO_2 (1.379Å in **1**) and O-NO_2 (1.449Å in **1**) bonds. Considering the charged forms, as the charge develops certain bonds are elongated or contracted as compared to the neutral state. Also, some univalent ionic forms actually stands for a dissociated molecule, in other words they are system of fragments or a hypothetical molecules having very elongated bonds (e.g 2.687Å in **5^-**). Univalent ionic forms lead to the bond rupture especially in the case of S-NO_2, O-NO_2 bonds. Considering molecule **6** (NENA) and its univalent ionic forms, r_5 (O-NO_2) bonds in univalent anionic state elongates to 2.248Å (bond rupture occurs) on the other hand, in the case of univalent cationic state no bond rupture takes place, so NENA, **6,** is much more sensitive to negative charges than the positive charging. On the other hand, bond rupture takes place after both the negative and positive charge developments in the cases of **4** and **5**. Interestingly, **1** (EGDN) positive charge development causes C-C (r_3) bond cleavage (1.873Å), whereas the univalent anion formation goes parallel with the elongation of mainly O-NO_2 (r_1) bond and rupture of this bond occurs (2.231Å) eventually. The calculations within the limitations of the used DFT method have revealed that these explosive materials are more prone to such kinds of electrical effects due to the presence of sensitive nitrated ester groups.

Table 3.11 Some selected structural parameters of neutral and univalent charged forms (-1, +1) of **1-6** are obtained at UB3LYP/6-311+G (d, p) level of theory (r in Å).

	r_1	**r_2**	**r_3**	**r_4**	**r_5**
1	1.449	1.438	1.516	1.442	1.430
1^{+}	1.746	1.304	1.873	1.306	1.757
1^{-}	2.231	1.355	1.536	1.465	1.382
2	1.379	1.463	1.528	1.455	1.369
2^{+}	1.444	1.387	1.688	1.387	1.445
2^{-}	1.341	1.453	1.530	1.467	1.501
3	1.851	1.822	1.533	1.822	1.851
3^{+}	2.038	1.832	1.531	1.832	2.038
3 -	2.191	1.815	1.531	1.815	2.191
4	1.837	1.825	1.526	1.457	1.381
4^{+}	2.084	1.831	1.532	1.479	1.488
4^{-}	2.678	1.829	1.529	1.454	1.337
5	1.853	1.823	1.521	1.442	1.428
5^{+}	2.169	1.809	1.537	1.442	1.536
5^{-}	2.687	1.822	1.519	1.463	1.384
6	1.388	1.457	1.527	1.447	1.434
6^{+}	1.468	1.361	1.818	1.312	1.756
6^{-}	1.346	1.461	1.555	1.368	2.248

Table 3.12 summarizes the computed homolytic BDE values of five bonds namely, N-NO_2, C-NO_2, S-NO_2, C-C, C-O, C-N, C-S bonds for the presently considered species (**1-6**) at UB3LYP/6-311+G (d, p) level of theory. For the initial stages in their thermal decompositions, it can be deduced (on the basis of the weakest BDE value) that the relative stability order of these isomers may be in the following sequence: **2**>**4**>**3**>**1**>**5**>**6** (see Table 3.12). As a result of the calculations, generally S-NO_2 bond strength is found to be weaker than the N-NO_2 bond strength, and S-NO_2 homolytic BDE values are comparable to O-NO_2 homolytic BDE values. In the case of C-C (r_3) bond values for the considered molecules, the biggest value belongs to **1** (301.4 kJ/mol) and the smallest value belongs to **3** (196.7 kJ/mol). This result is supported by the bond length values. Sulfur atom weakens the C-C bond strength.

Table 3.12 Calculated homolytic bond dissociation energies (in kJ/mol) of structures **1-6** at UB3LYP/6-311+G (d, p) level of theory. r_i stands for bonds shown in Figyre 3.7.

	r_1	**r_2**	**r_3**	**r_4**	**r_5**
1 (EGDN)	121.7	285.3	301.4		
2 (EDNA)	170.6	326.4	260.8		
3	121.9	249.2	196.7		
4	128.1	262.7	228.6	319.3	171.1
5	119.3	257.3	249.6	277.7	119.5
6 (NENA)	162.9	324.6	277.6	286.5	114.7

The products of detonation are postulated based on the assumptions that all N atoms change to nitrogen gas, O atoms change to water, S atoms change to sulfur dioxide if oxygen atoms are surplus, and C atoms change to carbon monoxide and/or carbon dioxide (if O atoms are surplus) [213]. In order to find the heat of detonation, detonation reactions are written as follows:

$C_2H_4N_2O_6 \rightarrow 2\ H_2O + 2\ CO_2 + N_2$ (for **1**)

$C_2H_6N_4O_4 \rightarrow 3\ H_2O + CO + C + 2\ N_2$ (for **2**)

$C_2H_4N_2O_4S_2 \rightarrow 2\ H_2O + SO_2 + N_2 + CS + C$ (for **3**)

$C_2H_5N_3O_4S \rightarrow 2.5\ H_2O + 0.75\ SO_2 + 1.5\ N_2 + 0.25\ CS + 1.75\ C$ (for **4**)

$C_2H_4N_2O_5S \rightarrow 2\ H_2O + SO_2 + CO + C + N_2$ (for **5**)

$C_2H_5N_3O_5 \rightarrow 2.5\ H_2O + 0.5\ CO_2 + 1.5\ CO + 1.5\ N_2$ (for **6**)

On the other hand, the oxygen balance (Ω) of these molecules is calculated according to the equation given in the literature [214]. The oxygen balance is of great importance for the reaction rate and the heat of the reaction. By varying the oxygen balance, it is possible to significantly influence both factors [215].

Table 3.13 tabulates the results of computations about the detonation parameters of the considered molecules **1-6**. Also, available experimental values [206] are seen in the table. In the case of **1** (EGDN), the calculated density and the experimental density is not so close to each other thus this fact has been reflected to the calculated detonation parameters of it. However, the values belong to the experimental data are according to the charging density so different charging density means different results of detonation pressure and velocity. On the other hand, calculated detonation parameters are generally for the maximum performance values. In the case of **2** (EDNA), the available experimental detonation velocity (7.57 km/s) of it and calculated detonation velocity (7.70 km/s) of EDNA are close to each other. According to the calculated detonation parameters (D, P), the power (or the high performance to low performance) of the explosive order is: **1**>**2**>**6**>**4**>**5**>**3**. Besides to problems of thionitrates that is insufficient stability for storage, thionitrates are not superior to the EDNA (**2**), EGDN (**1**) and **6** (NENA) in terms of the calculated detonation performances by using the well-known equations of Kamlet-Jacobs [22-27].

Table 3.13 Calculated properties of the concerned species. The values in paranthesis are experimental [206].

	Ω (%)	Mwt (g/mol))	ρ (g/cm^3)	Q (cal/g)	D (km/s)	P (kbar)
1	0.00	152.062	1.779 (1.480)	1449	8.78 (7.30)	340
2	-31.98	150.094	1.605 (1.650)	1304	7.70 (7.57)	245
3	-52.12	184.196	1.685	363	5.61	134
4	-43.08	167.145	1.687	944	7.18	220
5	-28.55	168.129	1.674	910	7.17	218
6	-15.89	151.078	1.667	1215	8.43	300

Table 3.14 lists energies (eV) of frontier orbitals (HOMO: highest occupied molecular orbital and LUMO: lowest unoccupied molecular orbital), their gaps ($\Delta\varepsilon = \varepsilon_{LUMO} - \varepsilon_{HOMO}$) and also dipole moments (Debye) at the UB3LYP/6-311+G(d,p) level of theory. The frontier molecular orbitals, the HOMO and LUMO are important in ionization processes [216]. The sensitivity of energetic materials to charge development is mainly dictated by the frontier orbital energies. In terms of the energy difference between HOMO and LUMO energy levels ($\Delta\varepsilon = \varepsilon_{LUMO} - \varepsilon_{HOMO}$), the order is: **1**>**6**>**2**>**5**>**3**>**4.** The stability here refers to the chemical or photochemical processes with electron transfer or electron leap. It is well known that hard molecules have a large HOMO-LUMO gap, and soft molecules have a small HOMO-LUMO gap. Accordingly, soft molecules will be

less stable than similar hard molecules. As a result of employed DFT method, molecule **1** (EGDN) is a hard molecule, whereas **4** is the soft molecule among these series of the compounds. Table 3.14 also tabulates the polarity or the dipole moments of the concerned molecules (**1**-**6**). According to the employed DFT method here, the polarity order is: **2**>**4**>**3**>**5**>**1**>**6**, however, these molecules are not rigid molecules so due to free rotations around the C-C (r_3) bond there are many conformers and their dipole moments should be different thus, here computed dipole moments are based on the orientations of the molecules seen in Figures 3.8 and 3.9.

Table 3.14 Calculated frontier orbital (HOMO-LUMO) energies (in eV) and dipole moments (DM in Debye) at UB3LYP/6-311+G (d, p) level of theory.

	1	**2**	**3**	**4**	**5**	**6**
HOMO	-9.306	-8.300	-8.082	-8.327	-8.082	-8.656
LUMO	-2.585	-2.531	-2.694	-2.966	-2.612	-2.831
$\Delta\varepsilon$	6.721	5.769	5.388	5.361	5.470	5.825
DM	4.475	6.833	5.429	5.711	5.150	2.830

$\Delta\varepsilon = \varepsilon_{LUMO} - \varepsilon_{HOMO}$

3.2.3.3 Summary of the Thionates (SNO_2) Part

Presently some of the N-NO_2 (nitramines), O-NO_2 (nitrate esters), S-NO_2 (thionitrates) containing molecules have been investigated in terms of the electronic structures, homolytic bond dissociation energies and possible detonation properties by using UB3LYP/6-311+G (d, p) level and well-known Kamlet-Jacobs equations. Some of the molecules (**3**, **4** and **5**) considered in this study were not studied either experimentally or computationally in the literature so far. These new molecules have been compared with their known nitrogen and oxygen analogs in terms of the detonation properties and thermal stabilities. It is found that compared to the known similar structures (**1** (EGDN), **2** (EDNA) **6** (NENA)), sulfur containing (thionitrates) (**3**, **4** and **5**) molecules can not be very good energetic materials in terms of the detonation velocity, detonation pressure and detonation heat. According to the calculated BDE values, thionitares (S-NO_2) are found to have similar strengths compared to nitrate esters (O-NO_2). An example consider molecule **5** which contains both thionitrate and nitrate ester groups, BDE values of S-NO_2 and O-NO_2 are calculated as 119.3 kJ/mol and 119.5 kJ/mol, respectively. However, the situation is markedly different in the case of C-C bond (r_3) strengths, this bond in thionitrate containing molecule **3** is very weak compared to the same bonds in other structures.

3.2.4 1,3,3-trinitroazetidine (TNAZ) and Some of Its Constitutional Isomers

3.2.4.1 Brief Information about TNAZ

TNAZ (1,3,3-trinitroazetidine), a relatively new explosive material that is of considerable interest to the energetic materials community, was first prepared by Archibald and co-workers in 1990 [217]. Recently, several research groups have been trying to develop improved methods for synthesis of TNAZ (**1**), as well as its more detailed characterization [218, 219] for several reasons: (i) it has density and detonation characteristics nearly that of standard high explosive HMX [220], (ii) it has melting transition without decomposition at about 100ºC making its melt casting possible [219-221], (iii) it has oxygen balance greater than that of HMX, which results in high detonation products heat and temperature [218-220]. These characteristics, together with its acceptable thermal stability and sensitivity, make TNAZ to be considered as a replacement for the most powerful high explosive HMX [220-224]. Chemically, TNAZ is of interest for many reasons, it contains a four-member ring (see Figure 3.10) with 37 kcal/mol strain energy [225]. Due in part to this strain energy, it is a more energetic than the many powerful explosives currently in use [226]. There is also interest in the chemistry of cyclic nitramines containing gem- dinitro groups; TNAZ having two NO_2 groups of that sort is the simplest molecule in this class [227].

In the literature, there exist many studies about TNAZ (**1**); molecular spectroscopic studies [227-229], synthesis [217, 230], decomposition mechanisms [231-233], thermochemistry [234] detonation parameters and strain energy calculations [235-237]. Although, there have been many studies about TNAZ, to the best of our knowledge, there has been no information about its constitutional isomers (see Figure 3.10). These structures derived from TNAZ have the same main skeleton of the ring, the position of the nitro group changes on the ring for different isomers of it. On the basis of the findings in the literature, it has concluded that TNAZ has the energy density 4% less than HMX, but 60% greater than the energy density of TNT [220]. Hence, constitutional isomers of TNAZ which were not studied isomers in the literature so far have been considered presently in terms of their explosive capability.

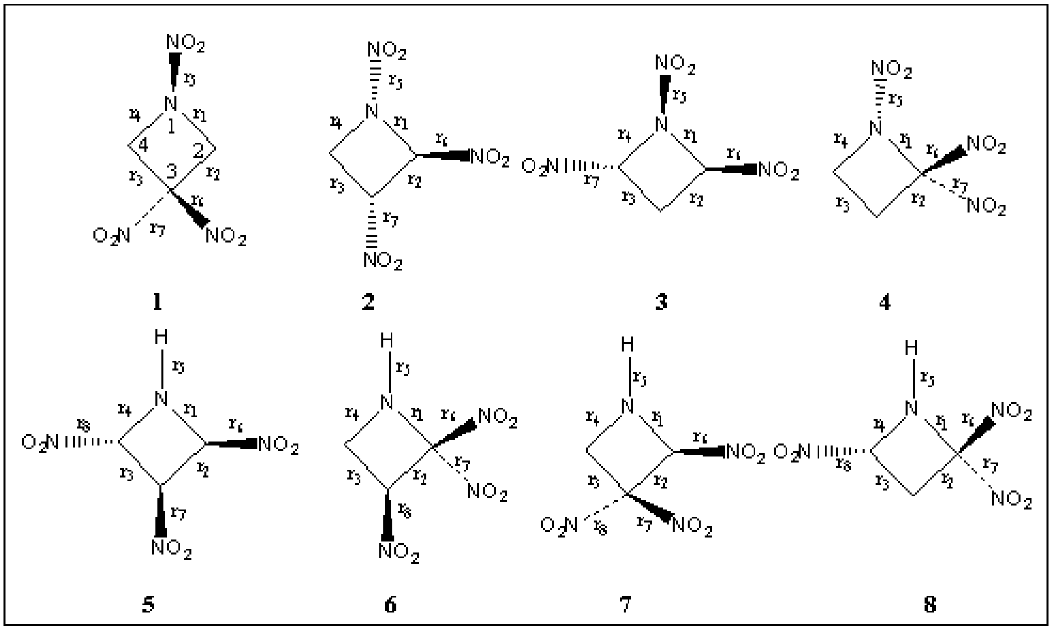

Figure 3.10 The numbering scheme and molecular structures of TNAZ (**1**) and its constitutional isomers.

3.2.4.2 Results and Discussions on the TNAZ and Its Constitutional Isomers

Figure 3.10 shows the chemical structures of TNAZ (**1**) and its constitutional isomers (**2–8**) and the numbering system used presently. The geometry optimized structures of the molecules calculated at the UB3LYP/6-311+G (d, p) level are presented in Figure 3.11. The bond lengths for the geometry optimized structures at the same theoretical level are presented in Table 3.15. The numbering in Table 3.15 is consistent with the numbering scheme employed in Figure 3.10. The position of the nitro groups affected the bond lengths (r_1, r_2, r_3 and r_4) in four membered rings (see in the Table 3.15). Comparing the nitramine bond lengths among the isomers, it is obtained that the longest bond length (1.492Å) belongs to the TNAZ, whereas the smallest one (1.404Å) is possessed by isomer **3**. Comparing the calculated bond lengths of C-NO_2 among the isomers considered r_6 having the value of 1.566Å in **6** stands for the longest bond length. The nitramine bond N-NO_2 was found to be smaller than the C-NO_2 bond in the case of TNAZ, **2**, **3** and **4**. The shortened N-N bond lengths and planar amino group geometry (usually seen together in nitramines) have been explained by invoking conjugation of a "p"-type lone pair on the amino nitrogen with the π-electron system of the nitro group [238]. On the other hand, the rings were found to be significantly puckered. According to the Archibald and coworkers [217], the pronounced nonplanarity of the nitramine indicates that the shortened N-N bond distance in **1 (TNAZ)** is probably not the result of increased double bond character, the explanation may lie rather in an analysis of the inductive effects produced by the strongly electron withdrawing geminal dinitro grouping across the ring.

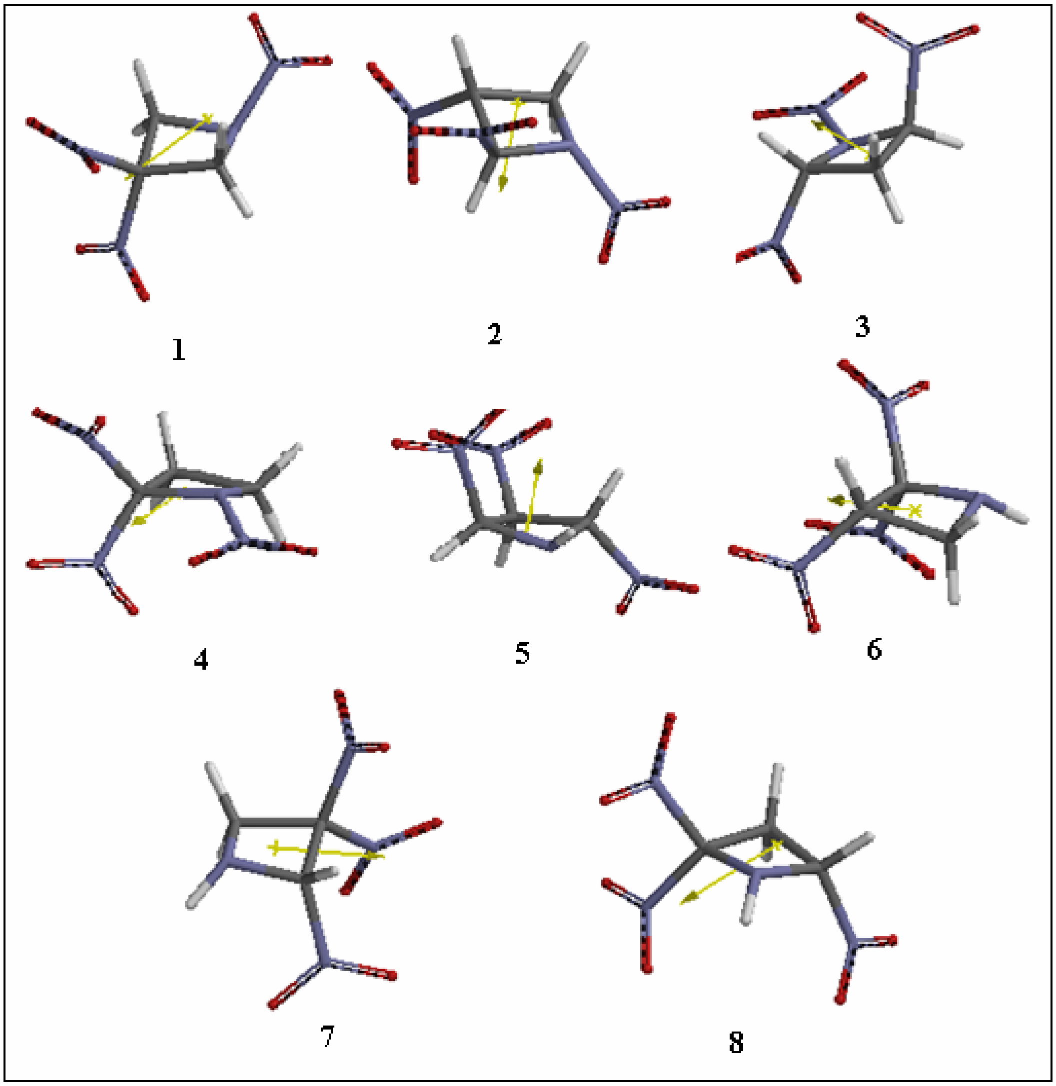

Figure 3.11 The geometry optimized (UB3LYP/6-311+G (d, p)) structures of **1-8** and direction of the dipole moments.

(Colors stand for; grey: carbon, blue: nitrogen, red: oxygen, white: hydrogen)

Table 3.15 Some calculated bond lengths (Å) of TNAZ and its constitutional isomers at UB3LYP/6-311+G (d,p) level of theory.

	1 (TNAZ)	**2**	**3**	**4**	**5**	**6**	**7**	**8**
$\mathbf{r_1}$	1.503	1.441	1.437	1.422	1.442	1.403	1.434	1.411
$\mathbf{r_2}$	1.525	1.543	1.558	1.543	1.554	1.545	1.549	1.537
$\mathbf{r_3}$	1.525	1.556	1.556	1.557	1.528	1.551	1.540	1.548
$\mathbf{r_4}$	1.503	1.481	1.435	1.481	1.453	1.485	1.487	1.445
$\mathbf{r_5}$	1.492	1.407	1.404	1.409	1.013	1.014	1.015	1.014
$\mathbf{r_6}$	1.526	1.529	1.542	1.564	1.550	1.566	1.557	1.552
$\mathbf{r_7}$	1.539	1.509	1.530	1.536	1.503	1.555	1.531	1.551
$\mathbf{r_8}$					1.530	1.509	1.529	1.536

Table 3.16 shows the calculated total energies in atomic units and relative energies in kJ/mol at UB3LYP/6-311+G (d,p) level of theory. In the limitations of the levels of the theory used, the most stable compound in terms of total energy consideration is isomer **8** and the least stable one is TNAZ **1**. The stability order in terms of total energy is: 8>5>6>3>2>7>4>1 at the UB3LYP/6-311+G(d,p) level. As seen from the calculations nitramine type explosives were found to be less stable than the aliphatic (C-NO_2) analogs.

Table 3.16 Calculated energies of **1**-**8** at UB3LYP/6-311+G (d,p) level of theory..

	UB3LYP/6-311+G(d,p)	
	Total E. (a.u)	Rel. E. (kJ/mol)
1	-786.8248289	116
2	-786.8516521	45
3	-786.8554770	35
4	-786.8415069	72
5	-786.8661485	7
6	-786.8566312	32
7	-786.8502188	49
8	-786.8689301	0

Early studies on decomposition of TNAZ (**1**) were reported by Brill and co-workers [225, 228, 239]. Using thermolysis of rapidly heated solid TNAZ to obtain information about the initial decomposition, they found that NO_2 was the initial and most abundant decomposition product when TNAZ was heated at a rate of 145 K/s at 15 psi of N_2 to a final temperature of 905 K. Other species produced included NO (second most abundant), HCN, H_2CO, CO, CO_2, and HONO [225]. The implication is that one or both of the reactions shown initiates the decomposition:

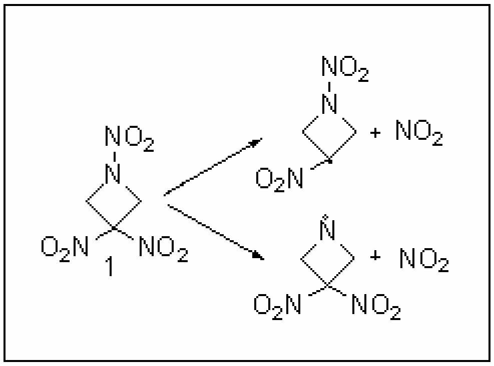

Figure 3.12 TNAZ decomposition.

Thermal decomposition studies of TNAZ in a solid form and in solution by Oxley et al. [240] show that the decomposition is first order with activation energy of 46.6 kcal/mol for the solid state TNAZ. Decomposition products of the reaction detected at different temperatures in the gas phase include N_2, NO, N_2O, CO_2, CO, and HCN. Isotope labeling experiments show that in the early stages of the decomposition, the nitrogen of the NO molecule originates from the nitro group on the azetidine nitrogen. This implies that there is preferential loss of NO_2 from the azetidine nitrogen, rather than from the carbon site.

Thompson and coworkers [233] performed a theoretical study of the decomposition pathways of 1,3,3-trinitroazetidine (TNAZ). Energy profiles for the pathways and possible routes to some of the experimentally observed species of TNAZ decomposition were presented in this study. The energy required to initiate the NO_2 bond fission pathways were found to be 4–8 kcal/mol lower than the HONO elimination pathways. In the gas phase, the NO_2 elimination pathways will be the dominant routes for TNAZ decomposition.

Keeping all these information in mind, thermal stabilities of presently considered species **1-8** are mainly related to the energy required for the initial reaction of decomposition. The common initial step of the thermal decomposition of nitramines is the NO_2 fission reaction through breaking of N-NO_2 bond as known as in the decomposition of hexahydro-1,3,5-trinitro-s-triazine (RDX) and 1,3,5,7-tetranitro-1,3,5,7-tetraazacyclooctane (HMX) [175]. So dissociation energy of the weakest bond in the molecule of energetic material is thought to play an important role in the initiation events. Table 3.17 summarizes the computed homolytic BDE values of C-NO_2 and N-NO_2 bonds for the presently considered species (**1-8**) at UB3LYP/6-311+G (d, p) level of theory. For the initial stages in their thermal decompositions, it can be deduced on the basis of the weakest BDE value that the relative stability order of these isomers may be in the following sequence: 5>3>2>7>4>8>1>6 (see Table 3.17). As a result of the calculations, generally N-NO_2 bond is found to be weaker than the C-NO_2 bond. In the case of **4**, the situation is reverse. This might be due to the streric repulsion occurring between the nitramine nitro group and geminally substituted nitro groups on the adjacent carbon atoms. The weakest nitramine bond belongs to TNAZ (see Table 3.17). According to the suggestion of Chung et. al [204], a molecule should have more than 20 kcal/mol (83.68 kJ/mol) barrier to dissociate in order to be considered as a viable candidate for high energy density material (HEDM), thus we can conclude that the molecules in Figure 3.10 are all viable candidates for HEDMs.

Table 3.17 Calculated homolytic bond dissociation energies in kJ/mol at UB3LYP/6-311+G (d, p).

	BDE							
Bond	**1**	**2**	**3**	**4**	**5**	**6**	**7**	**8**
r_5	101	138	153	141	-	-	-	-
r_6	138	160	176	-	164	92	140	-
r_7	-	190	-	128	174	-	137	114
r_8	-	-	-	-	-	-	-	188

Table 3.18 and 3.19 collect the predicted densities and detonation properties of the concerned isomers (**1-8**). The oxygen balance (*Ω*) and heats of formation (HOF) values were also calculated and listed in the tables. Furthermore, we have calculated the heat of formations at different approaches (see Table 3.18 and 3.19). Based on different heat of formation calculations, detonation parameters are presented in the tables and the results show parallelism. All these data gave some clue about the explosive character of the molecules derived from TNAZ, so far unknown compounds in the literature. The position of nitro group in the ring also has an important effect on the explosive properties of energetic materials (see the corresponding tables). On the basis of theoretical calculation of detonation parameters, isomers of TNAZ might be also very powerful explosives. For example considering isomer **2**, it has the highest detonation properties (9.05 km/s and 36.8 GPA (PM3 data)) among all the isomers (based on the T1 and PM3 heats of formation data). Also in terms of thermal sensitivity based on the calculated homolytic bond dissociation energy values ("trigger linkage"), **2** has to be an insensitive explosive compared to well-known explosive TNAZ **1** (see Tables 3.17, 3.18 and 3.19).

Table 3.18 Computed densities and estimated detonation properties of the concerned molecules **1-4**.

	1	**2**	**3**	**4**
ρ (g/cm^3)	1.80 (1.84)	1.84	1.78	1.79
Ω (%) CO$_2$	-16.66	-16.66	-16.66	-16.66
Ω (%) CO	8.33	8.33	8.33	8.33
V ^{a} (cm^3/mol)	106.715	104.195	107.93	107.35
HOF ^{b} (kJ/mol)	166.02	105.26	89.62	116.47
Q ^{b} (kJ/kg)	7485	7169	7087	7227
D ^{b} (km/s)	9.07 (8.73)	9.12	8.88	8.96
P ^{b} (GPa)	36.5 (37.2)	37.4	34.8	35.5
HOF ^{c} (kJ/mol)	94.96	64.14	66.57	78.08
Q ^{c} (kJ/kg)	7115	6954	6967	7027
D ^{c} (km/s)	8.96 (8.73)	9.05	8.85	8.90
P ^{c} (GPa)	35.6 (37.2)	36.8	34.5	35.0

[a] Average volume from 100 single-point calculations at the B3LYP/6-31G(d,p) level.
[b] Heat of formation values obtained from the T1 method.
[c] Heat of formation values obtained from the PM3 method.

Table 3.19 Computed densities and estimated detonation properties of the concerned molecules **5-8**.

	5	**6**	**7**	**8**
ρ (g/cm^3)	1.81	1.79	1.82	1.81
Ω (%) CO$_2$	-16.66	-16.66	-16.66	-16.66
Ω (%) CO	8.33	8.33	8.33	8.33
V ^{a} (cm^3/mol)	106.175	107.069	105.855	106.259
HOF ^{b} (kJ/mol)	54.8	73.17	86.53	50.38
Q ^{b} (kJ/kg)	6906	7001	7071	6883
D ^{b} (km/s)	8.93	8.89	9.02	8.92
P ^{b} (GPa)	35.5	34.9	36.3	35.4
HOF ^{c} (kJ/mol)	25.17	36.84	51.46	14.81
Q ^{c} (kJ/kg)	6752	6812	6888	6698
D ^{c} (km/s)	8.88	8.83	8.96	8.86
P ^{c} (GPa)	35.1	34.5	35.8	34.9

[a] Average volume from 100 single-point calculations at the B3LYP/6-31G(d,p) level.
[b] Heat of formation values obtained from the T1 method.
[c] Heat of formation values obtained from the PM3 method.

3.2.4.3 Summary of the TNAZ Part

This study employs theoretical methods to model TNAZ (**1**) and its constitutional isomers (**2-8**). Accurate molecular densities and molecular energies were calculated to obtain reliable detonation parameters (detonation velocities, detonation pressures). The calculation results indicate that the detonation velocity and detonation pressure of TNAZ and its seven isomers behave similar to TNAZ. Furthermore, homolytic bond dissociation energy calculations indicate that constitutional isomers of TNAZ might be much safer explosives (insensitive) compared to TNAZ. If these stable isomers of TNAZ can be synthesized successfully, they may be the potential candidates for the powerful insensitive energetic materials.

3.3 Studies on Design of Novel Explosives

3.3.1 Some Novel Nitropyrimidines

This part of the study has been published as a chapter in the book which is name of New Research on Hazardous Materials (2007) [4].

3.3.1.1 Brief Information about the Nitropyrimidines

Pyrimidine (I), (see Figure 3.13) also known as m-diazine, is the parent substance of a large group of heterocyclic compounds which have attracted much attention for a long time. Compounds belonging to this group were known as breakdown products of uric acid at a very early date in the history of organic chemistry, but the systematic study of the ring system really began with work of Pinner [241], who first applied the name pyrimidine to the unsubstituted parent heterocyclic skeleton. Pyrimidine derivatives play a vital role in many biological processes, the ring system being present in, for example, the nucleic acids, several vitamins and coenzymes, and uric acid and other purines. Many synthetic members of the group are also important as synthetic drugs (e.g., barbituric acid derivatives) and chemotherapeutic agents (e.g., sulfadiazine).

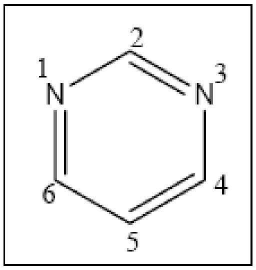

Figure 3.13 Structure of pyrimidine and numbering of it.

The isomeric nitropyrimidines will be numbered according to positional numbers of the nitro groups, eg. 2,4-dinitropyrimidine is called structure **24** etc. The known mononitro derivative of pyrimidine compound, 4-amino-2,6-dichloro-5- nitropyrimidine [242], is a key intermediate in the synthesis of a purine scaffold, as nucleophilic substitution of the chlorides allows access to a diverse array of potentially biologically active compounds. Furthermore the mono substituted nitropyrimidines were studied in the literature [243]. Nitropyrimidines are also known as explosive compounds, whereas there have not been any study (to the best knowledge of us), both theoretical and experimental, on dinitro, trinitro and tetranitro substituted pyrimidine derivatives. In this part of the study we aimed to investigate the mono- , di-, tri- and tetranitropyrimidine derivatives whether they are potential candidates for high energy density materials.

3.3.1.2 Results and Discussions on Nitropyrimidine Study

Although, wide variety of explosives exist and employed in usage, they have some common structural features. Usually, they are classified according to the types of groups present in their structures like nitro explosives, azides, nitramines etc. However, a deeper look into the groups considered primarily responsible for the explosive character of the compounds reveals that aliphatic or aromatic nitro compounds, aliphatic nitro esters, nitrogen halides etc., all have a common topological assembly of various atoms, that is the isoconjugate of methylene propenyl dianion [244]. This moiety is a non-Kekule alternating hydrocarbon structure. Figure 3.14 shows certain explosive groups (explosophores) and their isoconjugate non-Kekule alternant hydrocarbon structures. As seen there, when a nitro group is attached to a conjugated system, automatically an embedded non-Kekule moiety emerges. Although, the whole system becomes a Kekule or non-Kekule depending on the position of the attached nitro group, the embedded non-Kekule moiety isoconjugate with methylenepropenyl dianion system engenders a local unstable assembly of bonds due to the mesomeric and inductive electron attracting nature of the nitro group. If the nitro group is linked to a carbon atom in a π-structure, the effect of NO_2 group could be partly reduced by delocalization of electrons from the main body of the system to the nitro group. However, if this flow of electrons are hindered by some other electron withdrawing groups present at some other positions of the molecule, the local non-Kekule character due to the methylenepropenyl dianion system becomes more pronounced, hence unstability should increase. This is a general trend in practice.

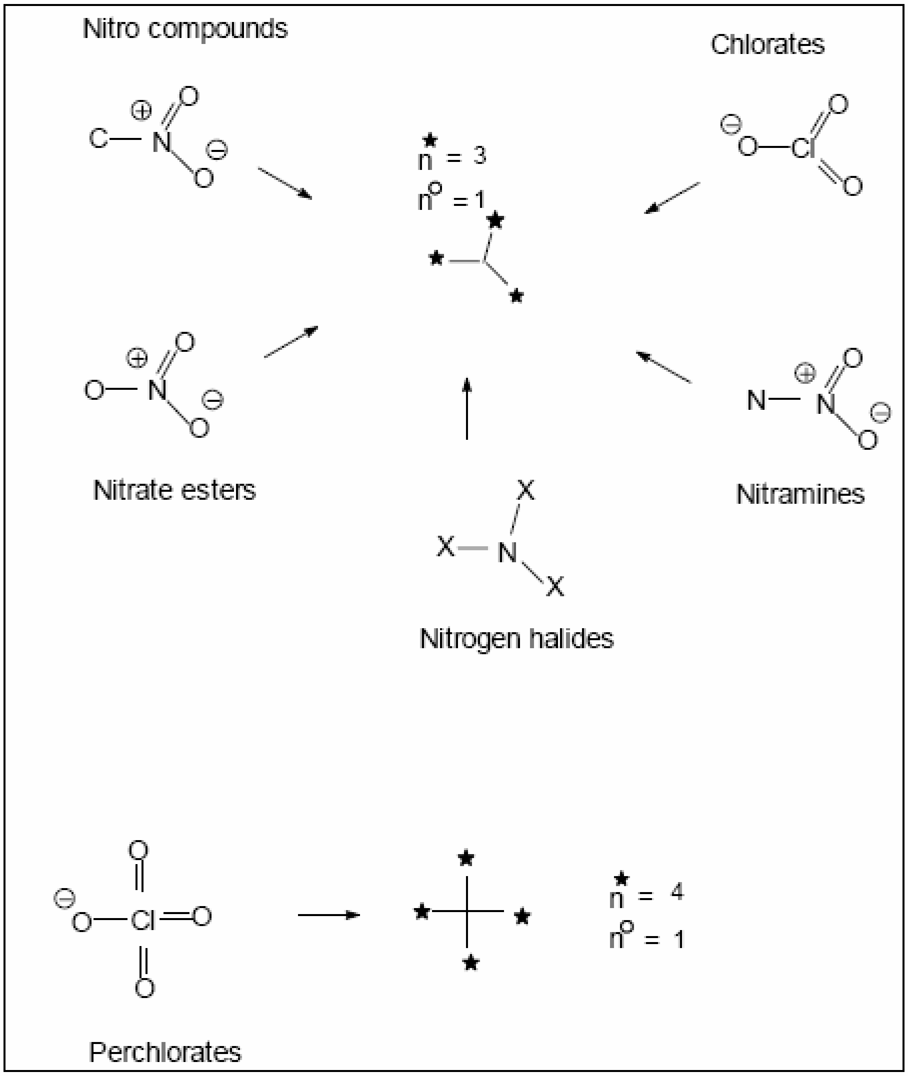

Figure 3.14 Some functional groups common in explosive molecules and their isoconjugates.

3.3.1.2.1 General Structural Considerations on Nitropyrimidines

Pyrimidine nucleus is isoconjugate with benzene skeleton. The lone-pairs of nitrogen atoms in the pyrimidine structure lie in the σ-plane, thus the orbital of nitrogens accommodating these electrons are orthogonal to the π-skeleton. Thus, π-skeleton of pyrimidine, like benzene contains six electrons but because of the electronegativity of aza-nitrogens it has a polarized π-skeleton. Due to some obvious structural reasons, the pyrimidine nucleus is an even alternant system. As seen below (see Figure 3.15), the 5th position has the same parity as the nitrogen centers. All the mono-nitration products of pyrimidine are isoconjugate with odd alternant hydrocarbon system. Of the four isomers of dinitro structures, **25** and **45** have even alternant hydrocarbon isoconjugates, but **24** and **46** are isoconjugate with non-Kekule alternant hydrocarbon systems. In the case of trinitro products, the symmetrical derivative has a non-Kekule, whereas **245** and **456** have odd alternant hydrocarbon isoconjugates. On the other hand, the tetra substituted compound is a non-Kekule system. (Note that in these part compound numbers are assigned according to the positional numbers of nitro groups, e.g. **25** stands for 2,5-dinitro pyrimidine. Nitro group has an odd conjugate system containing three atoms and four π-electrons, thus it is isoconjugate with the allyl anion. Although, in nitro compounds, the nitro group is attached to the adjacent aromatic system through the central, inactive atom of its isoconjugate allyl anion, it is not a – E substituent but according to Dewar, it is a + E substituent [245, 246]. Considering NO_2 structure, the negatively charged oxygen cannot donate or attract electrons to or from the adjacent conjugate system, but delocalization of electrons is possible to the NO group in NO_2 structure. Although, the oxygen atoms in NO_2 group are identical through resonance, one of them cannot be conjugated with the adjacent aromatic system. Hence, a nitro group acts as a nitroso group in the whole π-skeleton of the molecule. Following the Dewar's treatment of nitro groups, all the non-Kekule as well as the odd and even structures in Figure 3.15 becomes even alternant systems. Certain instability is associated with non-Kekule compounds. Since, the Dewar's treatment abolishes non-Kekule character, all the nitropyrimidines deserve to be treated in detail by using high level molecular orbital calculations.

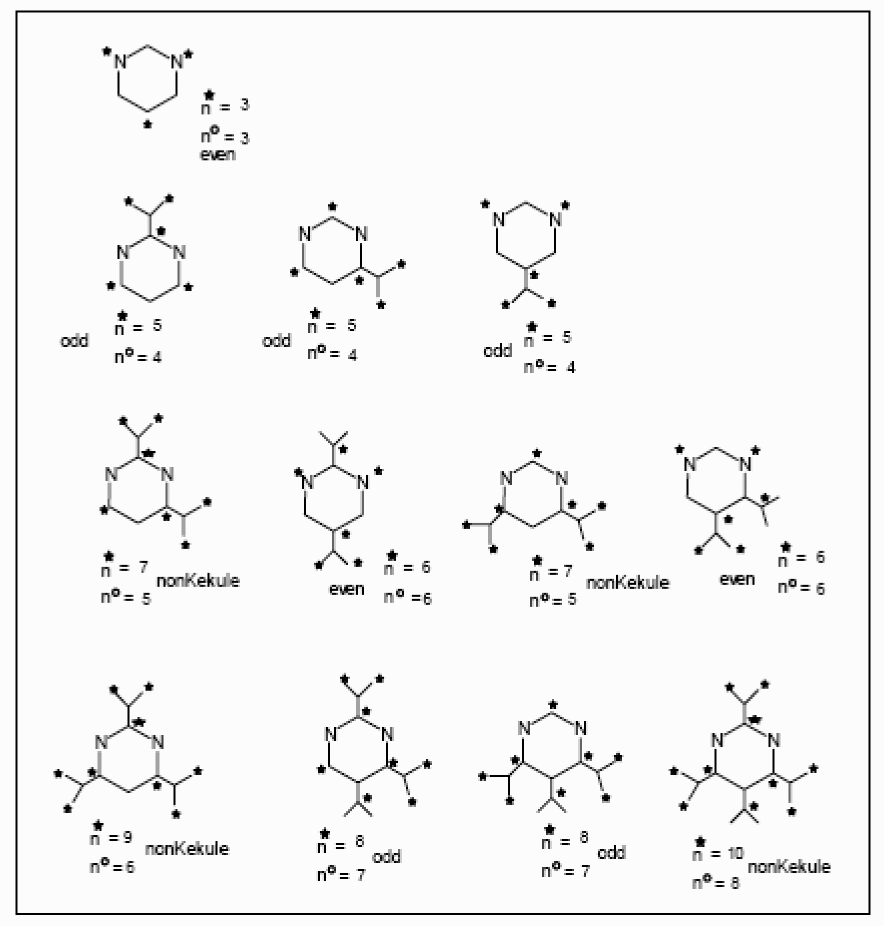

Figure 3.15 Isoconjugates of nitropyrimidines.

3.3.1.2.2 Explosion Products of Nitropyrimidines

According to the oxygen balance values of the nitropyrimidines; the mono nitro derivatives are highly oxygen deficient. As one goes to tetranitro derivative, the nitropyrimidines get less and less oxygen deficient and the tetra nitro derivative is an oxygen sufficient compound. The Kistiakowsky-Wilson rules [1] applied to tetra and trinitropyrimidines, (whose oxygen balance is higher than -40) estimate the formation of CO_2 and N_2 in the first case and CO, CO_2, H_2O and N_2 production from the trinitropyrimidines. On the other hand, the modified Kistiakowsky-Wilson rules [1] applied on the dinitro and mono nitropyrimidines forecast the detonation products as H_2O, CO and N_2, whereas the Springall-

Roberts rules [1] also consider the formation of CO_2 from CO. A more elaborate way to the decomposition products of such kind of molecules is based on the water-gas equilibrium. In general, the products of the explosion of propellant powders include a large variety of gases, those present in the greatest proportion are CO_2, CO, H_2O and N_2. The first four of these are components of a mixture of the water-gas reaction.

$$CO_2 + H_2 \rightleftharpoons CO + H_2O$$

When an explosive material of CHNO type explodes, these gases are formed according to the water-gas equilibrium. Table 3.20 shows the stoichiometric profile of explosion products of di-, tri- and tetranitro pyrimidines based on water-gas reaction. As seen there, dinitropyrimidines at the three temperatures tend to form CO rather than CO_2. In the absence of any extra oxidizer, dinitropyrimidines are quite oxygen deficient systems (the oxygen balances are ca. -47%). Thus, even hydrogens of the pyrimidine cannot be oxidized to H_2O. According to the calculations, the hydrogen formation is substantially low for a trinitropyrimidine at elevated temperatures. In the case of trinitropyrimidines, the water-gas equilibrium prefers the mutual formation of CO_2 and CO in such a way that at 3000 K the later one is preferred. Also, some water formation should occur. The raise of temperature disfavors the H_2 formation.

Table 3.20 Stoichiometric profile of the explosion products of di, tri and tetranitropyrimidines at different temperatures based on water-gas reaction.

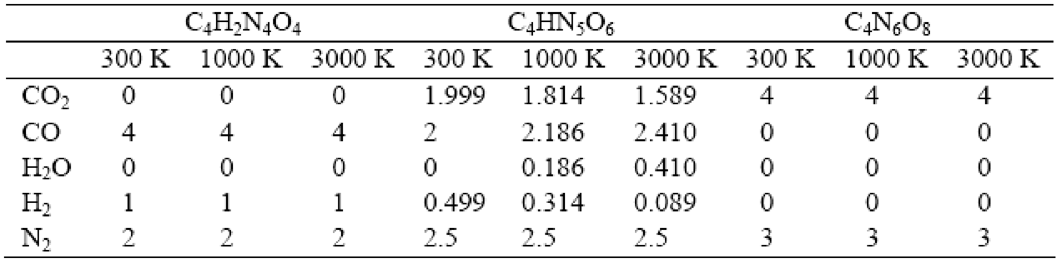

	$C_4H_2N_4O_4$			$C_4HN_5O_6$			$C_4N_6O_8$		
	300 K	1000 K	3000 K	300 K	1000 K	3000 K	300 K	1000 K	3000 K
CO_2	0	0	0	1.999	1.814	1.589	4	4	4
CO	4	4	4	2	2.186	2.410	0	0	0
H_2O	0	0	0	0	0.186	0.410	0	0	0
H_2	1	1	1	0.499	0.314	0.089	0	0	0
N_2	2	2	2	2.5	2.5	2.5	3	3	3

3.3.1.2.3 Geometry and Energy Considerations on Nitropyrimidines

Figure 3.16, 3.17 and 3.18 show the B3LYP/6-31G (d, p) level geometry optimized structures of the present molecules. Theoretically nitro-group can be either coplanar or not with the aromatic nucleus. In the case of coplanar nitro group, shift of electrons from the aromatic ring to the nitro group occurs through resonance. This effect produces a flat geometry for the NO_2 group with a sp^2 hybridized nitrogen atom and a relatively short C-N bond of “partially double” character (see Figure 3.16). The exact balance of these processes is subtle and depends on the possibility of forming resonance structures (the statistical weight of the contributing canonical structures).

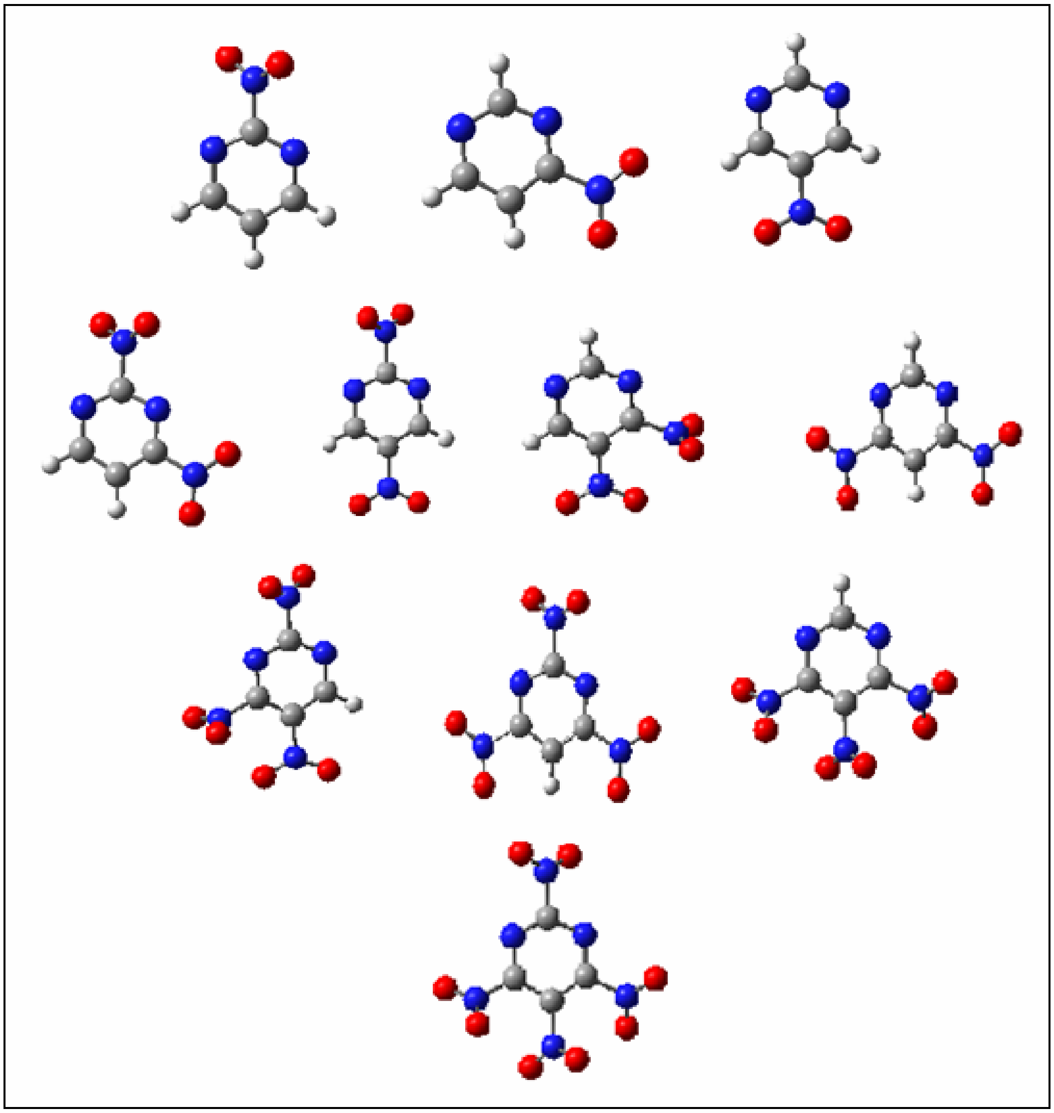

Figure 3.16 Geometry optimized structures of the nitropyrimidines at B3LYP/6-31G (d,p) level.

(Colors stand for; grey: carbon, blue: nitrogen, red: oxygen, white: hydrogen)

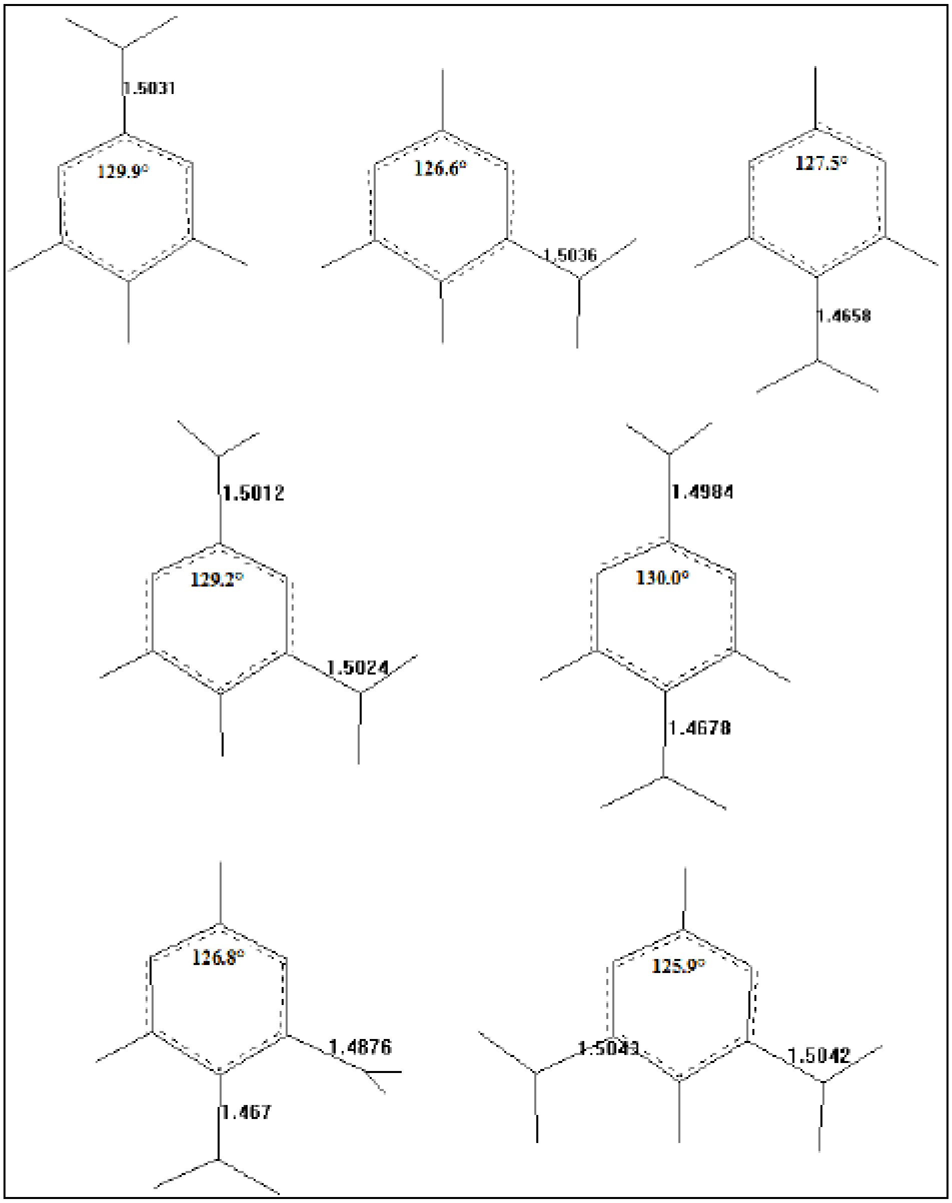

Figure 3.17 Some geometric features of the mono and dinitropyrimidines at B3LYP/6-31G (d, p) level.

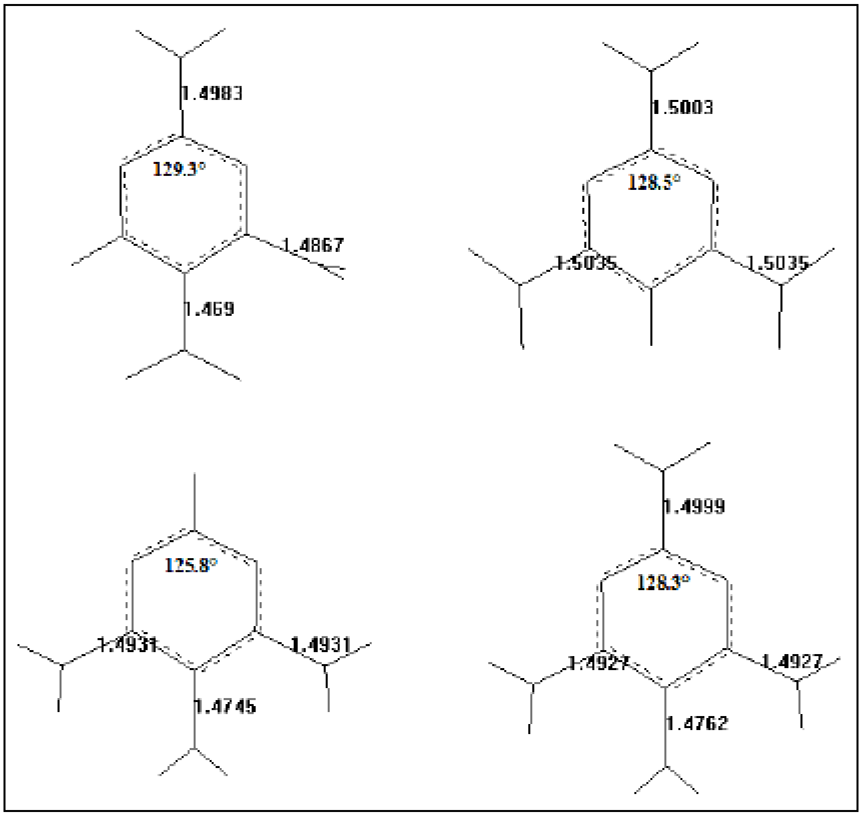

Figure 3.18 Some geometric features of the trinitropyrimidines and tetranitrpyrimidine calculated at B3LYP/6-31G (d, p) level.

Table 3.21 The homolytic BDEs of C-NO_2 (in kJ/mol) in the nitropyrimidines. (UB3LYP/6-31G (d, p)). The numbers in parentheses is the relevant positional number(s) where the bond dissociation occurs, see Figure 3.14 for numbering.

Structures	**BDE**
2 (2)	228
4 (4)	226
5 (5)	258
24 (2)	252
24 (4)	221
25 (2)	221
25 (5)	252
45 (4)	223
45 (5)	192
46 (4 or 6)	220
245 (2)	215
245 (4)	190
245 (5)	219
246 (2)	248
246 (4 or 6)	215
456 (5)	189
456 (4 or 6)	196
2456 (2)	212
2456 (5)	195
2456 (4 or 6)	188

Table 3.21 summarizes the computed homolytic BDE values of C-NO_2 linkage for the species considered at UB3LYP/6-31G (d, p) level of theory. As seen in the table, BDEs for these compounds are highly position dependent and it is hard to generalize certain trends. We can conclude that the molecules in Figure 3.17 are all viable candidate of HEDMs. When an explosion reaction takes place, the explosive molecule breaks apart. This is quickly followed by a rearrangement of the atoms into a series of small stable molecules. These molecules are usually water, carbon dioxide, carbon monoxide and nitrogen. The nature of the products will depend on the amount of oxygen available during the reaction. This supply of oxygen will depend on the quantity of oxidizing atoms which are present in the explosive molecule. Table 3.22 shows the oxygen balance (Ω) data for the molecules concerned. Di-substituted pyrimidines' oxygen balance data

resemble the powerful explosive tetryl (-47.39%). Tri-nitropyrimidines resemble RDX (1,3,5-trinitro-1,3,5-triazocyclohexane) (-21.60) and HMX (octahydro-1,3,5,7-tetranitro-1,3,5,7-tetrazocine) (-21.62%). Tetranitropyrimidine resembles EGDN (ethylene glycol dinitrate) which is oxygen sufficient.

Table 3.22 The oxygen balance (Ω) and NICS (0) (B3LYP/6-31G (d, p)) data for the nitropyrimidines.

Structure	Ω (%)	NICS (ppm)
2	-97	-8.05
4	-97	-8.63
5	-97	-7.59
24	-47	-9.68
25	-47	-8.73
45	-47	-9.02
46	-47	-10.09
245	-19	-10.01
246	-19	-11.24
456	-19	-8.98
2456	-19	-11.88

The aromaticity of pyrimidine itself is expected to be improved by the substitution of nitro groups due to the following reasoning; due the electro negativity of nitrogen, the ring of the pyrimidine suffers from homogeneous electron distribution and thus, poor aromaticity. Insertion of a nitro group(s) into the system will pull the electrons located on the nitrogen atoms of the pyrimidine ring and let these electrons delocalize over the ring better which will lead to an improved aromaticity. Therefore, the greater the number of nitro groups properly oriented in the system, more aromatic the structure will be. As can be seen in Table 3.22 the NICS (0) values of the systems increase (absolutely) as the number of nitro groups in the structures increase. The NICS values, therefore the aromaticity of the systems, increase in the case where nitro substitution is at the symmetrical positions 4 and 6. On the other hand, when nitro is located at position 5, NICS values generally decreases as compared to others.

3.3.1.2.4 Calculated Detonation Parameters of Nitropyrimidines

Table 3.23 collects the predicted densities and detonation properties (by using the Kamlet Jacobs equations) of the considered molecules. All these data in Table 3.23, gave some clue about the explosive character of the molecules derived from pyrimidine molecule, di-, tri- and tetra-nitrated pyrimidines are so far unknown compounds in the literature, to the best knowledge of the authors. It was clear that from mono-substituted to tetra-substituted nitro pyrimidines, density (ρ), velocity of detonation (D) and detonation pressure (P) all increase with the increasing number of the nitro groups. This might show good group additivity on the detonation properties and also supports the claim that introducing more nitro substituents into a molecule usually helps to increase its detonation performance. For RDX and HMX, experimental values of D and P are 8.75 km/s, 9.10 km/s and 34.70 GPa, 39.00 GPa, respectively. Comparing these values with tetra-substituted nitro pyrimidine compound which has velocity of detonation value of 9.23 km/s and detonation pressure value of 39.81 GPa, one finds it to be a more powerful explosive than the famous explosives HMX and RDX. Especially di-, tri- and tetra-nitro substituted pyrimidines can be novel high energy density materials (HEDMs) when they are succesfully synthesized.

Table 3.23 Computed densities and predicted detonation parameters of the considered molecules.

Structures	HOF[a] (kJ/mol)	Q (kJ/g)	V[b] (cm^3/mol)	ρ (g/cm^3)	D (km/s)	P (GPa)
2	148.83	1165.46	79.67	1.57	6.44	16.90
4	143.97	1156.18	80.04	1.56	6.41	16.68
5	130.10	1129.67	79.02	1.58	6.43	16.91
24	127.32	1348.19	96.18	1.77	7.76	26.40
25	120.01	1337.91	97.14	1.75	7.69	25.78
45	139.72	1365.60	96.46	1.76	7.77	24.56
46	142.58	1369.63	95.73	1.78	7.81	26.87
245	140.77	1493.30	115.20	1.87	8.54	33.08
246	133.50	1485.22	114.71	1.88	8.56	33.28
456	159.55	1514.17	112.85	1.91	8.70	34.72
2456	169.46	1602.20	131.83	1.97	9.23	39.81

[a] Heat of formation values calculated at PM3 level

[b] Average value from 100-single point volume calculations at B3LYP/6-31G(d,p).

[c] Heat of explosion, D: detonation velocity, P: detonation pressure.

3.3.1.2.5 Summary of Nitropyrimidine Part

As a conclusion, of the various nitropyrimidines studied presently, only the tetranitropyrimidine is oxygen sufficient material for explosive purposes. The rest is oxygen deficient in varying percentages. Thus, their usage necessitates oxidizing agents to be coupled with (as in the case of TNT). The homolytic bond dissociation energy (for C-NO_2 bond) for the tetranitro derivative is the minimum among the group (as expected). It is followed by 4, 5, 6 and 2, 4, 5- trinitro and 4, 5-dinitro derivatives. The tetra nitro derivative also has the maximum heat of explosion and pressure of explosion values among the series of compounds studied. Although, the others have lower values as compared to the tetranitro derivative, especially the trinitro derivatives possess quite comparable figures. Thus, combined with some oxidizing agents they can be utilized as explosive materials as well. Of course, all these predictions presently asserted are within the limitations of the calculation methods and Kamlet-Jacobs equations used.

3.3.2 Tetranitroparacyclophanes as Potential Candidates of High Explosives

3.3.2.1 Brief Information about Paracyclophane

[2.2] Paracyclophane, first prepared by Farthing in 1949 [247] and in following 20 years thoroughly investigated by Cram et al. [248]. It has become the archetype of strained compounds with bent aromatic rings [249]. Interest in this prototypical layered organic molecule is growing steadily. The investigations of its structural, spectroscopic, and chemical properties stood in the focus of numerous research projects [250-255] in recent years interest is beginning to shift more and more to applications [256, 257]. On the other hand, there is no study of its polynitro derivatives in terms of explosive capability. Compounds that contain polynitro groups are always highly energetic, they can provide a large amount of energy and heat after they are burned and are employed extensively as the main ingredient in explosive and propellants. Their corresponding detonation performance depends on whether they exhibit particular physical or chemical properties (such as heat of explosion, oxygen balance, and molecular density). In this study, we aimed to investigate the tetranitro substituted [2, 2] paracyclophanes (10 isomers, see Figure 3.19) as potential candidates of HEDMs.

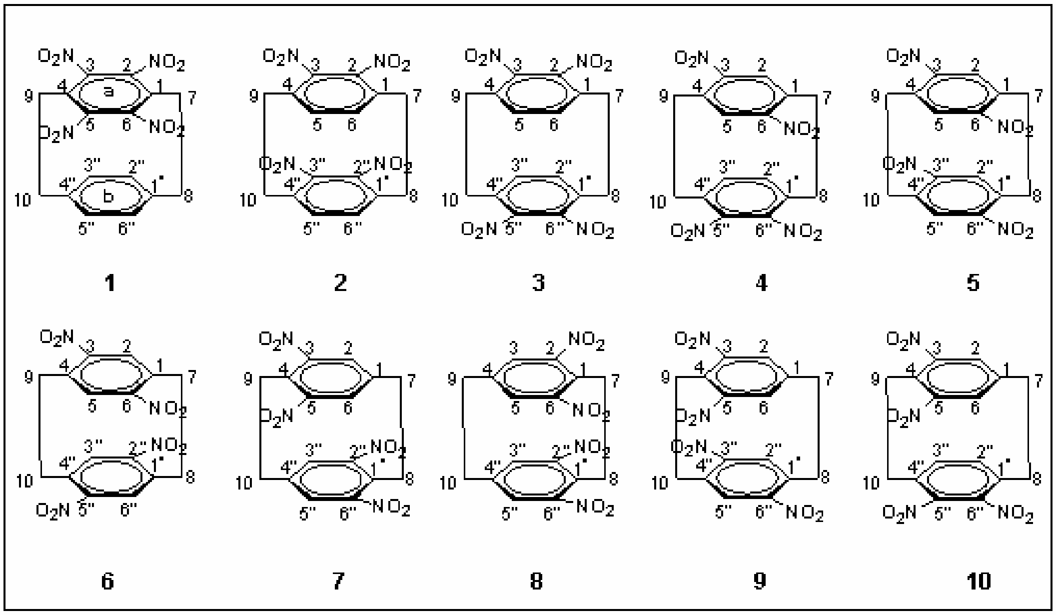

Figure 3.19 The numbering scheme and molecular structures of tetranitro [2, 2] paracyclophanes.

3.3.2.2 Results and Discussions on Nitroparacyclophanes

In the Table 3.24 and 3.25, presently calculated geometric parameters for considered species at the B3LYP/6-31G (d,p) level, as well as available experimental values [258] for [2,2] paracyclophane (PCP) are presented. The B3LYP/6-31G (d,p) bond lengths differ from the crystal averages with rms deviations of 0.015Å. Calculations about PCP give results qualitatively and quantitatively in agreement with experimental values.

Table 3.24 Some calculated bond lengths (Å) of the concerned species **1-5** at B3LYP/6-31G (d, p) level.

	1	**2**	**3**	**4**	**5**	**PCP**
C1-C2	1.403	1.405	1.402	1.396	1.398	1.402 (1.394)
C2-C3	1.395	1.400	1.403	1.396	1.393	1.394 (1.394)
C3-C4	1.404	1.406	1.400	1.408	1.407	1.402 (1.394)
C4-C5	1.403	1.400	1.403	1.403	1.398	1.402 (1.394)
C5-C6	1.395	1.391	1.389	1.392	1.393	1.394 (1.394)
C6-C1	1.404	1.402	1.405	1.409	1.407	1.402 (1.394)
C1”-C2"	1.403	1.406	1.405	1.404	1.400	1.402 (1.394)
C2"-C3"	1.396	1.400	1.389	1.390	1.393	1.394 (1.394)
C3"-C4"	1.402	1.405	1.403	1.402	1.408	1.402 (1.394)
C4"-C5"	1.403	1.402	1.400	1.400	1.400	1.402 (1.394)
C5"-C6"	1.396	1.391	1.403	1.399	1.393	1.394 (1.394)
C6"-C1"	1.402	1.400	1.402	1.404	1.408	1.402 (1.394)
C1-C7	1.518	1.516	1.517	1.516	1.518	1.514 (1.514)
C4-C9	1.518	1.517	1.518	1.519	1.518	1.514 (1.514)
C7-C8	1.607	1.605	1.600	1.609	1.599	1.612 (1.569)
C9-C10	1.607	1.605	1.610	1.599	1.599	1.612 (1.569)
C8-C1"	1.515	1.517	1.517	1.516	1.517	1.514 (1.514)
C4"-C10	1.515	1.516	1.518	1.515	1.517	1.514 (1.514)

Table 3.25 Some calculated geometrical data (bond angles and dihedral angles in degrees) of concerned species **6-10** at B3LYP/6-31G (d, p) level.

	6	**7**	**8**	**9**	**10**
C1-C2	1.401	1.398	1.409	1.398	1.396
C2-C3	1.394	1.397	1.397	1.391	1.394
C3-C4	1.407	1.407	1.396	1.413	1.410
C4-C5	1.401	1.408	1.398	1.408	1.410
C5-C6	1.394	1.391	1.391	1.399	1.395
C6-C1	1.407	1.399	1.413	1.396	1.399
C1”-C2"	1.407	1.408	1.413	1.397	1.404
C2"-C3"	1.394	1.391	1.391	1.396	1.389
C3"-C4"	1.400	1.399	1.398	1.407	1.403
C4"-C5"	1.407	1.398	1.396	1.402	1.403
C5"-C6"	1.394	1.397	1.397	1.391	1.402
C6"-C1"	1.400	1.407	1.409	1.407	1.401
C1-C7	1.517	1.514	1.521	1.517	1.515
C4-C9	1.517	1.518	1.514	1.521	1.521
C7-C8	1.596	1.608	1.599	1.592	1.601
C9-C10	1.596	1.608	1.601	1.598	1.601
C8-C1"	1.517	1.518	1.521	1.520	1.516
C4"-C10	1.517	1.514	1.514	1.516	1.518

The geometry optimized structures of the tetra nitro derivatives of [2, 2] paracyclophane are shown in Figure 3.20 and Figure 3.21 at the same theoretical level. Furthermore, calculated direction of the dipole moments is seen in the same figure. Comparing the calculated bond lengths of isomers and main skeleton [2, 2] paracyclophane (PCP), C7-C8 and C9-C10 bond lengths are equal lengths in the case of 1, 2, 5,6,10 and PCP. This might be due to symmetry of these molecules (except 10). It can bee seen from the table that C7-C8 and C9-C10 bonds stand for the longest bond lengths in the considered structures. The position of the nitro group affected the bond lengths in aromatic rings were seen in the Tables 3.24 and 3.25. Furthermore, the calculated longest C-NO_2 bond and its value are seen in Figure 3.20. The C-NO_2 bond length values for the considered isomers, 1-10, are found to be in between 1.474Å and 1.482Å. Considering the 2, 4, 6-trinitrotoluene, experimentally the longest C-NO_2 bond length was reported as 1.496Å [259] and 1.475Å [260].

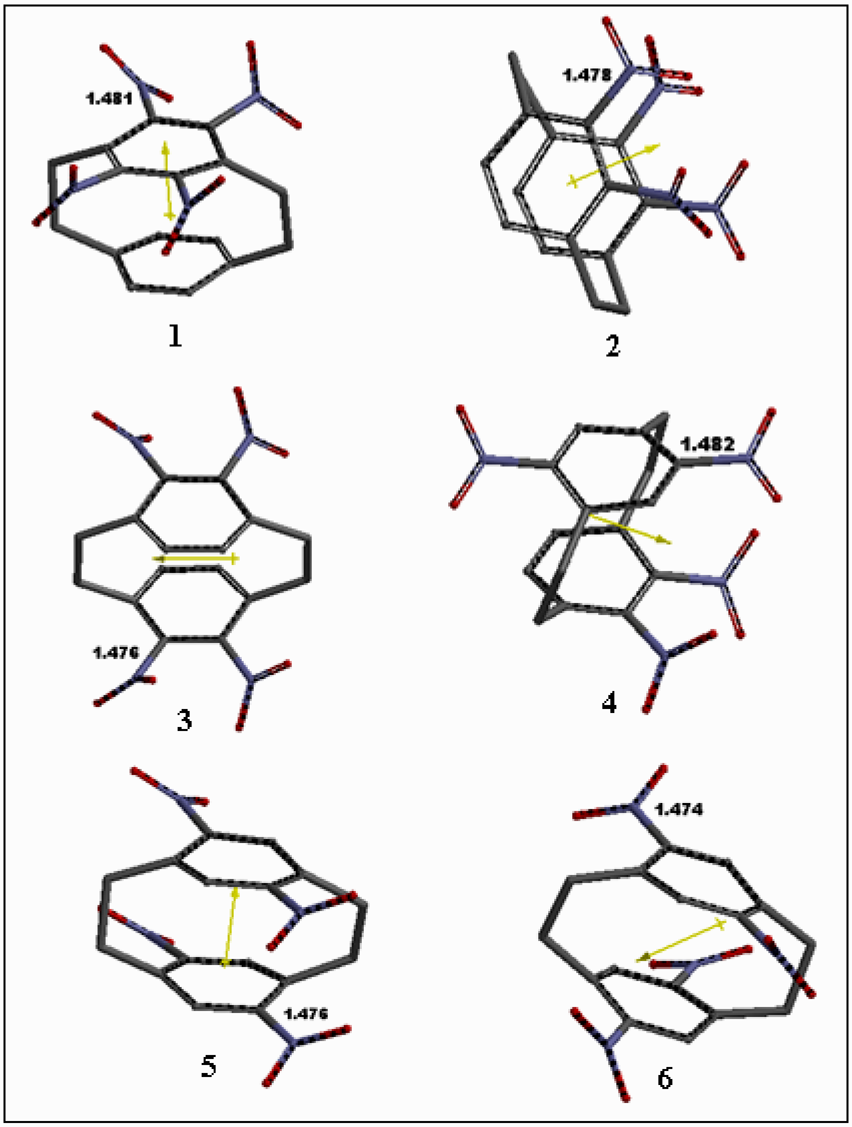

Figure 3.20 The geometry optimized (B3LYP/6-31G (d, p)) structures **1-6** and direction of the dipole moments of present concern.

(Colors stand for; black: carbon, blue: nitrogen, red: oxygen)

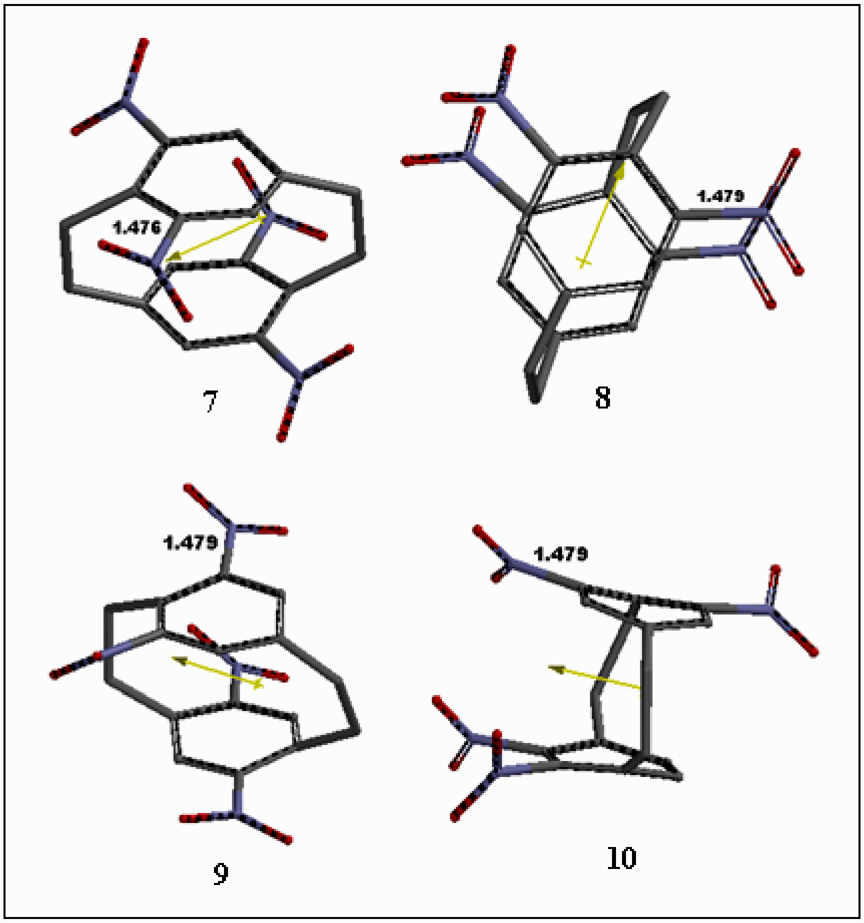

Figure 3.21 The geometry optimized (B3LYP/6-31G (d, p)) structures **7-10** and direction of the dipole moments of present concern.
(Colors stand for; black: carbon, blue: nitrogen, red: oxygen)

Table 3.26 shows the total, relative and homolytic bond dissociation energies for the considered isomers (**1-10**). As seen from the table, generally a good agreement of stability order among the calculated energies has been found. In the limitations of the used levels of the theory, the most stable compound in terms of total energy consideration is **6** and the least stable one is isomer **1**. This result is consistent with the calculated homolytic bond dissociation energy values. The weakest C-NO_2 bond belongs to the isomer **1** (216 kJ/mol), whereas the strongest C-NO_2 bond belongs to the isomer **6** (262 kJ/mol).

Table 3.26 Calculated total, relative and homolytic bond dissociation of C-NO_2 bond energies.

	B3LYP/6-31G (d,p)	Rel. En. [a]	T1	Rel. En. [b]	BDE [c]
	a.u	(kJ/mol)	a.u	(kJ/mol)	(kJ/mol)
1	-1437.267029	102	-1434.768317	76	216
2	-1437.271245	93	-1434.769538	73	221
3	-1437.284642	57	-1434.780933	43	236
4	-1437.289513	46	-1434.783563	36	248
5	-1437.299708	20	-1434.791164	16	260
6	-1437.307095	0	-1434.797280	0	262
7	-1437.300449	19	-1434.788770	22	254
8	-1437.295384	29	-1434.784647	33	247
9	-1437.301091	16	-1434.791226	16	246
10	-1437.288580	49	-1434.781923	40	241

[a] Calculated relative energies at B3LYP/6-31G(d,p) level of theory.
[b] Calculated relative energies at T1 level of theory.
[c] The BDEs calculated at UB3LYP/6-31G(d,p).
Atomic units; 1 hartree=2625.5 kJ/mol

The destability of isomer **1** is attributed to four nitro groups attached to the same aromatic ring; it is destabilized because of the repulsion between the neighboring lone pairs on the oxygen atoms of the nitro groups. This repulsion is also clearly seen from the orientations of the nitro groups in isomer **1** (see Figure 3.21). On the other hand, isomer **6** is evidently stabilized compared to isomer **1** and other isomers. We may ascribe this stability to the symmetrical distribution of nitro groups to the both aromatic rings. The stability order is in terms of total energy is : **6**>**9**>**7**>**5**>**8**>**4**>**10**>**3**>**2**>**1** at the B3LYP/6-31G(d,p) level. According to the T1 level of theory, the stability order is: **6**>**5**=**9**>**7**>**8**>**4**>**10**>**3**>**2**>**1**. At the B3LYP/6-31G (d, p) level, **1** is 102 kJ/mol less stable than **6**, and 76 kJ/mol with T1 level. See the relative energies in Table 3.26. On the other hand, the calculated heat of formation values at different levels is reported in Tables 3.27 and 3.28. As seen from the tables, the heat of formation values are endothermic, the values indicate that **6** is the least endothermic isomer, whereas the most endothermic structure is **1**. This result is consistent with the stability order with respect to total energies and BDEs. Table 3.26 summarizes the computed homolytic BDE values of C-NO_2 bond for the presently considered species (**1-10**) at B3LYP/6-

31G (d, p) level of theory. For the initial stages in their thermal decompositions, it can be deduced on the basis of the BDE that the relative stability order of these isomers may be in the following sequence: **6**>**5**>**7**>**4**>**8**>**9**>**10**>**3**>**2**>**1**. According to the suggestion of Chung et. al [204] a molecule should have more than a 84 kJ/mol barrier to dissociate in order to be considerede as a viable candidate for high energy density materials (HEDMs), we can conclude that the molecules in Figure 3.20 are all viable candidates for HEDMs.

Table 3.27 Computed densities and detonation properties of **1-5.**

	1	**2**	**3**	**4**	**5**
ρ (g/cm^3)	1.678	1.665	1.696	1.656	1.678
Ω (%) (CO_2)	-123.63	-123.63	-123.63	-123.63	-123.63
Ω (%) (CO)	-57.69	-57.69	-57.69	-57.69	-57.69
V ^{a} (cm^3/mol)	231.448	233.212	228.945	234.504	231.349
M (g/mol)	388.292	388.292	388.292	388.292	388.292
HOF ^{b} (kJ/mol)	278.178	254.453	227.454	223.804	205.329
Q ^{b} (kJ/kg)	5473.50	5412.36	5342.77	5333.87	5287.48
D ^{b} (m/s)	6457	6413	6471	6363	6402
P ^{b} (Gpa)	17.73	17.42	17.94	17.09	17.43
HOF ^{c} (kJ/mol)	359.502	331.064	307.905	314.273	296.083
Q ^{c} (kJ/kg)	5683.10	5612.22	5550.36	5568.41	5522.01
D ^{c} (m/s)	6518	6471	6533	6432	6472
P ^{c} (Gpa)	18.07	17.74	18.28	17.46	17.81
HOF ^{d} (kJ/mol)	222.30	218.12	186.01	180.40	161.02
Q ^{d} (kJ/kg)	5329.49	5318.72	5235.93	5221.50	5171.50
D ^{d} (m/s)	6414	6385	6438	6330	6366
P ^{d} (Gpa)	17.49	17.27	17.76	16.91	17.23

[a] Average volume from 100 single-point volume calculations at the B3LYP/6-31G (d,p) level. [b] Heat of formation values obtained from the PM3 level.
[c] Heat of formation values obtained from the PM3//B3LYP/6-31G(d,p) level.
[d] Heat of formation values obtained from the T1 level.

Table 3.28 Computed densities and detonation properties of **6-10**.

	6	**7**	**8**	**9**	**10**
ρ (g/cm^3)	1.702	1.669	1.66	1.667	1.680
Ω (%) (CO$_2$)	-123.63	-123.63	-123.63	-123.63	-123.63
Ω (%) (CO)	-57.69	-57.69	-57.69	-57.69	-57.69
V ^{a} (cm^3/mol)	228.100	232.611	233.954	232.969	231.149
M (g/mol)	388.292	388.292	388.292	388.292	388.292
HOF ^{b} (kJ/mol)	189.441	192.300	206.552	198.027	220.488
Q ^{b} (kJ/kg)	5246.24	5251.40	5290.06	5266.86	5326.14
D ^{b} (m/s)	6468	6365	6350	6369	6413
P ^{b} (Gpa)	17.98	17.16	17.02	17.19	17.49
HOF ^{c} (kJ/mol)	292.410	287.250	296.471	293.304	307.273
Q ^{c} (kJ/kg)	5511.7	5498.82	5522.01	5514.28	5550.36
D ^{c} (m/s)	6548	6438	6419	6443	6480
P ^{c} (Gpa)	18.43	17.56	17.39	17.58	17.85
HOF ^{d} (kJ/mol)	144.36	165.15	176.02	159.49	183.65
Q ^{d} (kJ/kg)	5130.26	5181.81	5210.16	5168.92	5230.78
D ^{d} (m/s)	6431	6344	6326	6340	6385
P ^{d} (Gpa)	17.78	17.05	16.89	17.02	17.33

[a] Average volume from 100 single-point volume calculations at the B3LYP/6-31G (d,p) level. [b] Heat of formation values obtained from the PM3 level.
[c] Heat of formation values obtained from the PM3//B3LYP/6-31G(d,p) level.
[d] Heat of formation values obtained from the T1 level.

Tables 3.27 and 3.28 collect the predicted densities and detonation properties of the concerned isomers (**1-10**). The oxygen balance (*Ω*) and heats of formation (HOF) values were calculated and listed in the tables. Based on different heat of formation calculations, detonation parameters are presented in the tables and the results show parallelism. All these data gave some clue about the explosive character of the molecules derived from PCP, so far unknown compounds in the literature. In terms of the predicted detonation parameters, the most powerful explosive among these isomers is compound **3** and the least effective explosive is compound **8** (see the detonation velocities and pressures in the Tables 3.28 and 3.29). It is known that detonation velocities of the secondary explosives are in the range of 5500 m/s and above [1]. Hence, the tetra nitro derivatives of PCP can be classified as secondary explosives. Compared to the nitro guanidine which is well known insensitive secondary type explosive, gave some information about the explosive character of the designed molecules. Nitro guanidine has detonation velocity of 4695 m/s (ρ=0.80 g/cm^3) to 6775 m/s (ρ=1.20 g/cm^3) [1]. It is not very sensitive to shock or impact, is also of interest as insensitive high explosive low vulnerability ammunition (LOVA). Therefore, if these stable tetra nitro substituted PCPs can be synthesized; they will have comparable exploitable values. In addition to the teranitro PCPs, we have calculated the octanitro PCP in order to see the limit of explosive capacity of this material. Based on the calculated heat of formation value at PM3//B3LYP/6-31G(d,p) level and calculated density at the same approach used for tetranitro PCPs, the detonation parameters of octanitro PCP were predicted as 8389 m/s (velocity of detonation), 33 Gpa (detonation pressure) and 6751 kJ/kg (heat of detonation). Also for the octanitro PCP case, homolytic bond dissociation energy was calculated as 198 kJ/mol. In terms of the oxygen balance values (Ω (CO_2) = -47% and Ω (CO) = -6% for octanitro PCP), the tetra nitro and also octanitro PCPs are oxygen deficient, thus their usages necessitates oxidizing agents to be coupled with.

We have investigated the NICS values to examine their aromaticity. Negative NICS values denote aromaticity and positive NICS values denote antiaromaticity while small NICS values indicate non-aromaticity. Calculated NICS (ppm) values, dipole moments and symmetries for the considered species at B3LYP/6-31G (d,p) level are presented in Table 3.29. NICS values were calculated at the center of each ring. Naming of **a** and **b** for the corresponding rings is given in Figure 3.19. The reference is the value of benzene (-9.9 ppm) and PCP (-9.6 ppm) computed at the same level of theory. Furthermore, the NICS values of octanitro PCP was calculated as -13.5 ppm for both aromatic rings. (Symmetry of D_2). In the octanitro PCP structure, all hydrogens in the aromatic rings were replaced by nitro group. The values are more negative for the nitro substituted PCPs. All the NICS values for the presently considered structures should be considered on the relative basis, just to compare relative aromaticities of the isomers. Since, no experimental values are available for the aromaticity of these structures, it is not possible to evaluate the precision of the NICS data presently. On the other hand, these results used for the purpose of comparing relative aromatcities of them and we have obtained generally comparable results for consiedered nitro substituted structures (**1-10**). According to the NICS data the most aromatic ring among the series is **1a** (-13.8 ppm), which can be explained by the presence of symmetry in this structure. The four nitro groups are arranged symmetrically in this structure **1a**, so that the pulling of electrons by the NO_2 groups is balanced and the ring current has been quite strongly increased; leading to a NICS of the most negative value. On the other hand, the least aromatic ring is **1b** (-10.1 ppm). This indicates that nitro groups have substantial effect on the aromaticity of the rings.

Table 3.29 Calculated NICS (ppm) values for the considered species at B3LYP/6-31G (d, p) level.

	a	**b**	**Dipole moments**[a]	**Symmetry**
1	-13.8	-10.1	2.261	C_2
2	-11.9	-11.5	11.901	C_2
3	-11.6	-11.7	0.057	C_2
4	-11.6	-12.2	5.795	C_1
5	-11.6	-11.6	0.192	C_2
6	-12.4	-12.0	0.001	C_2
7	-11.6	-13.0	0.001	C_i
8	-11.4	-11.4	6.666	C_2
9	-11.9	-12.0	3.208	C_1
10	-11.6	-11.8	6.550	C_1
PCP	-9.6		0.000	D_2
Benzene	-9.9		0.000	D_{6h}

[a] Dipole moments in Debye. a and b refer to the corresponding aromatic ring in the nitro PCPs, see Figure 3.20.

3.3.2.3 Summary of Tetranitroparacyclophane Part

[2,2] Paracyclophane (PCP) has become the archetype of strained compound with bent aromatic rings. Calculations and analysis of tetranitro PCPs show that this series can be a kind of novel energetic materials. They are all endothermic nature but stable compounds. Generally, the closer the nitro groups are the less stable the structure is. Calculation results of detonation velocities and detonation pressures for tetranitro substituted paracyclophanes indicate that they perform similarly to secondary type explosives (like nitroguanidine). However, compared to HMX, RDX, tetranitro PCPs show low detonation performances.

3.3.3 Mono and Polynitro-1,3-oxazetidines as Potential Candidates of High Explosives

3.3.3.1 Brief Information on 1,3-oxazetidines

In this part, 1, 3-oxazetidine main skeleton was taken as the basis for the design of new energetic material candidates by us (see Figure 3.22 for the structures **1**-**13**). Because modern HEDMs derive most of their energy from: i) oxidation of the carbon backbone, and ii) their high positive heats of formation. By substituting the carbon unit with nitrogen, more exotic metastable chemical systems can be obtained. This is especially true if we consider the fact that N_2 is one of the most stable species, therefore, any other arrangement of N_2 molecule into any other chemical system must be higher in energy than the free nitrogen molecule [261]. Another very important property about HEDMs is the oxygen balance (Ω) which is related with the thermochemistry of explosives.

Also we found no evidence of any theoretical or experimental studies of mono and polynitro-substituted 1,3-oxazetidines, to the best of our knowledge. On the other hand, there are few studies about 1,3-oxazetidines concerning its fluro derivatives (experimental studies) [262-264] and about its strain energy (theoretical studies) [265, 266] in the literature. Explosives' corresponding detonation performances depend on particular physical or chemical properties (such as heat of explosion, oxygen balance, and molecular density). In this study, we aimed to investigate the mono and polynitro derivatives of 1, 3-oxazetidines (13 molecules, see Figure 3.22) as potential candidates for HEDMs.

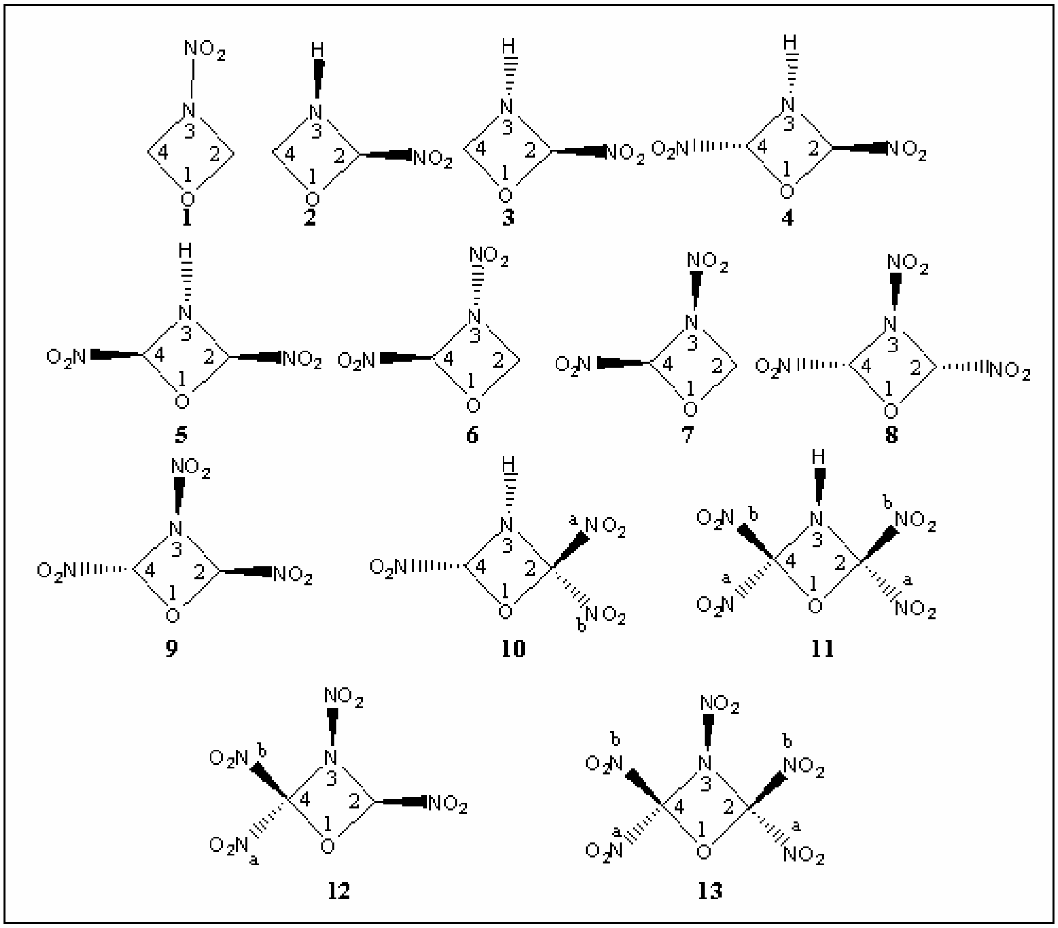

Figure 3.22 The numbering scheme and molecular structures of mono and polynitro-1,3-oxazetidines.

3.3.3.2 Results and Discussions on Mono and Polynitro-1,3-oxazetidines

Figure 3.22 shows the chemical structures of considered mono and polynitro derivatives of 1, 3-oxazetidines (**1–13**) and numbering system. The geometry optimized structures of the molecules and direction of the dipole moments calculated at the UB3LYP/6-311+G (d, p) level are presented in Figure 3.23. The bond lengths for the geometry optimized structures at the same theoretical level are presented in Table 3.30. The numbering in Table 3.30 is consistent with the numbering scheme employed in Figure 3.22. In the literature, as mentioned before no X-ray diffraction study exists for the considered molecules **1-13**. The position of the nitro group affected the bond lengths in four membered rings were seen in the Table 3.30. Comparing the nitramine bond (N-NO_2) lengths among them, the longest bond length (1.558Å) belongs to **13,** whereas the smallest one (1.392Å) belongs to **1**. Interestingly, comparing the calculated bond lengths of C-NO_2 among the considered molecules, **2** has the longest bond length, value of 1.590Å, whereas **13** which has bond length (C-NO_2) value of 1.555 Å The nitramine bond N-NO_2 was found to be smaller than the C-NO_2 bond in the case of these compounds. The shortened N-N bond lengths and planar amino geometry usually seen together in nitramines have been explained by invoking conjugation of a “p”-type lone pair on the amino nitrogen with the π-electron system of the nitro group [238]. Also C-N (C2-N3, N3-C4) bonds in the rings are found to be longer than C-O (O1-C2, C4-O1) bonds (see Table 3.30).

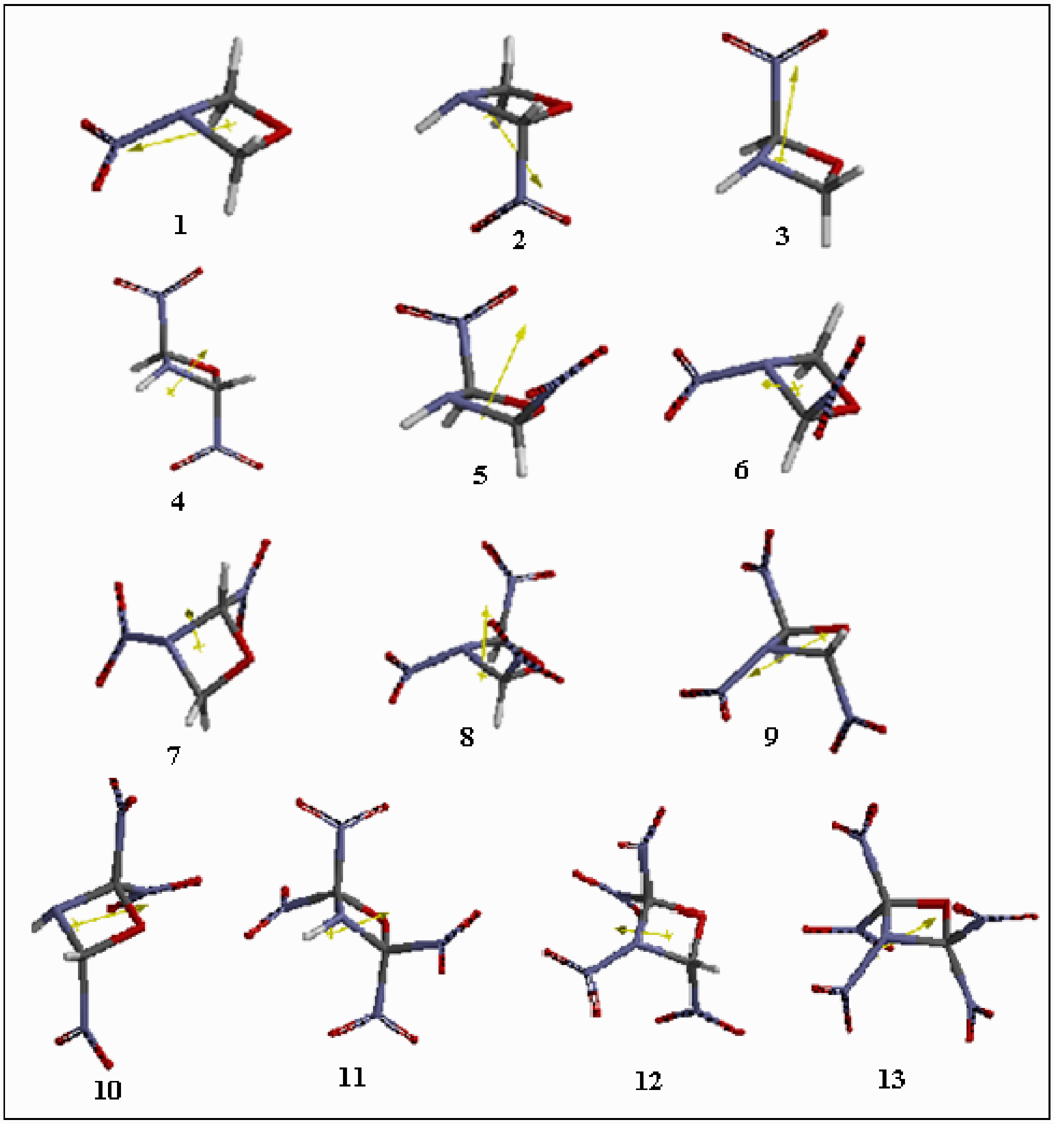

Figure 3.23 The geometry optimized (UB3LYP/6-311+G (d, p)) structures and direction of the dipole moments for **1-13**.

(Colors stand for; black: carbon, blue: nitrogen, red: oxygen, white: hydrogen)

Table 3.30 Some calculated bond lengths (Å) of mono and polynitro 1,3-oxazetidines at UB3LYP/6-311+G (d,p) level of theory.

	O1-C2	**C2-N3**	**N3-C4**	**C4-O1**	**N3-NO$_2$**	**C2-NO$_2$ a (b)**	**C4-NO$_2$ a (b)**
1	1.438	1.479	1.479	1.438	1.392		
2	1.399	1.432	1.476	1.458		1.590	
3	1.394	1.441	1.478	1.452		1.570	
4	1.415	1.445	1.440	1.415		1.551	1.563
5	1.412	1.445	1.445	1.412		1.544	1.544
6	1.451	1.480	1.452	1.398	1.410		1.558
7	1.457	1.475	1.449	1.398	1.403		1.571
8	1.426	1.444	1.444	1.426	1.420	1.539	1.539
9	1.412	1.450	1.445	1.421	1.418	1.559	1.547
10	1.391	1.421	1.444	1.435		1.562 (1.549)	1.544
11	1.406	1.426	1.426	1.406		1.546 (1.552)	1.546 (1.552)
12	1.436	1.435	1.426	1.397	1.425	1.548	1.552 (1.567)
13	1.403	1.440	1.440	1.403	1.558	1.555 (1.555)	1.555 (1.555)

See Figure 3.22 for a and b for structures **10-13**.

Table 3.31 shows the calculated total energies in atomic units and relative energies in kJ/mol at UB3LYP/6-311+G (d, p) and T1 levels of theory. As seen from the table, generally a good agreement of stability order among the calculated energies has been found. Within the limitations of the levels of the theory used, the most stable compound in terms of total energy consideration is **2** and the least stable one is isomer **1** among the mononitro substituted molecules. **2** is more stable than **3** about 7 kJ/mol. The calculated non-bonded distance between the hydrogen attached to the nitrogen (N3) and oxygen of nitro group in **2** is found to be 2.372 Å at UB3LYP/6-311+G(d,p) level, thus there might be some stabilizing interaction (like some extension of intra molecular hydrogen bonding) of this configuration rather than **3**. Among the dinitro substituted ones, the stability order is in terms of total energy is: **4**>**5**>**6**>**7** at the UB3LYP/6-311+G(d,p) level, whereas the stability order is: **4**>**5**>**7**>**6** at T1 method. Among the trinitro 1, 3-oxazetidines, **10** is the most stable species (see Table 3.31). As clearly seen from the Table 3.31, nitramine type molecules are less stable than the compounds lacking of nitramine type bonds. Also steric interactions are the other factor that affects the stability order among the molecules considered here.

Table 3.31 Calculated energies at UB3LYP/6-311+G(d,p) and T1 levels.

	UB3LYP/6–311+G(d,p)		**T1**	
	Total E. (a.u)	**Rel. E. (kJ/mol)**	**Total E. (a.u)**	**Rel. E. (kJ/mol)**
1	-413.6708695	55	-412.9411690	62
2	-413.6917280	0	-412.9648944	0
3	-413.6892466	7	-412.9622449	7
4	-618.2476683	0	-617.1799416	0
5	-618.2436317	11	-617.1757269	11
6	-618.2234176	64	-617.1534283	70
7	-618.2230492	65	-617.1555588	64
8	-822.7668465	57	-821.3572877	72
9	-822.7701351	48	-821.3631800	57
10	-822.7884668	0	-821.3847661	0
11	-1027.3246600	0	-1025.5869880	0
12	-1027.2969870	73	-1025.5619280	66
13	-1231.8154170	-	-1229.7399160	-

Atomic units, 1 hartree = 2625.5 kJ/mol.

Table 3.32 tabulates the calculated HOMO (highest occupied molecular orbital) and LUMO (lowest unoccupied molecular orbital) energies of the structures considered at UB3LYP/6-311+G (d, p) level. The sensitivity of energetic materials to charge development is mainly dictated by the frontier orbital energies. In the case of the energy difference between HOMO and LUMO energy levels ($\Delta\varepsilon = \varepsilon_{LUMO} - \varepsilon_{HOMO}$), the order is: **1**>**6**>**8**>**7**>**5**>**12**>**9**>**3**>**11**>**10**>**4**>**13**>**2**. The stability here refers to the chemical or photochemical processes with electron transfer or electron leap. It is well known that hard molecules have a large HOMO-LUMO gap, and soft molecules have a small HOMO-LUMO gap. Accordingly, soft molecules will be less stable than similar hard molecules. As a result of performed DFT method, molecule **1** is hard molecule. As seen from the Table 3.32, substitution of nitro lowers both the HOMO and LUMO levels.

Table 3.32 The calculated HOMO and LUMO energies and dipole moments.

	UB3LYP/6–311+G(d,p)			
	HOMO	**LUMO**	**Δε**	**Dipole M.**
1	-8.122	-2.287	5.835	2.71
2	-7.775	-2.644	5.131	3.43
3	-7.731	-2.352	5.380	5.38
4	-8.639	-3.410	5.229	1.95
5	-8.450	-2.976	5.474	6.11
6	-8.851	-3.136	5.715	3.51
7	-8.723	-3.223	5.500	4.35
8	-9.302	-3.625	5.677	3.78
9	-9.311	-3.928	5.384	1.52
10	-9.130	-3.806	5.324	3.26
11	-9.565	-4.217	5.348	1.66
12	-9.527	-4.102	5.424	3.20
13	-9.713	-4.524	5.189	0.48

$\Delta\varepsilon = \varepsilon_{LUMO} - \varepsilon_{HOMO}$ (ε in eV) and dipole moments in Debye.

Thermal stabilities of presently considered species **1-13** are mainly related to the energy required for the initial reaction of decomposition. As mentioned previous sections, the common initial step of the thermal decomposition of nitramines is the NO_2 fission reaction through breaking of N-NO_2 bond. So dissociation energy of the weakest bond in the molecule of energetic material is thought to play an important role in the initiation events. Table 3.33 summarizes the computed homolytic BDE values of C-NO_2 and N-NO_2 bonds for the presently considered species (**1-13**) at UB3LYP/6-311+G (d, p) level of theory. The BDEs include BSSE (basis set superposition error) and ZPVE (zero-point vibration energy) corrections. For the initial stages in their thermal decompositions, it can be deduced on the basis of the weakest BDE value that the relative stability order (or sensitivity order) of these isomers may be in the following sequence: **3**>**2**>**4**>**5**>**1**>**11**>**10**>**6**>**7**>**9**>**8**>**12**>**13** (see Table 3.33). As a result of the calculations, N-NO_2 bond is found to be weaker than the C-NO_2 bond. Also

BDE calculation indicates that when the number of nitro substituent increases, the bond strength decreases and sensitivity increases (for example **13** has value of 66.2 kJ/mol and **12** has value of 92.8 kJ/mol). Based on the calculated homolytic bond dissociation energies and in the light of literature knowledge [204] about definition of HEDMs (in terms of the weakest bond in the energetic or candidate molecule), we can conclude that the molecules in Figure 3.23 are all viable candidates for HEDMs (except **13**).

Table 3.33 Calculated homolytic bond dissociation energies in kJ/mol at UB3LYP/6-311+G (d, p) level of theory.

	BDE of C-NO_2 and N-NO_2 bonds
1	135
2	196.6
3	198.0
4	190.6
5	187.0
6	124.7 (173.9)
7	1.224
8	114.9 (166.7)
9	115.2 (173.1)
10	128.9
11	134.2
12	92.8 (117.2)
13	66.2 (89.0)

The BDE values in paranthesis belong to the C-NO_2 bonds in corresponding molecules.

Tables 3.34 and 3.35 tabulate the predicted densities and detonation properties of the concerned structures (**1-13**). The oxygen balance (*Ω*) and heats of formation (HOF) values were also calculated and listed in the tables. Furthermore, we have calculated the heat of formations at different approaches. Based on different heat of formation calculations, detonation parameters are presented in the table and the results show parallelism. All these data gave some clue about the explosive character of the molecules so far unknown compounds in the literature. The position of nitro group in the ring also has an important effect on the explosive properties of energetic materials (see Table 3.34 and 3.35). It was clear that in nitro-substituted 1,3-oxazetidines, density (ρ), velocity of detonation (D) and detonation pressure (P) all increase with increasing number of the nitro groups. This might show good group additivity on the detonation properties and also supports the claim that introducing more nitro substituents into a molecule usually helps to increase its detonation performance. On the other hand, in order to better understand the results of these detonation performance calculations, we also calculated detonation parameters of the well-known explosive TNAZ which is closely related to 1,3-oxazetidine structure, at the same theoretical treatment. According to the calculations, TNAZ has detonation velocity of 8.96 km/s (8.73 km/s literature value) and detonation pressure value of 35.6 GPa (37.2 GPa literature value), here the heat of formation values calculated at PM3 level. For RDX and HMX, experimental values of D are 8.75 km/s, 9.10 km/s, respectively [206]. Comparing these values (TNAZ, RDX and HMX) with the structures **1-13**, one finds seven structures **7-13** to be more powerful explosives than the famous explosives TNAZ, HMX and RDX. In terms of the bond strengths, we calculated the N-NO_2 bond dissociation energy in TNAZ, we found the value of it 101 kJ/mol. Thus, except structure **13**, all polynitro1,3-oxazetidines have higher homolytic bond dissociation energy value of N-NO_2 than the critical bond value of 84 kJ/mol. These structures (**1-12**) can be novel potential candidates for high energy density materials (HEDMs) when they are successfully synthesized. On the other hand, an increase in oxygen balance and heat of formation generally increase the sensitivity of an explosive as well as performance as the specific impulse of a propellant is proportional to the square root of its heat of formation [28, 206]. Based on this knowledge, structures **8-13** might be rather sensitive explosives due to their high oxygen balance (Ω) values (see Tables 3.34 and 3.35). BDE calculations indicate that **12** and **13** possess really weak bonds (see Table 3.33).

Table 3.34 Predicted densities and detonation properties of the concerned molecules.

	1	**2**	**3**	**4**	**5**	**6**
ρ (gcm$^{-3)}$	1.621	1.595	1.597	1.792	1.791	1.793
Ω (%)	-46.13	-46.13	-46.13	-5.37	-5.37	-5.37
Ω (%)	-15.38	-15.38	-15.38	16.10	16.10	16.10
V[a] (cm^{3}/mol)	64.195	65.263	65.148	83.198	83.217	83.146
M (g/mol)	104.065	104.065	104.065	149.062	149.062	149.062
HOF [b] (kJ/mol)	16.04	-45.52	-38.54	-55.47	-44.02	13.31
Q [b] (kJ/kg)	6700	6108	6175	6686	6763	7148
D [b] (m/s)	8107	7836	7864	8937	8959	9091
P [b] (GPa)	27.32	25.26	25.46	35.34	35.50	36.58
HOF [c] (kJ/mol)	-56.622	-102.219	-102.399	-107.795	-99.226	-56.693
Q [c] (kJ/kg)	6002	5563	5561	6335	6393	6658
D [c] (m/s)	7887	7655	7661	8817	8834	8931
P [c](GPa)	25.86	24.1	24.16	34.40	34.51	35.30

[a] Average volume from 100 single-point calculations at the B3LYP/6-31G(d,p) level.

[b] Heat of formation values obtained from the T1 method.

[c] Heat of formation values obtained from the PM3 method.

Table 3.35 Predicted densities and detonation properties of the concerned molecules.

	7	**8**	**9**	**10**	**11**	**12**	**13**
ρ	1.825	1.931	1.922	1.901	2.012	2.025	2.104
Ω	-5.37	16.49	16.49	16.49	30.12	30.12	39.43
Ω	16.10	32.98	32.98	32.98	43.51	43.51	50.70
V[a]	81.67	100.482	100.974	102.094	118.835	118.07	134.983
M	149.062	194.059	194.059	194.059	239.056	239.056	284.053
HOF [b]	8.14	35.00	17.43	-33.73	-5.93	54.79	146.07
Q [b]	7113	7514	7423	7160	7480	7734	8136
D [b]	9194	9823	9761	9598	10170	10329	10784
P [b]	37.8	44.6	43.92	42.19	48.89	50.70	56.35
HOF [c]	-53.633	-37.768	-45.874	-91.445	-67.4	-24.846	28.498
Q [c]	6699	7139	7082	6862	7223	7402	7722
D [c]	9057	9699	9647	9496	10081	10216	10644
P [c]	36.68	43.47	42.89	41.31	48.04	49.60	54.90

[a] Average volume from 100 single-pointcalculations at the B3LYP/6-31G(d,p) level.

[b] Heat of formation values obtained from the T1 method.

[c] Heat of formation values obtained from the PM3 method.

3.3.3.3 Summary of Mono and Polynitro-1,3-oxazetidines Part

1,3-oxazetidines having various numbers of nitro groups have been investigated by using quantum chemical calculations in order to find some novel potential candidates of HEDMs. The stabilities of these compounds were investigated in terms of the total energy and homolytic BDE values of N-NO_2 and C-NO_2 bonds. Accordingly, the C-NO_2 bond scission leads to the lowest sensitivity, the N-NO_2 bond rupture results in high sensitivity. To consider the initial step in thermal decompositions via the N-NO_2 bond scission, the sensitivity of **13** is the highest among all the title compounds. The detonation properties have been investigated and found that there might be some candidates of HEDMs among the investigated structures so far not reported in the literature. If these molecules can be synthesized successfully, they may be the potential candidates of the powerful energetic materials but some of them might be so sensitive due to very high oxygen balance values.

CHAPTER 4

CONCLUSION

Manufacture, development and testing of a new explosive is so costly in time and money, thus theoretical methods can help to eliminate any poor candidate due to performance or sensitivity reasons. Additionally, rapid development of computer technology and theoretical chemistry provide scientists with a more rigid and accurate approach to explosive phenomena. In the present study, our main objective has been to design novel energetic materials or suggest better candidates for high energy density materials without using sophisticated computational codes, e.g. TIGER. All the computed values in this study should be considered within the limitations of the Kamlet-Jacobs equations used and performed DFT calculations which are used mainly for the purpose of finding the densities of the molecules. In order to succeed this aim, initially well-known explosives were investigated, and based on structures of these well-known energetic molecules; some structural modifications were architected e.g constitutional isomers. Meanwhile, the tautomerism and charging effects on these well-known explosives' performances were analyzed in detail by using the molecular orbital approach. Totally 65 molecules were studied in a systematic way, and 54 of them were handled for the first time in the literature.

Stabilities of these compounds were investigated in terms of the total energy, heat of formation values and homolytic bond dissociation energy (BDE) values of N-NO_2, C-NO_2, O-NO_2, S- NO_2 bonds.Of these, S-NO_2 group has been handled for the first time in the literature for the explosive capability. The detonation properties have been investigated and found that there might be some candidates of HEDMs among these 54 studied molecules so far not mentioned in the literature. Table 4.1 tabulates some of the considered molecules as potential candidates of HEDMs and compares them with well-known and widely-used explosive molecules today.

Table 4.1 Some of the presently considered molecules and their detonation velocities and oxygen balance values and the respective values of some well known explosives. The values in parenthesis belong to the experimental values.

		Ω (%)	**D (m/s)**
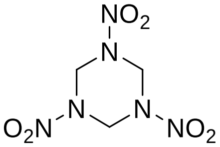	**RDX**[a]	-21.6	8830[b] (8750)
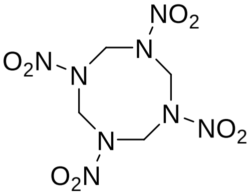	**HMX**[a]	-21.6	8990[b] (9100)
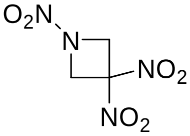	**TNAZ**[a]	-16.66	8960[b] (8730)
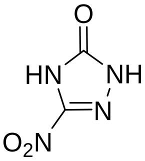	**NTO**[a]	-24.6	7950[b] (7940)

Table 4.1 Continued

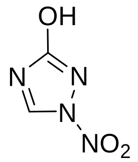	**3A**	-24.6	8210[c]
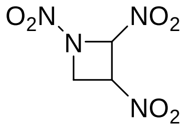	**2**	-16.66	9050[c]
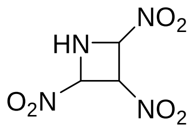	**5**	-16.66	8880[c]
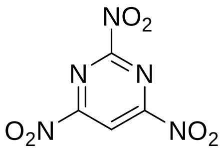	**246**	-18.60	8560[c]
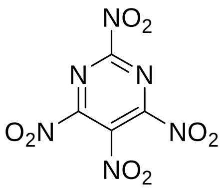	**2456**	0.00	9230[c]
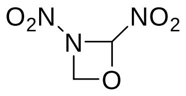	**6**	-5.37	8931[c]
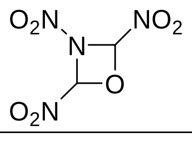	**8**	16.49	9699[c]

a Already existing explosives.
b Presently calculated values for the existing molecules.
c Calculated for presently proposed structures.

Conducted computational approach was mentioned in the results and discussion part about these molecules seen in Table 4.1. As it is clear from the Table 4.1, some of the designed molecules in this study show superior performance values compared to the well-known explosives. For example, based on the computed detonation performances and densities, some of the constitutional isomers of TNAZ might be better explosive than TNAZ (**1**) in terms of detonation parameters and sensitivity considerations. Furthermore, polynitro-1,3-oxazetidines have better performance than the RDX (Ω=-21.6) and TNT (Ω=-73.9). On the other hand, these polynitro-1,3-oxazetidines might have some sensitivity drawback due to high oxygen balance values, they should be more sensitive explosives, whereas structure **6** which is a derivative of 1,3-oxazetidine (Ω value (-5.37%) is not high so it is not expected to be sensitive energetic material), can be better alternative to TNAZ (**1**).Based on the calculated homolytic bond dissociation energy values, structure **6** (BDE value of 125 kJ/mol value) is even more insensitive than the TNAZ(**1**) (BDE value of 101 kJ/mol value).

Hence, if these molecules can be synthesized successfully, they may be the potential candidates for powerful energetic materials. Thus, the present study has shed some valuable light on to the new energetic materials.

REFERENCES

1. Akhavan, J., The Chemistry of Explosives, The Royal Society of Chemistry, Cambridge 1998.

2. Alam, N., Dictionary of Explosions & Explosives, Tisha Printers, Bangladesh 2005.

3. Davis, T., The Chemistry of Powder and Explosives, Angriff Press, 1943.

4. Türker, L., Gümüş, S., Atalar, T., Çamur Y., "Theoretical Treatment of some Novel Nitropyrimidines", in New Research on Hazardous Materials, Nova Publishers, 2007.

5. Brunswing, H., Explosivstoffe. Barth: Braunschweig; 1909, p.17.

6. Pletz, V.M., Zh. Obshch. Khim. 1935, 5, 173.

7. Lothrop W.C.; Handrick, G.R.The Relationship between Performance and Constitution of Pure Organic Explosive Compounds. Chem. 1949, 44, 419-445.

8. Schmidt, A., Chimie et Industrie 1952, 67, 253.

9. Stettbacher, A.,Die Sensibilität der Azide Angew. Chem. 1917, 30, 269.

10. Smolenski, D; Czuba, W. Zeszyty Nauk. Polit. Wroclawskiej, Chemia 1955, 2, 3-10.

11. Wöhler, L; Wenzelberg, O.Neues zur Schlagempfindlichkeit der Explosivstoffe. Angew. Chem. 1933, 46, 173-176.

12. Urbanski, T. Chemistry and technology of explosive, Warszawa, 1961; Vol. 10, 1-3.

13. Suceska, M., Test Methods for Explosives, Springer-Verlag, New York1995.

14. Cooper, P. W., Explosives Engineering, Wiley-VCH, New York 1996.

15. Politzer, P. A., Murray, J. S., Detonation, Combustion Theoretical and Computational Chemistry, Vol. 13, Chapter 7, Elsevier.

16. Fickett, W., Davis, W. C., University of California Press, Berkeley, 1979.

17. Andersen, W. H.Comments on “The chemistry of detonations, Combustion and Flame, 45 (1982) 309-316

18. Chapman, D. L., Philos, Mag, 47 (1899) 90.

19. Joguet, E., Mathem J., 6 (1904) 5.

20. Dremin, A. N., Towards detonation theory, Journal de Physique IV 5 (1995) C4-259-276.

21. Keshavarz, M. H., Simple procedure for determining heats of detonation, Thermochimica Acta, 428 (2005) 95-99.

22. Kamlet, M. J., Jacobs, S. F.Chemistry of Detonations. I. A Simple Method for Calculating Detonation Properties of C—H—N—O Explosives, J. Chem. Phys. 48 (1968) 23.

23. Kamlet, M. J., Ablard, J. E.Chemistry of Detonations. II. Buffered Equilibria, J. Chem. Phys. 48 (1968) 36-42.

24. Kamlet, M. J., Dickenson, C.Chemistry of Detonations. III. Evaluation of the Simplified Calculational Method for Chapman-Jouguet Detonation Pressures on the Basis of Available Experimental Information, J. Chem. Phys. 48 (1968) 43.

25. Kamlet, M. J., Hurwitz, H. J.Chemistry of Detonations. IV. Evaluation of a Simple Predictional Method for Detonation Velocities of C–H–N–O Explosives, J. Chem. Phys. 48 (1968) 3685-3692.

26. Hurwitz, H. J., Kamlet, M. J., Israel J. Tech. 7 (1968) 431.

27. Kamlet, M. J., Short, J. M.The chemistry of detonations. VI. A “Rule for Gamma” as a criterion for choice among conflicting detonation pressure measurements, Combust. Flame 38 (1980) 221.

28. Sikder, A. K., Sikder, N.1,3,3-Trinitroazetidine (TNAZ), a melt-cast explosive: synthesis, characterization and thermal behaviour, Journal of Hazardous Materials, A 112 (2004) 1.

29. Olah, G. A., Squire, D. R., Chemistry of Energetic Materials, Academic Press 1991.

30. Politzer, P. A., Murray, J. S., Energetic Materials, Part 1. Decomposition, Crystal and Molecular Properties Theoretical and Computational Chemistry, Vol. 12 Chapter 3, Elsevier 2003.

31. Sung, K. S., Wu, R. R., Sun, S. Y.Keto-enol tautomerism of -ketoamides and characterization of a sterically crowded -amido--ketoamide, J. Phys. Org. Chem. 15 (2002) 775-781.

32. Su, C. C., Lin, C. K., Wu, C. C., Lien, M. H.Keto-enol tautomerism of -ketoamides and characterization of a sterically crowded -amido--ketoamide, J. Phys. Chem. A. 103 (1999) 3289.

33. Rapport, Z., The Chemistry of Enols, Wiley Chichester, UK 1990.

34. Lammertsma, K., Prasad, B. V., J. Am. Chem. Soc., 116 (1994) 642.

35. Lin, J. F., Wu, C. C., Lien, M. H.Ab Initio Study on the Imine-Enamine Tautomerism of the .alpha.-Substituted Imines (XH2CCH:NH, X = H, BH2, CH3, NH2, OH, F, Cl, CN, NO), J. Phys. Chem. 99 (1995) 16903.

36. Long, J. A., Harris, N. J., Lammertsma, K., Formaldehyde oxime Nitrosomethane Tautomerism, J. Org. Chem. 6 (2001) 6762-6767.

37. Deleare, D., Raspoet, G., Nguyen, M. T., Thiol-Thione tautomersim in Thioformic acid: Importance of specific solvent interactions, J. Phys. Chem. A. 103 (1999) 171-177.

38. Wong, W. M., Wilberg, K. B., Frisch, M. J., Solvent effects.3. Tautomeric equilibra of formamide and 2-pyridone in the gas phase and solution: ab initio and SCRF study, J. Am Chem. Soc. 114 (1992) 1645-1652.

39. Albert, J., Gonzalez, A., Grannel, J., Moragas, R., Solans, X., Font-Bardia, M., Hydrazo-keto and azo-enol tautomerism in organometallic palladacycles. New bidentate monoanionic and tridentate bianionic ligands**,** J. Chem. Soc. Dalton Trans. 11 (1998) 1781-1786.

40. Nikiforov, E., Russ. Chem. Rev. 35 (1996) 817.

41. Manelis G. B., Nazin G. M., Rubtsov Yu. I., Strunin V. A., Thermal decomposition and combustion of explosives and powders, Taylor & Francis Group, CRC Press, Boca Raton, 2003.

42. Bharatam P. V., Lammertsma K. I., Nitro = aci-nitro tautomerizm in high-energetic nitro compounds, in: Politzer P., Murray J. (Eds.), Theoretical and computational chemistry, Vol. 13, Energetic Materials, Part 1, Detonation, combustion, Elsevier B. V., Amsterdam, 2003, 61.

43. Zeman, S., Atalar, T., Friedl, Z., Ju, X. H., Central European of Energtic Materials, in press.

44. Turker, L.Quantum chemical studies on charged forms of nitroglycerine, Journal of Molecular Structure (THEOCHEM) 680 (2004) 41.

45. M.A. Cook, The science of high explosives, Robert E. Krieger Pub. Co. Inc, New York, 1971.

46. H. Kolsky, Electromagnetic waves emitted on detonation of explosives, Nature 73 (1954) 77.

47. T. Takakura, Publ Astronom Soc Jpn 7 (1955) 210.

48. Davis, W. C., High Explosives the Interaction of Chemistry and Mechanics, Los Alamos.

49. Klapotke, T. M., Mingos, D. M. P., High Energy Density Materials, Springer, Vol. 125 2007.

50. Politzer, P., Murray, J. S., Energetic Materials, Part 1. Overview of Research in Energetic Materials (Rice, B. M.), Elsevier, 2003.

51. Sanderson, A. J., What makes a useable new energetic materials, Journal de Physique IV, 5 (1995) C4-573-580.

52. Smirnov, L. P., Chemical physics of decomposition of energetic materials, Problems and prospects, Russian Chemical Reviews, 73 (11) (2004) 1121-1141.

53. Shaw, R. W., Brill, T. B., Thompson, D. L., Advanced Series in Physical Chemistry 16, Overview of Recent Research on Energetic Materials, World Scientific, New Jersey.

54. Politzer, P., Murray, J. S., Energetic Materials, Part 1.Molecular Dynamics Simulations of Energetic Materials Chapter 6, Vol. 12, Elsevier, 2003.

55. Fried, L. E., Riad, M., Pagoria, P. F., Simpson, R. L., Annu. Rev. Mater. Res. 31 (2001) 291.

56. Bakhmatova, E. A., Korolev, V. L., Pivina, T. S., Central European Journal of Energetic Materials, 3 (4) (2006) 3.

57. Ilyushin, M. A., Tselinsky, I. V., Bachurina, I. V., Gruzdev, Y. A., Sinditskii, V. S., Serushkin, V. V., Egorshev, V. Y., Central European Journal of Energetic Materials, 3 (4) (2006) 41.

58. Agrawal, J. P., Hodgson, R. D., Organic Chemistry of Explosives, John Wiley & Sons, USA 2007.

59. Adam, C., New Directions in Energetic Materials, J. Def. Sci. 1 (3) (1997) 319.

60. Badgujar, D. M., Talawar, M. B., Asthana, S. N., Mahulikar, P. P.Advances in science and technology of modern energetic materials: An overview, Journal of Hazardous Materials, 151 (2008) 289-305.

61. Shreeve, J. M., Meshri, D. T., Verma, R. D., Singh, R. P.,Recent Developments in High Nitrogen Energetic Salts Including Ionic Liquids, Angew. Chem. Int. Ed. 45 (2006) 3584.

62. Klapotke, T. M., Steinhauser, G., "Green" Pyrotechnics: a chemists's challenge, Angew. Chem. Int. Ed. 47 (2008) 3330-3340.

63. Politzer, P., Murray, J. S., Seminario, J. M., Lane, P., Grice, M. E., Concha, M.C.Computational characterization of energetic materials, Journal of Molecular Structure (THEOCHEM), 573 (2001) 1-10.

64. Zhang, M. X., Eaton, P., Gilardi, E. R.Hepta- and Octanitrocubanes, Angew Chem. Int. Ed. (Engl) 39 (2000) 401-404.

65. Astakhov, A. M. Stepanow, R. S., Yu, Babushkin, A. Combustion Explosion Shock Waves 34 (1998) 85.

66. Zhang, G. F. J., Xiao, H. X. Gong,Theoretical studies on heats of formation for polynitrocubanes using the density functional theory B3LYP method and semiempirical MO methods J. Phys. Org. Chem. 14 (2001) 583–588.

67. Nielsen, A. T. Nirtrocarbons, VCH-Verlagsgesell Schaft, Weinheim 1995 97.

68. Eaton, P. E., Tang, D., Gilardi, R. A structural reassignment, J. Org. Chem., 66 (4) (2001) 1492-1493.

69. Politzer, P., Murray, J. S., Grice, M. E., Sjobers, P., in: Olah, G.A., Squire D.A. (Eds.), Chemistry of Energetic Materials, Academic Press, San Diego, 1990 89.

70. Sollot, G.P., Gilbert, E. E., A facile route to 1,3,5,7-tetraaminoadamatane, Synthesis of 1,3,5,7-tetranitroadamantane, J. Org. Chem. 45 (1980) 5405-5408.

71. Urbanski, T. Chemistry and Technology of Explosives, vol. 1, Pergamon, PWN-Polish Scientific Publishers, Warzawa, 1965.

72. Sheremetev, A. B., The chemistry of furazans fused to six and seven memeberede heterocycles with one heteroatom, Russ. Chem. Rev. 68 (1999) 137.

73. Coburn, M. D., Singleton, J. L., J. Heterocycl. Chem. 9 (1972) 1039.

74. Jadhav, H. S., Talwar, M. B., Dhavale, D.D., Asthana, S.N., Krishnamurthy, V. N., Ind. J. Heterocycl. Chem. 15 (4) (2006) 383.

75. Ritter, H., Licht, H. H.Synthesis and Characterization of Methylnitramino-Substituted pyridines and triazines, Propellants Explosives Pyrotechnics 18 (1993) 81.

76. Coburn, M. D., Explosives Synthesis at Los Alamos Proceedings of the American Defense Preparedness Association Compatibility of Plastics and Other materials with Explosives, Propellants, Pyrotechnics and Processing of Explosives, Propellants and Ingredients, Long Beach, California, 1986.

77. Nadentla, R. R., Molecular Modeling: A powerful tool for drug design and molecular docking, Resonance, (2004) 51-60.

78. Cramer, C. J., Essentials of Computational Chemistry, John-Wiley, 2004.

79. Hinchliffe, A., Computational Quantum Chemistry, John Wiley & Sons Ltd., New York, 1998

80. Richards, G. W., Cooper, D. L., Ab Initio Molecular Orbital Calculations for Chemists, Oxford University Press, New York, 1983.

81. Hehre, W. J., Random, L., Scheleyer, P. v. R., Pople, J. A. Ab Initio Molecular Orbital Theory; John Wiley & Sons: New York, 1986.

82. Daniel F.-Villar et al., On the limits of the HOMO driven reactions: The frontier effective for reaction molecular orbital concept, J. Phys. Chem. A 110 (2006) 1031-1040.

83. Stewart, J. J. P., Encyl. Comput. Chem. 3 (1998) 2080.

84. Holder, A. J., Encyl. Comput. Chem. 1 (1998) 8.

85. Young, D. C., Computational Chemistry, Wiley-Interscience, New York, 2001.

86. Jensen, F., Introduction to Computational Chemistry, John Wiley & Sons, New York 1999.

87. Levine, N., Quantum Chemistry, Prentice Hall, Englewood Cliffs, 1991.

88. Stubber, J. L., Paldus, J., Fundamental World of Quantum Chemistry, 1 (2003) 67.

89. Li, X., Paldus, J., Recent Advances in Computational Chemistry, 3 (1997) 183.

90. Pople, J.Nobel Lecture: Quantum chemical models , Reviews on Modern Physics, 7(5) (1999) 1267.

91. Møller, C.; Plesset, M. S. ,Note on an approximation many body electron system, *Phys. Rev.* 46 (1934) 618-622.

92. Cizek, J.On the Correlation Problem in Atomic and Molecular Systems. Calculation of Wavefunction Components in Ursell-Type Expansion Using Quantum-Field Theoretical Methods *J. Chem. Phys.*, 1966, 45, 4256.

93. Cizek, J. *Adv. Chem. Phys.* 14 (1969) 35.

94. Bartlett, R. J.Coupled-cluster approach to molecular structure and spectra: a step toward predictive quantum chemistry *J. Phys. Chem.* 1989, *93*, 1697-1708.

95. Sousa, S. F., Fernands, P. A., Ramos, M. J., J. Phys. Chem. A 111 (2007) 10439

96. Fermi, E., Rend. Accad. Naz. Lincei, 6 (1927) 602.chem phys

97. Thomas, L. H., Proc. Cambridge Philos. Soc. 23 (1927) 542.

98. Hohenberg, P., Kohn, W., Phys. Rev. B 136 (1964) 864.

99. Kohn, W., Sham, L.Self-Consistent Equations Including Exchange and Correlation Effects , J. Phys. Rev. A 140 (1965) 1133.

100. Becke, A. D.A new mixing of Hartree–Fock and local density-functional theories, J. Chem. Phys. 98 (1993) 1372.

101. Becke, A. D.Density-functional thermochemistry. IV. A new dynamical correlation functional and implications for exact-exchange mixing, J. Chem. Phys. 104 (1996) 1040.

102. Becke, A. D.Density-functional exchange-energy approximation with correct asymptotic behavior, Phys. Rev. A 38 (1998) 3098.

103. Perdew, J. P., Unified Theory of Exchange and Correlation Beyond the Local Density Approximation. In Electronic Strycture of Solids, 91 Ziesche, P., Esching, H., Eds., Akademie Verlag, Berlin, Germany, 1991.

104. Lee, C., Yang, W., Parr, R. G., Phys. Rev. B 37 (1998) 785.

105. Adamo, C., Barone, V.Exchange functionals with improved long-range behavior and adiabatic connection methods without adjustable parameters: The *m*PW and *m*PW1PW models, J. Chem. Phys., 108 (1998) 664.

106. Perdew, J. P., Schimidt, K., Jacob's ladder of density functional approximation for the exchange-correlation energy, In Density Functional Theory and Its Applications to Materials, Van Doren, V. E., Van Alseoy, K., Geerlings, P., Eds., AIP Press, New York 2001.

107. Krauss, M., Stevens, W. J., Ann. Rev. Phys. Chem., 35 (1984) 357.

108. Klobukowski, M., Huzinaga, S., Sakai, Y., Computational Chemistry Reviews of Current Trends Volume 3 49, Leszcynski, J. Ed., Worl Scientific, Singapore, 1999.

109. Balasubramanian, K., Pitzer, K. S., Adv. Chem. Phys. 67 (1987) 287.

110. Mitchell, K. A. R., Chem. Rev. 69 (1969) 157.

111. Hehre, W. J., Ditchfield, R., Pople, J. A.Self—Consistent Molecular Orbital Methods. XII. Further Extensions of Gaussian—Type Basis Sets for Use in Molecular Orbital Studies of Organic Molecules, *J. Chem. Phys.*, 1972, 56, 2257.

112. Jalbout, A. F., Nazari, F., Turker, L.Gaussian-based computations in molecular science, Journal of Molecular Structure (THEOCHEM), 671 (2004) 1-21.

113. Muthurojan, H., Sivabalan, R., Talawar, M. B., Asthana, S. N.Computer simulation for prediction of performance and thermodynamic parameters of high energy materials, Journal of Hazardous Materials A 112 (2004) 17-33.

114. Stine, J. R., Prediction of crystal densities of organic explosives by group additivity, Los Alamos National Laboratory's Report, New Mexico, 1981.

115. Pivina, T. S., Sukhaclev, D. V., Evtushenko, A. V., Khmelnitskii, L. I., Propel. Explos. Pyrotechn. 20 (1995) 5.

116. Zhang, J., Xiao, H.Computational studies on the infrared vibrational spectra, thermodynamic properties, detonation properties, and pyrolysis mechanism of octanitrocubane, Journal of Chemical Physics, 116 (24) (2002) 10674.

117. Liu, M. H., Chen, C., Hong, Y. S.Theoretical study on the detonation properties of energetic TNAD molecular derivatives, Journal of Molecular Structure (THEOCHEM), 710 (2004) 207.

118. Politzer, P. A., Murray, J. S., (Edts.), Energetic Materials, Part I. Decomposition, Crystal and Molecular Properties Theoretical and Computational Chemistry, Vol. 12, Chapter 6, Elsevier, 2003.

119. Persson, P. A., TIGER, WIN-a window PC code for computing explosive performance and thermodynamic properties, in Proceedings of 2000 High-Tech Seminar, State of the Art Blasting Technology and Explosives Applications, 2000.

120. Fried, L. E., CHEETAH 1.39, Lawrence Livermore National Laboratory 1996.

121. Muthurajan, H., Sivalan, R., Talawar, M., B., Asthana, S. N., Development of Computer Code for Qualitative Prediction of Heat of Formation of High Energetic Materials, New Trends in New Researc of Eneregtic Materials, 2007, 202.

122. Sućeska, M., Evaluation of Detonation Energy from EXPLO5 Computer Code Results, Propellants, Explos. Pyrotech. 24 (1999) 280-285.

123. Frisch, M.F., Trucks, G.W., Schleged, H.B., Scuseria, G.E. , Robb, M.A., J.R. Cheesman, et al., Gaussian 98, Gaussian 03, Gaussian Inc., Pittsburg, PA, 2003.

124. SPARTAN 06, Wavefunction Inc., Irvine CA, USA.

125. Hyperchem program, Hypercube, Canada, 1996.

126. Zeman, S., The study of chemical micromechanism governing detonation initation of organic polynitro and polynitroso compounds, Abridged version of D. Sc. Thesis, Institute of Chemical Technology, Department of Organic Technology, Prague 1997.

127. Zeman, S., Thermal stabilities of polynitro aromatic compounds and their derivatives, Thermochim. Acta. 31 (1979) 269-283.

128. Qasim, M.M., Moore, B., Taylor, L., Honea, P., Gorn, L., Leszczynski, Structural characteristics and reactivity relationships of nitroaromatic and nitramine explosives- a review of our computational chemistry and spectroscopic research, International Journal of Molecular Sciences, 8 (2007) 1234-1264.

129. Saraf, S.R., Rogers, W. J., Mannan, M. S., Prediction of reactive hazards based on molecular structure, Journal of Hazardous Materials A98 (2003) 15-29.

130. Song, X., Cheng, X., Yang, X., Li, D., Linghu, R., Correlation between the bond dissociation energies and impact sensitivities in nitramine and polynitro benzoate molecules with polynitro alkyl groupings, Journal of Hazardous Materials 150 (2008) 317-321.

131. Zhang, C., Review of the stablishment of nitro group charge method and its applications, Journal of Hazardous Materials 161 (2009) 21-28.

132. Khrapkovskii, G.M., Shamsutdinov, T. F., Chachkov, D.V., Shamov, A.G., Energy of the O-NO_2 bond dissociation and the mechanism of the gas-phase monomoleculae decomposition of aliphatic alcohol nitresters, THEOCHEM, 686 (2004) 185-192.

133. Türker, L., Gümüş, S., Atalar, T., Atlanel, S., A theoretical study on nitrourea and its tautomers, Journal of Energetic Materials 26 (2008) 1-16.

134. Gilman, J.J., Phil. Mag. B, 71 (1995) 1057.

135. Mana, M.R., Fried, L.E., Reed, E.J., Explosive chemistry: simulating the chemsitry of energetic materails at extreme conditions, Journal of Computer-Aided Materails Design, 10 (2003) 75-97.

136. Politzer, P., Lane, P., Grice, E.M., Concha, M.C., Redfren, P.C., Comparative computational analysis of some nitramine and difluoroamine structures, dissociation energies and heats of formation, THEOCHEM, 338 (1995) 249-256.

137. Tarver, C.M., Density estimations for explosives and related compounds using the group additivity approach,J. Chem. Eng. Data, 24 (2) (1979) 136-145.

138. Keshavarz, M.H., New method for calculating densities of nitroaromatic explosive compounds, Journal of Hazardous Materials 145 (2007) 263-269.

139. L. Qiu, H.M. Xiao, X.H. Ju, X.D. Gong, Theoretical study of the structures and properties of cyclic nitramines: tetranitrotetraazadecalin (TNAD) and its isomers Int, J. Quantum Chem. 105 (2005) 48–56.

140. X.J. Xu, H.M. Xiao, X.D. Gong, X.H. Ju, Z.X. Chen, Theoretical studies on the vibrational spectra, thermodynamic properties, detonation properties, and pyrolysis mechanisms for polynitroadamantanes, J. Phys. Chem.A109 (2005) 11268–11274.

141. L. Qiu, H. Xiao, X. Gong, X. Ju, W. Zhu, Theoretical studies on the structures, thermodynamic properties, detonation properties and pyrolysis mechanisms of spiro nitramines, J. Phys. Chem. A 110 (2006) 3797–3807.

142. G.S. Chung, M.W. Schimidt, M.S. Gordon, An *ab initio* study of potential energy surfaces for N8 isomers, J. Phys. Chem. A 104 (2000) 5647–5650.

143. J.J. Xiao, J. Zhang, D.Yang, H.M. Xiao, DFT comparative studies on the structures and properties of heterocyclic nitramines, Acta Chim. Sinica 60 (2002) 2110-2114.

144. P.E. Eaton, R.L. Gilardi, M.X. Zhang, Polynitrocubanes: Advanced high-density, high-enegy matrials, Advanced Materials, 12 (2000) 1143-1148.

145. Cho, S.G., Park, B.S., Cho, J.R., Theoretical studies on the structure of 1,2,4,5-tetranitroimidazole, Propellants, Explosives, Pyrotechnics, 24 (1999) 343-348.

146. Wang, G., Xiao, H., Ju, X., Gong, X., Calculation of detonation velocity, pressure, and electric sensitivity of nitro arenes on quantum chemsitry, Propellants, Explosives, Pyrotechnics, 31 (2006) 361-368.

147. Ling, Q. et. al, Theoretical study on the high energy density compound hexanitroazatricyclotetradecanedifuroxan, Chinese Journal of Chemistry, 24 (2006) 1538-1546.

148. Zhang, J.Z., Xiao, J., Xiao, H. Theoretical studies on heats of formation for cubylnitrates using density functional theory B3LYP method and semiemprical MO methods, Internationa Journal of Quantum Chemistry, 86 (3) 2001 305-312.

149. Walker, F.E., A new kinetics and the simplicity of detonation, Journal de Physique IV, 5 (1995) C4-309-335.

150. Klimenko, V.Y., Yakoventsev, M.Y., Dremin, A.N, Mnogoprotsesnaya model' detonatsii (multiprocess model of detonation), Khimicheskaya Fizika, 12 (1993) 671.

151. Kuklja, M., Stefanovich, E., Kunz, A.B., An exitonic mechanism of detonation initation in explosives, Journal of Chemical Physics, 12 (2000) 3417-3423.

152. Kuklja, M.M., Aduev, B.P., Aluker, E.D., Krasheninin, V.I., Krechetov, A.G., Mitrafanov, A.Y., Role of electronic excitations in explosive decomposition of solids, Journal of Applied Physics, 89 (2001) 4156.

153. Türker, L., Atalar, T., *Ab initio* and DFT study on 1,4-dinitroglycoluril configurational isomers: *cis*-DINGU and *trans*-DINGU, Journal of Hazardous Materials A137 (2006) 47–56.

154. J. Boileau, E. Wimmer, R. Gilardi, M. M. Stinecipher, R. Galio, M. Pierrot, Acta Cryst. 44 (1988) 696.

155. J. Boileau, E. Wimmer, M. Carail, R. Gallo, Fr. Bulletin de la Societe Chimique de France, 3 (1986) 465.

156. J. Boileau, E. Wimmer, M. Carail, R. Gallo, Propellants, Explosives, Pyrotechnics, 10(2) (1985) 53.

157. J. Boileau, J. M. Emeury, Y. De Longueville, P. Monteagudo, Chem. Mech. Technol. Treib-Explosivst, (1981),505.

158. L. Jiamin, X. Mod, Chem. Res. Inst., Xian, Peop. Rep. China. Proceedings of the International Pyrotechnics Seminar (1991), 17th (Vol. 1), 322.

159. J. P. Agrawal, Prog. Energy Combust. 24 (1998) 1.

160. J. Li, The Lova Composite explosives containing DINGU, in: Proceedings of the 17th International Pyrotechnology Seminar (Combined with Second Beijing International Symposium on Pyrotechnics & Explosives), Beijing Institute of Technology Press, Beijing, (1991) 322.

161. J.E. London, D.M. Smith, Toxicological study of the high-explosive formulation imidazo [4,5-d]imidazole-2,5(1H,3H)-dione, tetrahydro-1,4- dinitro, Avail. NTIS. Rep. 9 (14) (1984) (Absract no. 26903).

162. J. Boileau, E. Wimmer, R. Gilardi, M.M. Stinecipher, R. Galio, M. Pierrot, Structure of 1,4-dinitroglycoluril, Acta Crystallogr. 44 (1988) 696–699.

163. D. Mathieu, P. Simonetti, Evaluation of solid-state formation enthalpies for energetic materials and related compounds, Thermochim. Acta 384 (2002) 369–375.

164. V.H. Khire, M.B. Talawar, K.V. Prabhakaran, T. Mukundan, E.M. Kurian, Spectro-thermal decomposition study of 1,4-dinitroglycoluril (DINGU), J. Hazard. Mater. A 119 (2005) 63–68.

165. J. Yinon, S. Bulusu, T. Axenrod, Mass spectral fragmentation pathways in some glycoluril-type explosives. A study by collision-induced dissociation and isotope labeling, Org. Mass Spectrom. 29 (11) (1994) 625–631.

166. D. Delpeyroux, B. Blaive, R. Gallo, H. Graindorge, L. Lescop, Modelization by molecular mechanics (and X-rays) of five-membered heterocyclic nitramines, Propell. Explos. Pyrotech. 19 (2) (1994) 70–75.

167. D. Paz, J.G. Luis, J. Ciller, On the use of AM1 and PM3 methods on energetic compounds, Propell. Explos. Pyrotech. 18 (1) (1993) 33–40.

168. B.M. Rice, S. Sahu, F.J. Owens, Density functional calculation of bond dissociation energies for NO2 scission in some nitroaromatic molecules, J. Mol. Struct. (THEOCHEM) 583 (2002) 69–72.

169. J. Shao, X. Cheng, X. Yang, Density functional calculations of bond dissociation energies for removal of the nitrogen dioxide moiety in some nitroaromatic molecules, J. Mol. Struct. (THEOCHEM) 755 (2005) 127–130.

170. S.F. Boys, F. Bernardi, The calculation of small molecular interaction by the differences of separate total energies: some procedures with reduced errors, Mol. Phys. 19 (1970) 553–566.

171. Q. Zhao, S. Zhano, Q.S. Li, The influence of ring strain and conjugation on the reaction energies of the NO2 fission of nitramines: a DFT study, Chem. Phys. Lett. 407 (2005) 105–109.

172. M.A. Johnson, T.N. Truong, High-level ab initio and density functional theory evaluation of combustion reaction energetics: NO2 and HONO elimination from dimethylnitramine, J. Phys. Chem. A 103 (1999) 8840–8846.

173. N.J. Harris, K. Lammertsma, Ab initio and density functional computations of conformations and bond dissociation energies for hexahydro- 1,3,5-trinitro-1,3,5-triazine, J. Am. Chem. Soc. 119 (1997) 6583–6589.

174. D. Chakraborty, R.P. Muller, S. Dasgupta, W.A. Goddard, The mechanism for unimolecular decomposition of RDX (1,3,5-trinitro-1,3,5- triazine), an ab initio study, J. Phys. Chem. A 104 (2000) 2261–2272.

175. S.W. Zhang, T.N. Truong, Thermal rate constants of the NO2 fission reaction of gas phase α-HMX: a direct *ab initio* dynamics study, J. Phys. Chem. A 104 (2000) 7304–7307.

176. Türker, L., Atalar, T., Quantum chemical treatment of cyanogen azide and its univalent and divalent ionic forms, Journal of Hazardous Materials A153 (2008) 966–974.

177. Türker, L., Atalar, T., Quantum chemical study on 5-nitro-2,4-dihydro-3H-1,2,4-triazol-3-one (NTO) and some of its constitutional isomers, Journal of Hazardous Materials A137 (2006) 1333–1344.

178. E.F. Rothgery, D.E. Audette, R.C. Wedlich, D.A. Csejka, The study of the thermal decomposition of 3-nitro-1,2,4-triazol-5-one (NTO) by DSC, TGA-MS, and accelerating rate calorimetry (ARC), Thermochim. Acta 185 (2) (1991) 235-243.

179. B.C. Beard, J. Sharma, Early decomposition chemistry of NTO (3-nitro-1,2,4-triazol-5-one), J. Energ. Mater. 11 (4–5) (1993) 325–343.

180. Y. Xie, R. Hu, X. Wang, X. Fu, C. Zhunhua, Thermal behavior of 3-nitro-1,2,4-triazol-5-one and its salts, Thermochim. Acta 189 (1991) 283–296.

181. V.W. Manchot, R. Noll, Triazole derivatives, Justus Liebigs Ann. Chem. 343 (1905) 1–27.

182. C.F. Kroger, R. Mietchen, H. Fank, M. Siemer, S. Pilz, 1,2,4-Triazoles. XVII. Nitration and bromination of 1,2,4-triazolinones, Chem. Ber. 102 (1969) 755–766.

183. Y.M.Wang, C. Chen, S.T. Lin, Theoretical studies of theNTOunimolecular decomposition, J. Mol. Struct. (THEOCHEM) 460 (1999) 79–102.

184. K.Y. Lee, M.D. Coburn, 3-Nitro-1,2,4-triazol-5-one, a less sensitive explosive, Report, 1985, 7 pp. (LA-10302-MS; Order No. DE86009787).

185. D.C. Sorescu, T.R.L. Sutton, D.L. Thompson, D. Beardallm, C.A. Wight, Theoretical and experimental studies of the structure and vibrational spectra of NTO, J. Mol. Struct. 384 (1996) 87–99.

186. R.J. Spear, C.N. Louey, M.G.Wolfson, A Preliminary Assessment of NTO as an Insensitive High Explosive,MRL-TR-89-18 Materials Research Laboratory, Vic., Australia, 1989.

187. P.B.Kulkarni,T.S. Reddy, J.K. Nair, A.N. Nazare, M.B.Talawar,T. Mukundan, S.N. Asthana, Studies on salts of 3-nitro-1,2,4-triazol-5-one (NTO) and 2,4,6-trinitroanilino benzoic acid (TABA): potential energetic ballistic modifiers, J. Hazard. Mater. 123 (1–3) (2005) 54–60.

188. K. Mitsuo,W. Jemmy, K. Yoshihito, Kayagu Gakkaishi 62 (6) (2001) 283.

189. F.J. Owens, Calculation of energy barriers for bond ruptures in some energetic molecules, J. Mol. Struct. (THEOCHEM) 370 (1) (1996) 11–16.

190. K.Y. Lee, L.B. Chapman, M.D. Coburn, 3-Nitro-1,2,4-triazol-5-one, a less sensitive explosive, J. Energ. Mater. 5 (1987) 27.

191. Y. Kohno, O. Takahashi, K. Saito, Phys. Chem. Chem. Phys. 3 (14) (2001) 2742.

192. R.I. Hiyoshi, Y. Kohno, J. Nakamura, Vibrational assignment of energetic material 5-nitro-2,4-dihydro-1,2,4-triazol-3-one (NTO) with labeled isomers, J. Phys. Chem. A 108 (27) (2004) 5915–5920.

193. H.M. Ma, J.R. Song, W. Dong, R.Z. Hu, G.H. Zhai, Z.Y. Wen, Molecular structure, the quantum chemical investigation and the thermal behavior of the dimethylamine salt of 3-nitro-1,2,4-triazol-5-one, (CH3)2NH2 +C2N4O3H−, J.Mol. Struct. (THEOCHEM) 678 (1–3) (2004) 217–222.

194. G. Singh, S.P. Felix, Studies on energetic compounds. Part 32. Crystal structure, thermolysis and applications of NTO and its salts, J. Mol. Struct. 649 (1–2) (2003) 71–83.

195. J. Vagenknecht, P. Marecek, W.A. Trzcinski, Sensitivity and performance properties of TEX explosives, J. Energ. Mater. 20 (3) (2003) 245–253.

196. V.L. Zbarskii, V.V. Kuz'min, N.V. Yudin, Synthesis and properties of 1-nitro-4,5-dihydro-1H-1,2,4-triazol-5-one, Russ. J. Org. Chem. 40 (7) (2004) 1069–1070.

197. C. Meredith, T.P. Russell, R.C. Mowrey, J.R. McDonald, Decomposition of 5-nitro-2,4-dihydro-3H-1,2,4-triazol-3-one (NTO): energetics associated with several proposed initial routes, J. Phys. Chem. A. 102 (1998) 471–477.

198. N.B. Bolotina, E.A. Zhurova, A.A. Pinkerton, Energetic materials: variable-temperature crystal structure of _-NTO, J. Appl. Crystallogr. 36 (2003) 280–285.

199. J.A. Ciezek, S.F. Trevino, Theoretical and experimental study of the inelastic neutron scattering spectra of _-5-nitro-2,4-dihydro-3H-1,2,4-triazol-3-one, J. Mol. Struct. (THEOCHEM) 732 (2005) 211–218.

200. Yi, X. et. al., Thermal behavior 3-nitro-1,2,4-triazol-5-one and its salts, Thermochimica Acta, 189(2) (1991) 283-296.

201. W. Leung, Y.Z.F. Liu, Application of *ab initio* molecular dynamics for a priori elucidation of the mechanism in unimolecular decomposition: the case of 5-nitro-2,4-dihydro-3H-1,2,4-triazol-3-one (NTO), J. Am. Chem. Soc. 123 (2001) 2243–2250.

202. T.B. Brill, K.J. James, Kinetics and mechanisms of thermal decomposition of nitroaromatic explosives, Chem. Rev. 93 (1993) 2667.

203. J. Shao, X. Cheng, X. Yang, Density functional calculations of bond dissociation energies for removal of the nitrogen dioxide moiety in some nitroaromatic molecules, J. Mol. Struct. (THEOCHEM) 755 (2005) 127–130.

204. G.S. Chung, M.W. Schimidt, M.S. Gordon, An *ab initio* study of potential energy surfaces for N8 isomers, J. Phys. Chem. A 104 (2000) 5647–5650.

205. G. Subramanian, P.V.R. Scheleyer, F. Jiao, Are the most stable fused heterobicycles the most aromatic, Angew. Chem. Int. Ed. 35 (1996) 2638–2641.

206. Meyer, R., Kohler, J., Homburg, A., Explosives, Fifth Ed.,Wiley-VCH Verlag GmnH, Weinheim, 2002.

207. K. Dudek, P. Marecek, J. Skladal, Z. Jalovy, Synthesis and some properties of Bu-NENA, New Trends in Research of Energetic Materials, Proceedings of the Seminar, 7th, Pardubice, Czech Republic, Apr. 20-22, 2004 (2004), Meeting Date 2004, 2 464-471

208. Cameron, D.R., Borajo, A. M. P., Bennett, B. M., Thatcher, G. R. J., Organic nitrates, thionitrates, peroxynitrates, and nitric oxide: a molecular orbital study of the $RXNO_2 \rightarrow RXONO$ (X=O, S) rearrangement, a reaction of potential biological significance, Can. J. Chem. 73 (1995) 1627-1638.

209. Choi, Y. J., Lee, Y. S., The rearrangement reaction of CH3NO2 to CH3ONO studied by a density functional theory method, Bulletin of the Korean Chemical Society, 25 (11) (2004) 1657-1660.

210. George, R. S., Production of organic thionitrates (as for use in improving the ignition quality of Diesel fuels), US 2307624 19430105 Patent, 1943.

211. Ozias, Y., Julg, A., Effect of the substitution of oxygen by sulfur on the structure of carbonate and nitrate ions, Journal of Molecular Structure, 57 (1) 1979 183-188.

212. M.E. Sitzmann, W.H. Gilligan, D.L. Ornellas, J.S. Thracher, Polynitroaliphatic explosives containing the pentafluorosulphenyl group (SFs). The selection and the study of the model compound, J. Energ. Matals 8 (4) (1990) 352–374.

213. J. Simons, Molecular anions, J. Phys. Chem. A. 112 (29) (2008) 6401-6511.

214. Steinhauser, G., Klapotke, T. M., “Green” pyrotechnics: a chemist’s challenge, Angew. Chem. Int. Ed. 47 (2008) 3330-3347.

215. Berger, B., Chinica, 58 (2004) 363-368.

216. Zhang, C., Computational investigation of the detonation properties of furazans and foroxans, THEOCHEM, 765 (2006) 77-83.

217. T. G. Archibald, R. Gilardi, K. Baum, C. George, Synthesis and x-ray crystal structure of 1,3,3-trinitroazetidine, J. Org. Chem. 55 (1990) 2920-2927.

218. M. Suceska, S. Zeman, Z. Jalovy, M. Rajic, 1,3,3-trinitroazetidine (TNAZ). Part 2. Study of thermal Behaviour, J. Energ. Mater. in press.

219. R. I. Simpson, R. G. Garza, M. F. Foltz, D. L. Ornellas, P. A.: Urtiew, Characterization of TNAZ, Report UCRL-ID-119672, Lawrance Livermore National Laboratory, December 1994.

220. R. L. Mc Kenney, T. G. Floyd, W. E. Stevens, T. G. Archibald, A. P: Marchand, G. V. M. Sharma, S. G. Bott, Synthesis and Termal Properties of 1,3-dinitro-3-(1'3'-dinitroazetidine-3'-yl)azetidine (TNDAZ) and its Admixtures with 1,3,3-trinitroazetidine (TNAZ), J. Energ. Mater. 16 (1998)1-22.

221. K. Anderson, J. Homsy, R. Behrens, Modeling the Thermal Decomposition of TNAZ and DNNAZ, Proc. Of 11th Symposium (International) on Detonation , Snowmass Village, Colorado, August 31- SEptember 4, 1998, pp 367-375.

222. L. G. Hill, W. L. Seitz, J. F. Kramer, D. M. Murk, R. S. Medina, Wedge Test for Three New Explosives,: LAX112, 2,4-DNI, and TNAZ, Report LA-UR-95-2762, Los Alamos National Laboratory, 1995.

223. M. Suceska, Calculation of the Detonation properties of CHNO Explosives, Propellants, Explos. Pyrotech. 16 (1991) 197–202.

224. O. Oyumi, T. B. Brill,Thermal decomposition of energetic materials 4. High-rate, in situ, thermolysis of the four, six, and eight membered, oxygen-rich, gem-dinitroalkyl cyclic nitramines, TNAZ, DNNC, and HNDZ Combust, Flame, 62 (1985) 225-231.

225. S. A. Oehrle, J. Energ. Mater. 14 (1996) 47.

226. A. T. Craig, J. K. Rice, T. P. Russelljorge, M. Seminario, P. Politzer, Vibrational Analysis of 1,3,3-trinitroazetidine Using Matrix Isolation Infrared Spectroscopic and Quantum Chemical Calculations, J. Phys. Chem. A. 101(42) (1997) 7742-7748.

227. O. Oyumi, T. B. Brill, A. L. Rheingold, T. M. Haller, J. Phys. Chem. 89 (1985)4317.

228. T. G. Archibald, L. C. Garver, A. A. Malik, O. F. Bonsu, D. D. Tzeng, S. B. Preston, K. Baum, Research in Energetic Compounds. Contact 200014–78-C-0147; Fluorochem, inc. : Azusa, CA.; ONR-2-10, Feb 1998. 78 p.

229. K. Dudek, P. Maracek, Z. Jalovy, Synthesis and Some Properties of 1,3,3-trinitroazetidine (TNAZ), New Trends in Reseach of Energetic Materials, 2001.

230. N. L. Garland, H. H. Nelson, Laser-induced Decomposition of TNAZ, J. Phys. Chem. B. 102 (15) (1998) 2663-2667.

231. J. C. Oxlel, A. B. Kooh, R. Szekeres, W. Zheng, Mechanism of Nitramine Thermolysis, J. Phys. Chem. B. 98 (28) (1994) 7004-7008.

232. S. Alavi, L. M. Reilly, D. L. Thompson, Theoretical Prediction of the decomposition mechanism of 1,3,3-trinitroazetidine (TNAZ), Journal of Chemical Physics, 119 (16) (2003) 8297–8304.

233. C. F. Wilcox, Y. X. Zhang, S. H. Bauer, The thermochemsitry of TNAZ (1,3,3-trinitroazetidine) and related species: G3 (MP2)/B3LYP heats of formation, J. Mol. Struct. (THEOCHEM). 538 (2001) 67-72.

234. M. H. Liu, C. Cheng, Y. S. Hong, Emprical methods for estimating the detonation properties of energetic TNAZ molecular derivatives, Journal of Theoretical and Computational Chemistry, 3 (3) (2004) 379-389.

235. M. Suceska, S. Zeman, M. Rajic, Z. Jalovy, Theoretical Prediction of TNAZ detonation properties, New Trends in Reseach of Energetic Materials, 2001.

236. X. W. Fan, X. H. Ju, Theoretical studies on four-membered ring compounds with NF_2, ONO_2, N_3 and NO_2 groups, J. Comput. Chem. 29 (2008) 505–513.

237. Q. Zhao, S. Zhang, Q. S. Li, The influence of ring strain and conjugation on the reaction energies of the NO_2 fission of nitramines: A DFT study, Chemical Physics Letters 407 (2005) 105-109.

238. J. P. Ritchie, J. Am. Chem. Soc. 111 (1989) 2517.

239. Y. Oyumi, T. B. Brill,Thermal decomposition of energetic materials 22. The contrasting effects of pressure on the high-rate thermolysis of 34 energetic compounds Combust. Flame, 68 (1987) 209.

240. J. Oxley, J. Smith, W. Zheng, E. Rogers, M. Coburn, J. Phys. Chem. A. 101 (1997) 4375.

241. Elderfield, R.C. Heterocyclic Compounds, John Wiley and Sons Inc: New York, 1957; Vol. 6, 234-235.

242. McKeveney, D; Quinn, R.J.; Janssen, C.O.; Healy, P.C. Acta Cryst. 2004, E60, 241-243.

243. Politzer, P; Murray, J.S.; Concha, M.C. J. Phys. Chem. A. 1998, 102, 6697 6701.

244. Türker, L. J. Mol. Struct. (Theochem), 2004, 681, 15-19.

245. Dewar, M.J.S. The molecular orbital theory of organic chemistry, McGraw-Hill: New York, 1969.

246. Dewar, M.J.S; Dougherty, R.C. PMO Theory of organic chemistry, Plenum-Rosetta: New York, 1975.

247. C.J. Brown, A.C. Farthing, Preparation and structure of di-p-Xylylene-, Nature, 164 (1949) 915-916.

248. D.J. Cram, H. Steinberg, Maxro Rings.1. Preparation and spectra of the paracyclophanes, J. Am. Chem. Soc. 73 (1951) 5691-5704.

249. G. J. Bodwell, The new inductees in the "Hall of Phane" - no phane, no gain, Angew. Chem. Int. Ed. Engl. 35 (1996) 2085-2088.

250. B.H. Smith, Bridged aromatic compounds, Academic Press, Newyork, (1964).

251. P. M. Keehn, S. M. Rosenfeld, Cyclophanes, Academic Press,1–2 (1983)

252. F. Diedrich, Cyclophane, Royal Society of Chemistry, Cambridge (1991)

253. F. Vögtle, Cyclophane Chemistry, Wiley-VCH, NewYork, 1993.

254. H. Takamura, Cyclophane chemistry for the 21st Century, Research Signpost, Trivan-drum, 2002.

255. R. Gleiter, H. Hopf, Modern cyclophane chemistry, Wiley-VCH, Weinheim, 2004.

256. H. Nandivada, H.Y. Chen, L. Bondarenko, J. Lahann, Reactive polymer coatings that "Click", Angew. Chem. Int. Ed. 45 (2006) 3360–3363.

257. H. Hopf, [2.2] Paracyclophanes in polymer chemistry and materials science, Angew. Chem. Int. Ed. 47 (2008) 2–7.

258. H. Hope, J. Bernstein, K.N. Trueblood, The crystal and molecular structure of 1,1,2,2,9,9,10,10-octafluoro-[2.21paraeyelophane and a reinvestigation of the structure of [2.2]Paracyclophane, *Acta Cryst. B28* (1972) 1733–1743.

259. W. R. Carper, L. P. Davis, M. W. Extlne, Molecular structure of 2,4,6-trinitrotoluene, *J. Phys.* Chem. 86 (1982) 459–462.

260. J. Clarksona, W. E. Smitha, D. N. Batchelderb, D. A. Smithb, A. M. Coatsc, A theoretical study of the structure and vibrations of 2,4,6-trinitrotolune, Journal of Molecular Structure, 648 (2003) 203–214.

261. F. A. Cotton, G. Wilkinson, Advanced Inorganic Chemistry, 5, Wiley, New York, 1998.

262. R.A. Falk, J.D. Readio, Perfluorooxazetidines, J. Org. Chem. 34 (1969) 4088-4090.

263. J.D. Readio, R.A. Falk, Conformational studies of perfluoro-2-halo-1,2-oxazetidines using nuclear magnetic resonance spectroscopy J. Org. Chem. 35 (1970) 927–930.

264. J.D. Readio, Nuclear magnetic resonance evidence for restricted nitrogen inversion and nonplanarity in perfluoro-4-chloro-2-halo-1,2-oxazetidines, J. Org. Chem. 35 (1970) 1607–1611.

265. D. H. Magers, S. R. Davis, Ring strain in the oxazetidines, J. Mol. Struct. (THEOCHEM) 487 (1999) 205–210.

266. C. W. Benton, D. H. Magers, Conventional strain energy in the oxadiazetidines, International Journal of Quantum Chemistry, 100 (2004) 788–800.

APPENDIX

- ZPVE (Zero point vibrartion energy) in kJ/mol.
- Coordinates in Angstroms
- The numbering is done separately for each part; see the corresponding molecules in the results and discussion (chapter 3).

Table A.1 Cartesian coordinates of the optimized geometries of cis-DINGU (1) and trans-DINGU (2) at B3LYP/6-31G (d,p).

Cis-DINGU (1) ZPE=332.6792

Center	Atomic	Coordinates (Angstroms)		
Number	Number	X	Y	Z
1	6	1.278378	-1.486830	-0.213520
2	6	0.563779	0.533359	0.925475
3	6	-0.563740	-0.533641	0.925336
4	6	-1.278390	1.486898	-0.213008
5	7	1.527272	-0.081802	0.001315
6	7	0.085002	-1.714263	0.443161
7	7	-1.527272	0.081803	0.001404
8	7	-0.084984	1.714128	0.443689
9	7	-2.790510	-0.515354	-0.104036
10	7	2.790509	0.515384	-0.103990
11	8	-2.862718	-1.627694	0.425136
12	8	3.658080	-0.071818	-0.712848
13	8	2.862736	1.627566	0.425511
14	8	1.956504	-2.272304	-0.815951
15	8	-1.956545	2.272557	-0.815164
16	8	-3.658103	0.072027	-0.712692
17	1	1.027309	0.690931	1.900786
18	1	-1.027228	-0.691511	1.900618
19	1	-0.435293	-2.561646	0.264708
20	1	0.435302	2.561567	0.265474

Table A.1 Continued

Trans-DINGU (2) ZPVE= 333.1260655

Center Number	Atomic Number	Coordinates (Angstroms) X	Y	Z
1	6	0.466171	0.566961	-0.193597
2	6	-0.466171	-0.566961	0.193599
3	7	1.696017	-0.007985	0.323467
4	6	1.621656	-1.442481	-0.048282
5	7	0.271768	-1.681464	-0.343650
6	7	-0.271768	1.681464	0.343653
7	7	-1.696017	0.007985	-0.323467
8	6	-1.621656	1.442481	0.048283
9	8	-2.533412	2.216221	0.082524
10	8	2.533412	-2.216219	-0.082524
11	7	2.884568	0.720577	0.027463
12	7	-2.884568	-0.720577	-0.027464
13	8	2.683211	1.870085	-0.360099
14	8	3.943866	0.173656	0.233365
15	8	-2.683211	-1.870086	0.360096
16	8	-3.943866	-0.173657	-0.233366
17	1	0.544167	0.639643	-1.287246
18	1	-0.544169	-0.639642	1.287247
19	1	-0.053315	-2.628850	-0.189715
20	1	0.053315	2.628850	0.189721

Table A.2 Cartesian coordinates of the optimized geometries of cis-DINGU (1) and trans-DINGU (2) at MP2/6-31 G (d,p) // RHF/6-31 G(d,p).

Cis-DINGU (1) ZPVE= 367.4098445

Center Number	Atomic Number	Coordinates (Angstroms)		
		X	Y	Z
1	6	-0.563848	0.523815	0.958517
2	6	0.563848	-0.523815	0.958517
3	7	0.000000	1.531279	0.065538
4	7	-1.684515	-0.181464	0.447240
5	1	-0.764191	0.953900	1.926193
6	6	-1.384434	-1.349640	-0.188503
7	6	1.384434	1.349640	-0.188503
8	7	1.684515	0.181464	0.447240
9	7	0.000000	-1.531279	0.065538
10	7	-0.687293	2.686933	-0.130053
11	1	0.764191	-0.953900	1.926193
12	1	-2.557559	0.264926	0.278186
13	7	0.687293	-2.686933	-0.130053
14	8	-0.189009	3.544377	-0.763080
15	8	-1.779360	2.700475	0.368862
16	8	2.110047	2.049739	-0.793725
17	8	-2.110047	-2.049739	-0.793725
18	1	2.557559	-0.264926	0.278186
19	8	0.189009	-3.544377	-0.763080
20	8	1.779360	-2.700475	0.368862

Table A.2 Continued

Trans-DINGU (2) ZPVE= 369.1269215

Center Number	Atomic Number	Coordinates (Angstroms) X	Y	Z
1	6	-0.451516	0.555074	0.224426
2	6	0.451516	-0.555074	-0.224422
3	6	-1.604491	-1.424475	0.056330
4	6	1.604491	1.424475	-0.056329
5	7	-1.687715	-0.007337	-0.260326
6	7	-0.261121	-1.672779	0.304046
7	7	0.261121	1.672779	-0.304043
8	7	1.687715	0.007337	0.260331
9	7	-2.841070	0.704859	-0.029641
10	7	2.841071	-0.704859	0.029639
11	8	2.493633	2.186934	-0.096481
12	8	-2.493632	-2.186934	0.096480
13	8	-2.660032	1.827285	0.345502
14	8	-3.869429	0.182861	-0.257040
15	8	2.660030	-1.827282	-0.345511
16	8	3.869430	-0.182863	0.257041
17	1	-0.492948	0.598804	1.308052
18	1	0.492948	-0.598803	-1.308047
19	1	0.046992	-2.606079	0.131579
20	1	-0.046993	2.606079	-0.131581

Table A.3 Cartesian coordinates of the optimized geometries of nitrotriazole (NTO), its constitutional isomers (1-6) at ROB3P86/6-311 G (d,p).

NTO (1) ZPVE=177.0138355

Center Number	Atomic Number	Coordinates (Angstroms) X	Y	Z
1	6	-1.820424	-0.230306	-0.000006
2	7	-0.558852	-0.833210	-0.000012
3	6	0.372742	0.156008	0.000005
4	7	-0.128518	1.342408	0.000016
5	7	-1.459121	1.115092	-0.000011
6	8	-2.912806	-0.728779	0.000005
7	7	1.787102	-0.132887	0.000001
8	8	2.560228	0.795706	-0.000013
9	8	2.062409	-1.324339	0.000012
10	1	-0.372927	-1.823479	-0.000020
11	1	-2.103910	1.888736	0.000031

Table A.3 Continued

1A ZPVE= 177.546812

Center Number	Atomic Number	Coordinates (Angstroms) X	Y	Z
1	6	0.000000	0.000000	0.000000
2	7	0.000000	0.000000	1.309558
3	7	1.261609	0.000000	-0.476728
4	8	-1.043540	0.000000	-0.813857
5	6	1.324007	0.000000	1.571714
6	7	2.139860	0.000000	0.547587
7	1	1.582817	0.000000	-1.432486
8	1	-1.838361	-0.000001	-0.266375
9	7	1.842772	-0.000002	2.937234
10	8	3.049454	0.000014	3.063864
11	8	1.018068	-0.000016	3.826900

1B ZPVE= 175.85599

Center Number	Atomic Number	Coordinates (Angstroms) X	Y	Z
1	6	1.700619	-0.096919	0.000003
2	7	0.544596	-0.793358	0.000001
3	6	-0.401753	0.191145	0.000002
4	7	0.127726	1.374245	0.000007
5	7	1.479999	1.196935	0.000008
6	8	2.875264	-0.702532	0.000002
7	7	-1.800679	-0.138992	-0.000001
8	8	-2.045732	-1.340701	-0.000012
9	8	-2.603083	0.763862	-0.000007
10	1	0.381659	-1.789208	-0.000002
11	1	3.552059	-0.012982	0.000005

1C ZPVE= 177.3814055

Center Number	Atomic Number	Coordinates (Angstroms) X	Y	Z
1	7	-0.595057	-0.891812	0.000007
2	7	-0.143851	1.249091	0.000005
3	7	-1.484785	1.197060	0.000010
4	6	-1.699629	-0.113159	0.000006
5	8	-2.932369	-0.602990	-0.000016
6	6	0.354933	0.010114	0.000002
7	7	1.781901	-0.216449	-0.000003
8	8	2.465791	0.798421	-0.000013
9	8	2.173842	-1.358629	0.000006
10	1	0.362324	2.122469	-0.000003
11	1	-2.859711	-1.563834	0.000007

Table A.3 Continued

2 ZPVE= 174.7401525

Center Number	Atomic Number	Coordinates (Angstroms) X	Y	Z
1	6	2.078430	0.408191	0.000000
2	6	0.416500	-1.117960	0.000000
3	7	1.019647	1.142195	0.000000
4	7	-1.341222	0.714478	0.000000
5	7	1.796999	-0.929210	0.000000
6	7	0.000000	0.238396	0.000000
7	8	-2.183238	-0.144245	0.000000
8	8	-0.202496	-2.140160	0.000000
9	8	-1.467043	1.907690	0.000000
10	1	3.079182	0.810759	0.000000
11	1	2.445483	-1.699440	0.000000

2A ZPVE= 175.8113565

Center Number	Atomic Number	Coordinates (Angstroms) X	Y	Z
1	6	0.886198	0.746858	0.000000
2	7	2.077180	0.231343	0.000001
3	7	-0.041921	-0.292210	-0.000002
4	8	0.569362	2.015314	0.000001
5	6	1.836933	-1.116428	0.000000
6	7	0.585002	-1.495728	0.000000
7	7	-1.437184	-0.191729	-0.000002
8	1	-0.406678	2.072415	0.000000
9	8	-2.071226	-1.199621	0.000002
10	8	-1.854321	0.962494	0.000000
11	1	2.635824	-1.842226	0.000001

3 ZPVE= 173.7897215

Center Number	Atomic Number	Coordinates (Angstroms) X	Y	Z
1	6	-0.217025	1.313963	0.072443
2	6	-1.801176	-0.145904	-0.066074
3	7	0.367715	0.098275	0.447837
4	7	1.715278	-0.181166	-0.034670
5	7	-1.461984	1.228836	-0.187281
6	7	-0.593311	-0.848865	0.166425
7	8	1.957143	-1.335690	-0.241735
8	8	-2.882115	-0.647155	-0.133812
9	8	2.440082	0.779249	-0.073220
10	1	0.400519	2.200312	0.035384
11	1	-0.606075	-1.659455	0.770364

Table A.3 Continued

3A ZPVE= 175.0919695

Center Number	Atomic Number	Coordinates (Angstroms) X	Y	Z
1	6	1.653434	-0.175381	0.000000
2	7	1.493836	1.184725	-0.000001
3	6	0.195785	1.327871	0.000003
4	7	0.372068	0.093165	0.000002
5	7	0.551900	-0.888506	0.000002
6	8	2.851051	-0.741463	-0.000002
7	7	-1.770202	-0.197488	0.000003
8	8	-2.472936	0.785514	-0.000003
9	8	-2.071206	-1.352836	-0.000003
10	1	-0.375584	2.241430	0.000004
11	1	3.500736	-0.029366	-0.000004

4 ZPVE= 174.863551

Center Number	Atomic Number	Coordinates (Angstroms) X	Y	Z
1	6	-0.513301	-1.440840	-0.000003
2	7	-1.790728	-1.302421	0.000001
3	7	-2.009458	0.044522	0.000000
4	6	-0.880248	0.825841	0.000000
5	8	-0.755983	2.014956	0.000004
6	7	0.115855	-0.209775	-0.000007
7	7	1.515546	-0.040780	0.000000
8	8	2.144156	-1.074727	0.000008
9	8	1.920316	1.087010	-0.000005
10	1	0.023677	-2.373834	-0.000005
11	1	-2.948800	0.405106	0.000012

Table A.3 Continued

4A ZPVE= 173.4274025

Center Number	Atomic Number	Coordinates (Angstroms) X	Y	Z
1	6	0.518851	-1.496530	0.000003
2	7	1.797750	-1.339510	0.000003
3	7	2.072130	0.022577	-0.000001
4	6	0.944201	0.652941	-0.000003
5	8	0.749608	1.957300	0.000002
6	7	-0.099197	-0.253878	-0.000007
7	7	-1.504670	-0.029074	-0.000003
8	8	-1.859070	1.116020	0.000004
9	8	-2.169700	-1.033380	0.000000
10	1	-0.035390	-2.419740	0.000007
11	1	1.628280	2.360920	0.000003

5 ZPVE= 172.910179

Center Number	Atomic Number	Coordinates (Angstroms) X	Y	Z
1	7	2.072040	0.181767	-0.235865
2	6	1.801900	-1.075670	-0.117875
3	7	0.508909	-1.372970	0.150637
4	6	0.900326	0.876962	0.036838
5	8	0.668198	2.040470	0.010554
6	7	-0.097441	-0.163329	0.421879
7	7	-1.463310	-0.080901	-0.018105
8	8	-1.938620	1.017060	-0.028166
9	8	-1.987840	-1.145110	-0.253448
10	1	2.525030	-1.873450	-0.231921
11	1	0.186279	-2.185650	0.656802

6 ZPVE= 171.0066915

Center Number	Atomic Number	Coordinates (Angstroms) X	Y	Z
1	6	0.560883	-1.447531	0.000021
2	7	1.975040	-1.070433	-0.000017
3	7	2.134244	0.157172	-0.000023
4	6	0.837977	0.863339	0.000006
5	8	0.690852	2.037938	-0.000009
6	7	0.099223	-0.177102	0.000055
7	7	1.492885	-0.062379	0.000002
8	8	-2.077636	-1.125472	-0.000037
9	8	-1.952261	1.045787	0.000005
10	1	0.349519	-2.045846	0.890275
11	1	0.349463	-2.045828	-0.890232

Table A.4 Cartesian coordinates of the optimized geometries of nitrotriazole (NTO), its constitutional isomers (1-6) at MP2/6-311 G (d, p)// RHF/6-311 G (d, p).

NTO (1) ZPVE= 192.4832815

Center Number	Atomic Number	Coordinates (Angstroms) X	Y	Z
1	6	-0.903581	-1.564343	0.193508
2	7	-0.979528	-0.186250	0.123269
3	6	0.288005	0.270531	-0.048616
4	7	1.156718	-0.632192	-0.096770
5	7	0.442945	-1.771855	0.050573
6	7	0.571329	1.684624	-0.162198
7	8	-0.383185	2.390345	-0.092867
8	8	1.689856	2.012060	-0.309575
9	8	-1.773697	-2.352596	0.338728
10	1	-1.808712	0.357286	0.187471
11	1	0.898127	-2.653178	0.048770

1A ZPVE= 193.756649

Center Number	Atomic Number	Coordinates (Angstroms) X	Y	Z
1	6	1.647217	-0.182911	-0.000004
2	7	0.552633	-0.869056	-0.000015
3	6	-0.367574	0.111357	0.000001
4	7	0.061474	1.314279	0.000021
5	7	1.391484	1.122889	0.000021
6	8	2.875726	-0.634464	-0.000015
7	7	-1.795814	-0.177104	-0.000002
8	8	-2.528158	0.750780	-0.000041
9	8	-2.101764	-1.318234	0.000036
10	1	2.025561	1.887414	0.000025
11	1	2.861710	-1.579801	-0.000028

Table A.4 Continued

1B ZPVE= 192.2154805

Center Number	Atomic Number	Coordinates (Angstroms)		
		X	Y	Z
1	6	1.689825	-0.086096	0.000010
2	7	0.548914	-0.791078	-0.000008
3	6	-0.394016	0.188220	-0.000014
4	7	0.115278	1.344336	-0.000001
5	7	1.466201	1.179581	0.000009
6	8	2.854133	-0.686603	-0.000008
7	7	-1.796743	-0.137064	-0.000001
8	8	-2.040169	-1.305057	0.000013
9	8	-2.571658	0.745027	-0.000003
10	1	0.412327	-1.775958	-0.000015
11	1	3.538815	-0.034143	0.000031

1C ZPVE= 192.2154805

Center Number	Atomic Number	Coordinates (Angstroms)		
		X	Y	Z
1	7	-0.579763	-0.869925	0.000000
2	7	-0.137007	1.245188	0.000005
3	7	-1.477422	1.176815	0.000006
4	6	-1.689123	-0.099742	0.000000
5	8	-2.902227	-0.610716	-0.000008
6	6	0.344370	0.024332	0.000003
7	7	1.774221	-0.217451	0.000000
8	8	2.450021	0.762517	-0.000012
9	8	2.139329	-1.332729	0.000007
10	1	0.353837	2.109523	0.000007
11	1	-2.842496	-1.552024	0.000002

Table A.4 Continued

2 ZPVE= 190.9394875

Center Number	Atomic Number	Coordinates (Angstroms) X	Y	Z
1	6	0.317526	-1.131591	0.000000
2	7	1.691783	-1.056501	0.000000
3	6	2.075088	0.254868	0.000000
4	7	1.101039	1.054179	0.000000
5	7	0.000000	0.235328	0.000000
6	8	-0.361795	-2.087929	0.000000
7	7	-1.253501	0.796171	0.000000
8	8	-1.297863	1.970104	0.000000
9	8	-2.152931	0.036516	0.000000
10	1	2.271975	-1.862277	0.000000
11	1	3.097808	0.568853	0.000000

2A ZPVE= 192.622433

Center Number	Atomic Number	Coordinates (Angstroms) X	Y	Z
1	6	-0.874187	0.735370	0.000001
2	7	-2.041495	0.216361	-0.000004
3	6	-1.798093	-1.127737	-0.000002
4	7	-0.570632	-1.486041	0.000004
5	7	0.059695	-0.278066	0.000004
6	8	-0.598277	2.000308	-0.000002
7	7	1.417882	-0.182035	0.000000
8	8	2.033959	-1.167897	-0.000006
9	8	1.842476	0.938586	0.000005
10	1	-2.589398	-1.847771	0.000007
11	1	0.339675	2.142469	-0.000006

3 ZPVE= 192.0369465

Center Number	Atomic Number	Coordinates (Angstroms) X	Y	Z
1	6	-0.210738	1.305410	0.113323
2	6	-1.766578	-0.151864	-0.077258
3	7	0.382749	0.076261	0.454007
4	7	1.666264	-0.175096	-0.026648
5	7	-1.429210	1.218042	-0.157750
6	7	-0.576066	-0.867930	0.125070
7	8	1.948762	-1.299667	-0.189140
8	8	-2.831580	-0.631352	-0.149891
9	8	2.357521	0.777127	-0.142117
10	1	0.383914	2.194987	0.120393
11	1	-0.623805	-1.644070	0.749642

Table A.4 Continued

3A ZPE=191.782273

Center Number	Atomic Number	Coordinates (Angstroms)		
		X	Y	Z
1	6	1.628940	-0.179378	0.000002
2	7	1.452896	1.176664	0.000004
3	6	0.177307	1.308371	0.000005
4	7	-0.388376	0.084049	0.000007
5	7	0.559281	-0.885658	0.000005
6	8	2.826810	-0.713647	-0.000011
7	7	-1.730882	-0.196868	0.000000
8	8	-2.433442	0.759399	-0.000012
9	8	-2.039944	-1.322060	0.000004
10	1	-0.387827	2.214891	0.000005
11	1	3.472521	-0.025695	-0.000002

4 ZPE=191.052384

Center Number	Atomic Number	Coordinates (Angstroms)		
		X	Y	Z
1	6	-0.867529	0.818683	0.000001
2	7	0.126198	-0.195795	0.000003
3	6	-0.508135	-1.435357	0.000002
4	7	-1.755210	-1.294019	-0.000002
5	7	-1.984075	0.050717	-0.000003
6	8	-0.750532	1.987423	0.000003
7	7	1.486006	-0.036630	0.000000
8	8	1.898109	1.057779	-0.000004
9	8	2.105846	-1.047304	0.000001
10	1	0.026214	-2.358190	0.000004
11	1	-2.910056	0.405149	-0.000002

Table A.4 Continued

4 A ZPE=190.8292165

Center Number	Atomic Number	Coordinates (Angstroms)		
		X	Y	Z
1	6	-0.937304	0.644155	0.000003
2	7	0.115273	-0.245371	0.000009
3	6	-0.498506	-1.494142	0.000003
4	7	-1.749544	-1.341224	-0.000003
5	7	-2.033474	0.010372	-0.000004
6	7	1.469539	-0.019489	0.000000
7	8	1.822953	1.097929	0.000001
8	8	2.136140	-0.993880	-0.000006
9	8	-0.763446	1.937101	-0.000001
10	1	0.053247	-2.406964	0.000007
11	1	-1.616119	2.347673	-0.000008

5 ZPE=190.92636

Center Number	Atomic Number	Coordinates (Angstroms)		
		X	Y	Z
1	6	0.871547	0.865185	0.051245
2	7	2.059967	0.181177	-0.187408
3	6	1.796565	-1.054351	-0.123765
4	7	0.489896	-1.382005	0.070911
5	7	-0.109130	-0.166896	0.364285
6	8	0.664608	2.009582	0.039779
7	7	-1.439298	-0.075772	-0.014953
8	8	-1.893072	1.000994	-0.088487
9	8	-1.995559	-1.109842	-0.157507
10	1	2.524577	-1.836405	-0.231313
11	1	0.248888	-2.130001	0.686298

6 ZPE= 0.072140

Center Number	Atomic Number	Coordinates (Angstroms)		
		X	Y	Z
1	6	-0.827901	0.852831	0.000011
2	7	0.113421	-0.171538	0.000064
3	6	-0.547305	-1.448980	0.000020
4	7	-1.945387	-1.052373	-0.000037
5	7	-2.100246	0.149747	-0.000034
6	8	-0.700886	2.006450	0.000025
7	7	1.466995	-0.054487	0.000002
8	8	1.923236	1.025198	-0.000044
9	8	2.051028	-1.088497	-0.000004
10	1	-0.339677	-2.033886	0.884869
11	1	-0.339596	-2.033867	-0.884823

Table A.5 Cartesian coordinates of the optimized geometries of nitroglycol (EDNA) 1, ethylenedinitramine (EDNA) 2 and their thionates 3-6 at UB3LYP/6-311+ G (d, p).

1 (EGDN) ZPVE=234.8956085

Center Number	Atomic Number	Coordinates (Angstroms)		
		X	Y	Z
1	6	-0.799063	1.478317	0.400886
2	6	0.660080	1.306904	0.026578
3	8	0.988035	-0.067333	0.315109
4	7	2.320976	-0.439424	-0.045311
5	8	2.552987	-1.590819	0.177679
6	8	3.023921	0.423871	-0.511152
7	8	-1.651456	0.790582	-0.530873
8	1	-1.000123	1.137694	1.415908
9	1	0.821408	1.515542	-1.032095
10	1	1.280923	1.976310	0.628085
11	7	-2.228699	-0.452599	-0.062933
12	8	-2.794583	-1.030790	-0.941626
13	8	-2.099742	-0.729867	1.099260
14	1	-1.071790	2.532293	0.312978

2 (EDNA) ZPVE=304.017147

Center Number	Atomic Number	Coordinates (Angstroms)		
		X	Y	Z
1	6	0.636936	1.306680	0.080039
2	1	0.742066	1.759276	-0.909009
3	1	1.278073	1.868556	0.768140
4	6	-0.808670	1.419844	0.562470
5	1	-0.921685	0.991834	1.561301
6	1	-1.058581	2.480842	0.622422
7	7	-1.791645	0.810662	-0.334002
8	1	-2.517545	1.372333	-0.758461
9	7	1.054721	-0.085460	0.021300
10	1	0.528144	-0.822277	0.477521
11	7	-2.275225	-0.451440	-0.061629
12	8	-1.601799	-1.160827	0.680678
13	8	-3.317737	-0.763820	-0.611929
14	7	2.386077	-0.374460	-0.108166
15	8	3.125523	0.549935	-0.430610
16	8	2.714318	-1.538390	0.081927

Table A.5 Continued

3 ZPVE=216.76128

Center Number	Atomic Number	Coordinates (Angstroms)		
		X	Y	Z
1	1	-0.705848	1.023283	2.615064
2	6	-0.133393	0.754556	1.723116
3	1	0.793839	1.330803	1.737004
4	6	0.133393	-0.754556	1.723116
5	1	0.705848	-1.023283	2.615064
6	1	-0.793839	-1.330803	1.737004
7	16	-1.080188	1.378732	0.297395
8	16	1.080188	-1.378732	0.297395
9	7	0.255531	2.248446	-0.644133
10	8	1.371537	2.307465	-0.176801
11	8	-0.133393	2.713925	-1.690717
12	7	-0.255531	-2.248446	-0.644133
13	8	0.133393	-2.713925	-1.690717
14	8	-1.371537	-2.307465	-0.176801

4 ZPVE=260.822421

Center Number	Atomic Number	Coordinates (Angstroms)		
		X	Y	Z
1	6	-0.571751	1.510390	0.706995
2	1	-0.776627	2.577032	0.829414
3	1	-0.814680	1.021738	1.652348
4	6	0.890735	1.326808	0.311836
5	1	1.519725	1.790460	1.082960
6	1	1.103351	1.831503	-0.630856
7	7	1.207693	-0.086983	0.155661
8	1	0.792653	-0.771907	0.777701
9	16	-1.804948	0.955417	-0.518768
10	7	2.509782	-0.427961	-0.151375
11	8	3.221392	0.452824	-0.615694
12	8	2.820333	-1.595553	0.035625
13	7	-2.072761	-0.777289	0.029572
14	8	-2.883691	-1.379336	-0.633201
15	8	-1.454555	-1.192067	0.993111

Table A.5 Continued

5 ZPVE=225.892769

Center	Atomic	Coordinates (Angstroms)		
Number	Number	X	Y	Z
1	1	0.673257	2.583628	0.729500
2	6	0.482588	1.513956	0.613113
3	1	0.748758	1.017190	1.548246
4	6	-0.982613	1.302029	0.265640
5	1	-1.617888	1.766259	1.024938
6	1	-1.236015	1.716847	-0.711424
7	16	1.656774	0.923169	-0.650110
8	7	2.170309	-0.695256	0.092362
9	8	1.813949	-0.967884	1.214791
10	8	2.873459	-1.348562	-0.644320
11	7	-2.513208	-0.518036	-0.116448
12	8	-2.653952	-1.705296	-0.126151
13	8	-3.299134	0.363605	-0.367707
14	8	-1.193829	-0.124047	0.261710

6 (NENA) ZPVE=271.0067355

Center	Atomic	Coordinates (Angstroms)		
Number	Number	X	Y	Z
1	6	-2.844400	-0.137282	1.506204
2	6	-2.120160	0.890747	2.353485
3	8	-2.180786	-0.106711	0.221116
4	7	-2.731898	-1.010522	-0.746893
5	8	-2.184309	-0.933052	-1.805671
6	8	-3.640888	-1.711142	-0.381075
7	1	-2.755736	-1.131014	1.948334
8	1	-3.897950	0.118146	1.383178
9	1	-2.567770	0.910922	3.346501
10	1	-1.063109	0.620630	2.460973
11	7	-2.286983	2.211551	1.756213
12	7	-1.887403	3.313693	2.508270
13	8	-1.843608	3.176130	3.720350
14	8	-1.665670	4.332403	1.875939
15	1	-1.969931	2.333402	0.801574

Table A.6 Cartesian coordinates of the optimized geometries of 1, 3, 3-trinitroazetidine (TNAZ) and its constitutional isomers 2-8 at UB3LYP/6-311+ G (d, p).

1 (TNAZ) ZPVE=275.922065

Center Number	Atomic Number	Coordinates (Angstroms) X	Y	Z
1	6	0.436000	-0.172000	1.069000
2	6	0.436000	-0.172000	-1.069000
3	7	1.336000	-0.724000	0.000000
4	6	-0.641000	-0.024000	0.000000
5	7	-1.699000	-1.141000	0.000000
6	8	-2.078000	-1.524000	1.089000
7	8	-2.078000	-1.524000	-1.089000
8	7	-1.448000	1.272000	0.000000
9	8	-1.735000	1.727000	1.090000
10	8	-1.735000	1.727000	-1.090000
11	7	2.687000	-0.092000	0.000000
12	8	2.739000	1.124000	0.000000
13	8	3.606000	-0.867000	0.000000
14	1	0.238000	-0.866000	-1.882000
15	1	0.238000	-0.866000	1.882000
16	1	0.750000	0.804000	1.443000
17	1	0.750000	0.804000	-1.443000

2 ZPVE=279.996198

Center Number	Atomic Number	Coordinates (Angstroms) X	Y	Z
1	6	-0.033000	0.484000	-0.214000
2	6	0.082000	-1.198000	1.083000
3	7	-0.955000	-0.345000	0.496000
4	6	1.101000	-0.134000	0.612000
5	7	2.218000	-0.687000	-0.184000
6	8	1.937000	-1.192000	-1.228000
7	8	3.299000	-0.620000	0.300000
8	7	-2.049000	-0.867000	-0.123000
9	8	-2.486000	-0.243000	-1.033000
10	8	-2.461000	-1.885000	0.330000
11	7	-0.205000	1.945000	-0.001000
12	8	-1.226000	2.341000	0.442000
13	8	0.745000	2.590000	-0.325000
14	1	1.523000	0.495000	1.375000
15	1	0.184000	-2.147000	0.579000
16	1	0.025000	0.329000	-1.279000
17	1	-0.016000	-1.332000	2.148000

Table A.6 Continued

3 ZPVE=279.565855

Center Number	Atomic Number	Coordinates (Angstroms) X	Y	Z
1	6	0.136000	-1.699000	0.128000
2	6	-0.908000	-0.689000	0.692000
3	7	0.036000	0.346000	0.373000
4	6	0.922000	-0.468000	-0.410000
5	7	-0.266000	1.695000	0.127000
6	8	-1.284000	2.103000	0.648000
7	8	0.542000	2.296000	-0.548000
8	7	2.382000	-0.429000	0.044000
9	8	2.644000	0.068000	1.119000
10	8	3.160000	-0.961000	-0.730000
11	7	-2.164000	-0.680000	-0.203000
12	8	-3.164000	-1.162000	0.288000
13	8	-2.037000	-0.241000	-1.333000
14	1	0.931000	-0.298000	-1.484000
15	1	0.660000	-2.242000	0.912000
16	1	-0.236000	-2.376000	-0.636000
17	1	-1.269000	-0.754000	1.714000

4 ZPVE=277.578685

Center Number	Atomic Number	Coordinates (Angstroms) X	Y	Z
1	6	-0.978000	1.342000	1.407000
2	6	0.531000	1.035000	1.638000
3	6	0.502000	0.229000	0.322000
4	7	-0.804000	0.731000	0.069000
5	7	-1.816000	0.030000	-0.618000
6	8	-2.947000	0.407000	-0.384000
7	8	-1.448000	-0.843000	-1.375000
8	7	1.568000	0.589000	-0.724000
9	8	2.700000	0.674000	-0.284000
10	8	1.198000	0.776000	-1.860000
11	7	0.579000	-1.319000	0.531000
12	8	1.406000	-1.945000	-0.085000
13	8	-0.229000	-1.740000	1.337000
14	1	-1.274000	2.388000	1.364000
15	1	-1.652000	0.766000	2.041000
16	1	1.193000	1.895000	1.576000
17	1	0.759000	0.437000	2.516000

Table A.6 Continued

5 ZPVE=280.079055

Center Number	Atomic Number	Coordinates (Angstroms)		
		X	Y	Z
1	7	-0.418000	-1.561000	0.186000
2	6	-1.004000	-0.329000	-0.314000
3	6	-0.063000	0.437000	0.614000
4	6	0.725000	-0.894000	0.759000
5	7	1.981000	-0.929000	-0.148000
6	8	1.796000	-0.764000	-1.345000
7	8	3.042000	-1.141000	0.400000
8	7	-2.496000	-0.242000	0.013000
9	8	-3.201000	-1.007000	-0.617000
10	8	-2.859000	0.553000	0.862000
11	7	0.640000	1.645000	0.060000
12	8	0.055000	2.279000	-0.796000
13	8	1.719000	1.909000	0.561000
14	1	-0.305000	-2.360000	-0.426000
15	1	-0.535000	0.756000	1.541000
16	1	-0.919000	-0.114000	-1.379000
17	1	1.077000	-1.220000	1.735000

6 ZPVE=278.383825

Center Number	Atomic Number	Coordinates (Angstroms)		
		X	Y	Z
1	7	-0.621000	0.047000	1.757000
2	6	0.794000	-0.349000	1.973000
3	6	0.827000	-0.816000	0.494000
4	6	-0.515000	-0.063000	0.363000
5	7	-0.488000	1.280000	-0.441000
6	8	-0.607000	2.296000	0.208000
7	8	-0.361000	1.169000	-1.642000
8	7	-1.698000	-0.836000	-0.287000
9	8	-2.762000	-0.251000	-0.267000
10	8	-1.478000	-1.958000	-0.693000
11	7	1.987000	-0.319000	-0.333000
12	8	2.318000	0.846000	-0.179000
13	8	2.515000	-1.127000	-1.073000
14	1	-1.006000	0.901000	2.146000
15	1	1.470000	0.488000	2.154000
16	1	0.924000	-1.134000	2.717000
17	1	0.729000	-1.881000	0.310000

Table A.6 Continued

7 ZPVE=278.526750

Center Number	Atomic Number	Coordinates (Angstroms)		
		X	Y	Z
1	7	0.671000	1.893000	0.518000
2	6	-0.173000	1.078000	1.431000
3	6	-0.486000	0.170000	0.226000
4	6	0.685000	0.881000	-0.498000
5	7	1.978000	0.014000	-0.552000
6	8	2.919000	0.383000	0.123000
7	8	1.946000	-0.930000	-1.317000
8	7	-0.391000	-1.345000	0.426000
9	8	0.394000	-1.708000	1.280000
10	8	-1.073000	-2.042000	-0.291000
11	7	-1.850000	0.441000	-0.409000
12	8	-2.794000	0.338000	0.350000
13	8	-1.881000	0.734000	-1.586000
14	1	1.578000	2.205000	0.850000
15	1	0.516000	1.169000	-1.534000
16	1	0.371000	0.529000	2.201000
17	1	-1.030000	1.602000	1.852000

8 ZPVE=277.559792

Center Number	Atomic Number	Coordinates (Angstroms)		
		X	Y	Z
1	7	0.245000	0.479000	1.067000
2	6	1.243000	1.053000	0.194000
3	6	0.270000	0.903000	-1.001000
4	6	-0.623000	0.155000	0.002000
5	7	-0.826000	-1.352000	-0.307000
6	8	-0.282000	-2.143000	0.433000
7	8	-1.500000	-1.593000	-1.289000
8	7	-2.064000	0.680000	0.229000
9	8	-2.392000	1.684000	-0.369000
10	8	-2.717000	0.061000	1.045000
11	7	2.525000	0.220000	0.046000
12	8	3.210000	0.474000	-0.928000
13	8	2.777000	-0.580000	0.928000
14	1	1.603000	2.048000	0.457000
15	1	-0.166000	1.831000	-1.361000
16	1	0.637000	0.303000	-1.831000
17	1	0.458000	-0.169000	1.818000

Table A.7 Cartesian coordinates of the optimized geometries of Nitropyrimidines at B3LYP/6-31 G (d, p).

2 ZPVE=208.112883

Center Number	Atomic Number	Coordinates (Angstroms)		
		X	Y	Z
1	6	0.180497	-0.000001	-0.000001
2	7	-0.378741	1.182648	-0.187276
3	7	-0.378741	-1.182648	0.187274
4	6	-1.718265	1.170121	-0.199896
5	6	-1.718267	-1.170121	0.199896
6	6	-2.449417	0.000000	0.000001
7	7	1.683636	0.000000	0.000000
8	8	2.231255	-0.986400	-0.474232
9	8	2.231253	0.986400	0.474234
10	1	-2.208580	2.125296	-0.371003
11	1	-2.208580	-2.125296	0.371003
12	1	-3.533271	0.000002	0.000002

4 ZPVE=208.3675565

Center Number	Atomic Number	Coordinates (Angstroms)		
		X	Y	Z
1	6	-1.726706	-1.157621	-0.000023
2	7	-2.498823	-0.065997	-0.000001
3	7	-0.388450	-1.189046	-0.000022
4	6	-1.859217	1.109478	0.000022
5	6	0.198124	-0.008419	-0.000001
6	6	-0.466996	1.209192	0.000021
7	7	1.701651	-0.015771	0.000001
8	8	2.243386	1.089257	-0.000006
9	8	2.266237	-1.096105	0.000006
10	1	-2.233556	-2.118856	-0.000042
11	1	-2.479475	2.002682	0.000040
12	1	0.064167	2.150874	0.000036

Table A.7 Continued

5 ZPVE=208.921537

Center Number	Atomic Number	Coordinates (Angstroms) X	Y	Z
1	6	2.413157	-0.000020	-0.000016
2	7	1.820636	-1.201025	0.000001
3	7	1.820646	1.201030	0.000004
4	6	0.485333	-1.198314	-0.000018
5	6	0.485367	1.198321	0.000017
6	6	-0.224385	-0.000003	0.000008
7	7	-1.690166	0.000002	0.000018
8	8	-2.252867	1.092773	-0.000027
9	8	-2.252867	-1.092766	0.000007
10	1	3.500499	-0.000008	0.000013
11	1	-0.034646	-2.151334	0.000015
12	1	-0.034627	2.151333	0.000024

24 ZPVE=213.2982455

Center Number	Atomic Number	Coordinates (Angstroms) X	Y	Z
1	6	-1.104391	0.193352	-0.025461
2	7	-1.225826	1.508275	-0.082294
3	7	-0.006688	-0.543963	0.012020
4	6	-0.070372	2.183532	-0.123069
5	6	1.110729	0.158175	-0.000649
6	7	2.387990	-0.629817	0.070499
7	8	3.422258	0.029490	-0.017156
8	6	1.170139	1.543308	-0.078023
9	8	2.300237	-1.836027	0.209534
10	8	-2.395265	-1.647136	-0.590907
11	8	-3.320498	-0.060372	0.605743
12	7	-2.392870	-0.576587	-0.000904
13	1	-0.142039	3.265597	-0.189302
14	1	2.113300	2.071203	-0.100438

Table A.7 Continued

25 ZPVE=213.8601025

Center Number	Atomic Number	Coordinates (Angstroms)		
		X	Y	Z
1	7	0.725129	1.189895	-0.154295
2	6	1.284021	0.000000	0.000000
3	6	-0.610961	1.188087	-0.170131
4	7	0.725129	-1.189895	0.154295
5	6	-1.318890	0.000000	0.000000
6	6	-0.610961	-1.188087	0.170131
7	7	2.782521	0.000000	0.000000
8	8	3.323541	0.899774	0.626635
9	8	3.323541	-0.899774	-0.626635
10	7	-2.786617	0.000000	0.000000
11	8	-3.344186	-1.082747	0.155175
12	8	-3.344186	1.082747	-0.155175
13	1	-1.126033	2.132256	-0.313552
14	1	-1.126033	-2.132255	0.313552

45 ZPVE=213.5292895

Center Number	Atomic Number	Coordinates (Angstroms)		
		X	Y	Z
1	6	-2.061091	-1.575464	0.000218
2	7	-2.674194	-0.387801	0.000005
3	7	-0.740658	-1.795600	0.000283
4	6	-1.878663	0.683531	-0.000158
5	6	0.030569	-0.724046	0.000121
6	7	0.342668	1.779327	-0.000307
7	6	-0.487870	0.570092	-0.000108
8	8	1.558796	1.619590	-0.000370
9	8	-0.245003	2.856785	-0.000401
10	7	1.486623	-1.029457	0.000222
11	8	2.000162	-1.169744	-1.097853
12	8	2.000122	-1.169181	1.098390
13	1	-2.695292	-2.457526	0.000352
14	1	-2.336072	1.667969	-0.000335

Table A.7 Continued

46 ZPVE=213.4872815

Center	Atomic	Coordinates (Angstroms)		
Number	Number	X	Y	Z
1	6	0.000000	2.091125	0.000000
2	7	-1.191684	1.483193	0.000000
3	7	1.191684	1.483193	0.000000
4	6	-1.157762	0.165477	0.000001
5	6	1.157762	0.165477	0.000000
6	6	0.000000	-0.603661	0.000000
7	7	2.488980	-0.534999	-0.000001
8	7	-2.488980	-0.534999	0.000001
9	8	3.490469	0.158154	0.000011
10	8	-3.490469	0.158154	-0.000012
11	8	2.443129	-1.763066	-0.000015
12	8	-2.443129	-1.763066	0.000015
13	1	0.000000	3.176743	0.000000
14	1	0.000000	-1.683366	0.000000

245 ZPVE=218.0293965

Center	Atomic	Coordinates (Angstroms)		
Number	Number	X	Y	Z
1	7	-1.341096	-1.542906	-0.056419
2	6	-1.654040	-0.259138	-0.020014
3	6	-0.031432	-1.803247	-0.077027
4	7	-0.857950	0.797696	0.010072
5	6	0.919162	-0.782302	-0.029896
6	6	0.435688	0.525831	0.019577
7	7	-3.119974	0.050011	-0.012049
8	8	-3.815053	-0.668998	0.689457
9	8	-3.474623	0.989149	-0.708237
10	7	1.307103	1.729494	0.066293
11	8	1.685624	2.145869	-1.015828
12	8	1.500261	2.199219	1.174278
13	7	2.348894	-1.119943	-0.021751
14	8	2.636323	-2.301895	-0.175961
15	8	3.134632	-0.194344	0.144630
16	1	0.287584	-2.839317	-0.125569

Table A.7 Continued

246 ZPVE=217.816731

Center Number	Atomic Number	Coordinates (Angstroms)		
		X	Y	Z
1	7	1.191667	0.675384	-0.002088
2	6	0.000001	1.249834	0.000000
3	6	1.161219	-0.643774	-0.016737
4	7	-1.191667	0.675384	0.002087
5	6	-0.000001	-1.409428	0.000000
6	6	-1.161219	-0.643774	0.016737
7	7	0.000000	2.750085	0.000000
8	8	0.897749	3.285984	0.631384
9	8	-0.897749	3.285984	-0.631384
10	7	-2.493305	-1.340277	0.048916
11	8	-2.446624	-2.565567	-0.019575
12	8	-3.486308	-0.643532	0.140908
13	7	2.493305	-1.340278	-0.048916
14	8	3.486308	-0.643532	-0.140908
15	8	2.446623	-2.565567	0.019575
16	1	-0.000001	-2.489388	0.000000

456 ZPVE=218.257815

Center Number	Atomic Number	Coordinates (Angstroms)		
		X	Y	Z
1	7	-1.189641	1.958901	0.009761
2	6	0.000000	2.568129	0.000001
3	6	-1.171403	0.641515	0.018443
4	7	1.189644	1.958901	-0.009762
5	6	-0.000001	-0.113848	-0.000006
6	6	1.171404	0.641515	-0.018453
7	7	2.507235	-0.019508	-0.107556
8	8	2.593383	-0.910403	-0.944880
9	8	3.376770	0.402668	0.631761
10	7	-0.000001	-1.588335	-0.000001
11	8	0.660688	-2.124163	0.877061
12	8	-0.660690	-2.124167	-0.877060
13	7	-2.507236	-0.019509	0.107556
14	8	-3.376776	0.402670	-0.631752
15	8	-2.593376	-0.910403	0.944881
16	1	0.000002	3.653384	0.000004

Table A.7 Continued

2456 ZPVE=222.301085

Center	Atomic	Coordinates (Angstroms)		
Number	Number	X	Y	Z
1	7	-1.208461	-1.189787	0.004771
2	6	-1.785300	-0.000001	0.000000
3	6	0.110231	-1.174756	-0.000095
4	7	-1.208462	1.189786	-0.004770
5	6	0.863115	0.000000	0.000000
6	6	0.110230	1.174757	0.000095
7	7	2.339336	0.000000	0.000000
8	8	2.870440	-0.607460	-0.915819
9	8	2.870440	0.607461	0.915819
10	7	0.769802	2.513051	-0.046455
11	8	1.682094	2.610876	-0.858121
12	8	0.326171	3.363957	0.700041
13	7	0.769806	-2.513050	0.046455
14	8	0.326179	-3.363954	-0.700046
15	8	1.682093	-2.610876	0.858125
16	7	-3.285163	-0.000002	0.000000
17	8	-3.817936	-0.904176	0.623500
18	8	-3.817938	0.904171	-0.623500

Table A.8 Cartesian coordinates of the optimized geometries of nitro [2,2] paracyclophanes (1-10) at UB3LYP/6-311 + G (d, p).

1 ZPVE=744.828038

Center Number	Atomic Number	Coordinates (Angstroms) X	Y	Z
1	6	0.069000	2.833000	-0.023000
2	6	0.259000	2.796000	1.571000
3	6	0.050000	1.443000	-0.631000
4	6	-0.050000	-1.443000	-0.631000
5	6	-1.148000	0.738000	-0.834000
6	6	1.197000	0.655000	-0.812000
7	6	1.148000	-0.738000	-0.834000
8	6	-1.197000	-0.655000	-0.812000
9	6	0.128000	1.406000	2.160000
10	6	-0.128000	-1.406000	2.160000
11	6	1.256000	0.586000	2.308000
12	6	-1.130000	0.804000	2.314000
13	6	-1.256000	-0.586000	2.308000
14	6	1.130000	-0.804000	2.314000
15	6	-0.069000	-2.833000	-0.023000
16	6	-0.259000	-2.796000	1.571000
17	7	-2.513000	-1.316000	-0.955000
18	8	-3.164000	-0.991000	-1.940000
19	8	-2.837000	-2.150000	-0.116000
20	7	2.416000	-1.501000	-0.893000
21	8	3.291000	-1.207000	-0.084000
22	8	2.480000	-2.384000	-1.739000
23	7	2.513000	1.316000	-0.955000
24	8	2.837000	2.150000	-0.116000
25	8	3.164000	0.991000	-1.940000
26	7	-2.416000	1.501000	-0.893000
27	8	-2.480000	2.384000	-1.739000
28	8	-3.291000	1.207000	-0.084000
29	1	0.872000	3.433000	-0.451000
30	1	-0.866000	3.336000	-0.265000
31	1	2.029000	-1.414000	2.299000
32	1	2.249000	1.025000	2.280000
33	1	-0.486000	3.476000	1.994000
34	1	1.248000	3.202000	1.792000
35	1	-2.029000	1.414000	2.299000
36	1	-2.249000	-1.025000	2.280000
37	1	-1.248000	-3.202000	1.792000
38	1	0.866000	-3.336000	-0.265000
39	1	-0.872000	-3.433000	-0.451000
40	1	0.486000	-3.476000	1.994000

Table A.8 Continued

2 ZPVE=747.458625

Center Number	Atomic Number	Coordinates (Angstroms) X	Y	Z
1	6	1.178000	-2.642000	1.393000
2	6	-0.377000	-2.912000	1.102000
3	6	1.569000	-1.182000	1.280000
4	6	1.206000	1.643000	1.145000
5	6	1.597000	-0.384000	2.433000
6	6	1.722000	-0.483000	0.071000
7	6	1.556000	0.905000	0.000000
8	6	1.417000	0.993000	2.367000
9	6	-1.206000	-1.643000	1.145000
10	6	-1.569000	1.182000	1.280000
11	6	-1.556000	-0.905000	0.000000
12	6	-1.417000	-0.993000	2.367000
13	6	-1.597000	0.384000	2.433000
14	6	-1.722000	0.483000	0.071000
15	6	0.377000	2.912000	1.102000
16	6	-1.178000	2.642000	1.393000
17	7	-2.090000	1.259000	-1.131000
18	8	-3.124000	0.931000	-1.697000
19	8	-1.375000	2.214000	-1.426000
20	7	-1.643000	-1.585000	-1.309000
21	8	-1.189000	-1.008000	-2.288000
22	8	-2.181000	-2.691000	-1.311000
23	7	2.090000	-1.259000	-1.131000
24	8	3.124000	-0.931000	-1.697000
25	8	1.375000	-2.214000	-1.426000
26	7	1.643000	1.585000	-1.309000
27	8	1.189000	1.008000	-2.288000
28	8	2.181000	2.691000	-1.311000
29	1	-0.737000	-3.617000	1.857000
30	1	-0.468000	-3.397000	0.134000
31	1	-1.278000	-1.553000	3.288000
32	1	-1.616000	0.871000	3.404000
33	1	-1.401000	2.966000	2.413000
34	1	0.468000	3.397000	0.134000
35	1	0.737000	3.617000	1.857000
36	1	-1.747000	3.280000	0.715000
37	1	1.747000	-3.280000	0.715000
38	1	1.278000	1.553000	3.288000
39	1	1.616000	-0.871000	3.404000
40	1	1.401000	-2.966000	2.413000

Table A.8 Continued

3 ZPVE=746.479856

Center	Atomic	Coordinates (Angstroms)		
Number	Number	X	Y	Z
1	6	-0.486273	0.641376	2.823050
2	6	0.486273	-0.641376	2.823050
3	6	-0.890853	1.097099	1.433050
4	6	-0.856168	1.086054	-1.423950
5	6	-1.944768	0.538241	0.698050
6	6	-0.014091	1.917303	0.707050
7	6	0.000000	1.916103	-0.680950
8	6	-1.921065	0.526570	-0.704950
9	6	0.890853	-1.097099	1.433050
10	6	0.856168	-1.086054	-1.423950
11	6	1.944768	-0.538241	0.698050
12	6	0.014091	-1.917303	0.707050
13	6	0.000000	-1.916103	-0.680950
14	6	1.921065	-0.526570	-0.704950
15	6	-0.425252	0.677907	-2.819950
16	6	0.425252	-0.677907	-2.819950
17	7	-3.015533	-0.146780	-1.424950
18	8	-4.156133	0.182869	-1.121950
19	8	-2.712619	-0.962870	-2.295950
20	7	-2.965461	-0.252102	1.413050
21	8	-3.530194	0.289649	2.357050
22	8	-3.151861	-1.410582	1.039050
23	7	3.015533	0.146780	-1.424950
24	8	4.156133	-0.182869	-1.121950
25	8	2.712619	0.962870	-2.295950
26	7	2.965461	0.252102	1.413050
27	8	3.151861	1.410582	1.039050
28	8	3.530194	-0.289649	2.357050
29	1	-0.204593	-1.472022	-3.221950
30	1	0.204593	1.472022	-3.221950
31	1	-1.272522	0.535478	-3.492950
32	1	1.272522	-0.535478	-3.492950
33	1	0.039804	1.463634	3.314050
34	1	-1.359714	0.413320	3.434050
35	1	-0.039804	-1.463634	3.314050
36	1	1.359714	-0.413320	3.434050
37	1	-0.774337	-2.442004	1.236050
38	1	0.796586	2.438263	-1.199950
39	1	0.774337	2.442004	1.236050
40	1	-0.796586	-2.438263	-1.199950

Table A.8 Continued

4 ZPVE=748.134469

Center Number	Atomic Number	Coordinates (Angstroms)		
		X	Y	Z
1	6	-0.646430	-1.964970	-2.094600
2	6	-0.115430	-3.096970	-1.081600
3	6	-0.343430	-0.549970	-1.644600
4	6	0.836570	1.576030	-0.144600
5	6	0.848570	0.067030	-2.056600
6	6	-1.069430	0.152030	-0.668600
7	6	-0.500430	1.208030	0.050400
8	6	1.430570	1.093030	-1.320600
9	6	0.681570	-2.523970	0.074400
10	6	1.843570	-0.380970	1.597400
11	6	0.141570	-2.108970	1.308400
12	6	1.991570	-2.095970	-0.148600
13	6	2.563570	-1.067970	0.602400
14	6	0.689570	-1.052970	2.030400
15	6	1.704570	2.146030	0.958400
16	6	2.068570	1.048030	2.062400
17	7	-1.068430	-2.742970	1.881400
18	8	-1.680430	-2.127970	2.747400
19	8	-1.342430	-3.877970	1.495400
20	7	-2.456430	-0.246970	-0.370600
21	8	-3.298430	0.641030	-0.379600
22	8	-2.672430	-1.441970	-0.173600
23	7	-1.232430	1.804030	1.187400
24	8	-1.738430	1.035030	2.002400
25	8	-1.248430	3.029030	1.251400
26	7	3.904570	-0.639970	0.172400
27	8	4.603560	-1.470970	-0.403600
28	8	4.254560	0.520030	0.405400
29	1	-0.968430	-3.658970	-0.715600
30	1	2.545570	-2.464970	-1.003600
31	1	3.099570	1.226030	2.368400
32	1	1.224570	2.986030	1.464400
33	1	2.633570	2.503030	0.513400
34	1	2.432570	1.425030	-1.569600
35	1	1.396570	-0.361970	-2.890600
36	1	0.127570	-0.687970	2.881400
37	1	1.426570	1.210030	2.932400
38	1	-1.715430	-2.127970	-2.231600
39	1	-0.163430	-2.118970	-3.063600
40	1	0.520570	-3.778970	-1.652600

Table A.8 Continued

5 ZPVE=748.409680

Center Number	Atomic Number	Coordinates (Angstroms)		
		X	Y	Z
1	6	1.744000	-2.221000	-0.798000
2	6	1.435000	-2.420000	0.758000
3	6	0.904000	-1.118000	-1.418000
4	6	-0.904000	1.118000	-1.418000
5	6	1.346000	0.206000	-1.595000
6	6	-0.476000	-1.293000	-1.557000
7	6	-1.346000	-0.206000	-1.595000
8	6	0.476000	1.293000	-1.557000
9	6	0.776000	-1.209000	1.389000
10	6	-0.776000	1.209000	1.389000
11	6	-0.610000	-1.229000	1.586000
12	6	1.361000	0.056000	1.593000
13	6	0.610000	1.229000	1.586000
14	6	-1.361000	-0.056000	1.593000
15	6	-1.744000	2.221000	-0.798000
16	6	-1.435000	2.420000	0.758000
17	7	-2.784000	-0.523000	-1.708000
18	8	-3.168000	-1.595000	-1.241000
19	8	-3.494000	0.287000	-2.298000
20	7	2.784000	0.523000	-1.708000
21	8	3.494000	-0.287000	-2.298000
22	8	3.168000	1.595000	-1.241000
23	7	-2.823000	-0.229000	1.699000
24	8	-3.223000	-1.209000	2.318000
25	8	-3.548000	0.621000	1.179000
26	7	2.823000	0.229000	1.699000
27	8	3.548000	-0.621000	1.179000
28	8	3.223000	1.209000	2.318000
29	1	-0.747000	3.261000	0.873000
30	1	-2.801000	2.003000	-0.918000
31	1	-1.544000	3.173000	-1.298000
32	1	-2.376000	2.682000	1.242000
33	1	1.544000	-3.173000	-1.298000
34	1	2.801000	-2.003000	-0.918000
35	1	-1.145000	-2.171000	1.603000
36	1	2.376000	-2.682000	1.242000
37	1	0.747000	-3.261000	0.873000
38	1	0.907000	2.286000	-1.515000
39	1	-0.907000	-2.286000	-1.515000
40	1	1.145000	2.171000	1.603000

Table A.8 Continued

6 ZPVE=748.292392

Center Number	Atomic Number	Coordinates (Angstroms)		
		X	Y	Z
1	6	0.000000	0.000000	0.000000
2	6	0.000000	0.000000	1.596366
3	6	1.402259	0.000000	-0.578817
4	6	4.253511	0.391468	-0.577195
5	6	2.309082	-1.076223	-0.588700
6	6	1.972792	1.227544	-0.935778
7	6	3.353885	1.416751	-0.923819
8	6	3.690614	-0.890127	-0.598515
9	6	1.347753	0.385575	2.175705
10	6	4.196852	0.792732	2.175043
11	6	1.924573	1.669465	2.185663
12	6	2.233022	-0.638110	2.532825
13	6	3.612844	-0.440275	2.521196
14	6	3.303951	1.870439	2.196007
15	6	5.631758	0.561428	0.033467
16	6	5.568621	1.008318	1.564705
17	7	3.804890	2.801198	-1.148906
18	8	4.803249	3.195087	-0.540425
19	8	3.146539	3.482502	-1.929311
20	7	1.859515	-2.470852	-0.434875
21	8	2.544355	-3.339653	-0.966677
22	8	0.835662	-2.684288	0.219562
23	1	5.791674	2.074269	1.615939
24	1	-0.498970	0.908120	-0.338871
25	1	-0.582104	-0.861792	-0.327108
26	1	-0.230925	-1.010230	1.935093
27	1	-0.796555	0.669510	1.923118
28	1	6.347834	0.461562	2.097054
29	1	6.231204	1.300466	-0.498525
30	1	6.138600	-0.402412	-0.017622
31	1	4.326579	-1.758559	-0.472603
32	1	1.337263	2.092893	-1.083267
33	7	1.108457	2.886323	2.031689
34	8	1.527840	3.909800	2.564893
35	8	0.065463	2.811106	1.376874
36	7	4.427521	-1.646951	2.746432
37	8	5.496005	-1.752159	2.138526
38	8	3.981601	-2.482593	3.527811
39	1	1.860415	-1.644856	2.680267
40	1	3.676119	2.880296	2.070339

Table A.8 Continued

7 ZPVE=750.047302

Center Number	Atomic Number	Coordinates (Angstroms) X	Y	Z
1	6	0.981000	2.431000	1.368000
2	6	0.580000	1.381000	2.518000
3	6	0.808000	1.856000	-0.026000
4	6	-0.009000	-0.086000	-1.980000
5	6	-0.438000	1.909000	-0.681000
6	6	1.712000	0.981000	-0.655000
7	6	1.335000	0.045000	-1.621000
8	6	-0.862000	0.956000	-1.602000
9	6	0.009000	0.086000	1.980000
10	6	-0.808000	-1.856000	0.026000
11	6	0.862000	-0.956000	1.602000
12	6	-1.335000	-0.045000	1.621000
13	6	-1.712000	-0.981000	0.655000
14	6	0.438000	-1.909000	0.681000
15	6	-0.580000	-1.381000	-2.518000
16	6	-0.981000	-2.431000	-1.368000
17	7	3.117000	0.883000	-0.215000
18	8	3.366000	0.990000	0.988000
19	8	3.953000	0.691000	-1.090000
20	7	-1.453000	2.899000	-0.270000
21	8	-1.086000	4.061000	-0.112000
22	8	-2.610000	2.498000	-0.135000
23	7	-3.117000	-0.883000	0.215000
24	8	-3.366000	-0.990000	-0.988000
25	8	-3.953000	-0.691000	1.090000
26	7	1.453000	-2.899000	0.270000
27	8	2.610000	-2.498000	0.135000
28	8	1.086000	-4.061000	0.112000
29	1	-2.012000	-2.735000	-1.537000
30	1	0.143000	-1.872000	-3.176000
31	1	-1.476000	-1.172000	-3.105000
32	1	-0.354000	-3.314000	-1.469000
33	1	2.012000	2.735000	1.537000
34	1	0.354000	3.314000	1.469000
35	1	1.900000	-0.962000	1.915000
36	1	-0.143000	1.872000	3.176000
37	1	1.476000	1.172000	3.105000
38	1	2.082000	-0.663000	-1.962000
39	1	-1.900000	0.962000	-1.915000
40	1	-2.082000	0.663000	1.962000

Table A.8 Continued

8 ZPVE=746.547170

Center Number	Atomic Number	Coordinates (Angstroms)		
		X	Y	Z
1	6	0.183000	0.778000	-2.153000
2	6	-0.183000	-0.778000	-2.153000
3	6	0.082000	1.413000	-0.774000
4	6	-0.050000	1.393000	2.098000
5	6	1.222000	1.569000	0.046000
6	6	-1.117000	1.623000	-0.065000
7	6	-1.194000	1.617000	1.330000
8	6	1.175000	1.520000	1.436000
9	6	-0.082000	-1.413000	-0.774000
10	6	0.050000	-1.393000	2.098000
11	6	-1.222000	-1.569000	0.046000
12	6	1.117000	-1.623000	-0.065000
13	6	1.194000	-1.617000	1.330000
14	6	-1.175000	-1.520000	1.436000
15	6	-0.138000	0.789000	3.483000
16	6	0.138000	-0.789000	3.483000
17	7	-2.415000	1.745000	-0.759000
18	8	-2.568000	1.170000	-1.836000
19	8	-3.266000	2.436000	-0.207000
20	7	2.575000	1.686000	-0.541000
21	8	2.685000	2.315000	-1.590000
22	8	3.510000	1.193000	0.090000
23	7	-2.575000	-1.686000	-0.541000
24	8	-3.510000	-1.193000	0.090000
25	8	-2.685000	-2.315000	-1.590000
26	7	2.415000	-1.745000	-0.759000
27	8	2.568000	-1.170000	-1.836000
28	8	3.266000	-2.436000	-0.207000
29	1	1.135000	-0.972000	3.891000
30	1	-1.135000	0.972000	3.891000
31	1	0.579000	1.255000	4.167000
32	1	2.115000	1.478000	1.974000
33	1	-2.177000	1.664000	1.782000
34	1	-0.579000	-1.255000	4.167000
35	1	-0.492000	1.261000	-2.858000
36	1	1.199000	0.894000	-2.517000
37	1	-2.115000	-1.478000	1.974000
38	1	0.492000	-1.261000	-2.858000
39	1	-1.199000	-0.894000	-2.517000
40	1	2.177000	-1.664000	1.782000

Table A.8 Continued

9 ZPVE=748.261346

Center Number	Atomic Number	Coordinates (Angstroms)		
		X	Y	Z
1	6	0.000000	0.000000	0.000000
2	6	0.000000	0.000000	1.597747
3	6	1.397885	0.000000	-0.586608
4	6	4.244496	-0.406551	-0.635931
5	6	1.959970	-1.238828	-0.922060
6	6	2.307096	1.073483	-0.623417
7	6	3.689097	0.875395	-0.633262
8	6	3.337340	-1.433063	-0.955347
9	6	1.320142	-0.484054	2.178336
10	6	4.119914	-1.133034	2.074010
11	6	2.333215	0.432269	2.539421
12	6	1.793329	-1.808794	2.130560
13	6	3.152251	-2.138569	2.088398
14	6	3.691550	0.143216	2.453633
15	6	5.598717	-0.620598	0.018959
16	6	5.475843	-1.349006	1.428603
17	7	1.862446	2.475025	-0.505672
18	8	0.806302	2.702089	0.087250
19	8	2.579072	3.328411	-1.018370
20	1	6.290740	-0.982345	2.061406
21	1	-0.582876	0.864359	-0.317934
22	1	-0.500313	-0.908424	-0.334039
23	1	4.392773	0.960524	2.581249
24	1	-0.830503	-0.627144	1.921955
25	1	-0.185784	1.013692	1.941937
26	1	3.416540	-3.176770	1.922535
27	1	5.636042	-2.421702	1.285520
28	1	6.046438	0.364819	0.171835
29	1	6.277441	-1.201688	-0.605912
30	1	4.322294	1.743120	-0.490292
31	7	2.001695	1.820200	2.925604
32	8	2.790195	2.705058	2.593623
33	8	0.988724	1.993152	3.598757
34	7	0.874470	-2.951230	1.964486
35	8	-0.160326	-2.790077	1.314731
36	8	1.211235	-4.005815	2.493875
37	1	1.320825	-2.109257	-1.017203
38	7	3.801620	-2.818646	-1.161421
39	8	2.989601	-3.728148	-0.999208
40	8	4.976085	-2.983652	-1.492494

Table A.8 Continued

10 ZPVE=748.140145

Center	Atomic	Coordinates (Angstroms)		
Number	Number	X	Y	Z
1	6	0.617000	-1.800000	1.855000
2	6	1.819000	-1.911000	0.804000
3	6	-0.110000	-0.469000	1.791000
4	6	-0.827000	2.047000	0.638000
5	6	-1.341000	-0.291000	1.144000
6	6	0.567000	0.712000	2.128000
7	6	0.215000	1.936000	1.571000
8	6	-1.685000	0.941000	0.570000
9	6	1.703000	-0.914000	-0.338000
10	6	0.733000	1.480000	-1.598000
11	6	2.422000	0.300000	-0.331000
12	6	0.679000	-0.925000	-1.308000
13	6	0.191000	0.231000	-1.917000
14	6	1.953000	1.473000	-0.919000
15	6	-0.794000	3.177000	-0.373000
16	6	-0.087000	2.746000	-1.743000
17	7	-2.205000	-1.460000	0.886000
18	8	-2.437000	-2.198000	1.836000
19	8	-2.614000	-1.614000	-0.263000
20	7	3.654000	0.438000	0.468000
21	8	3.835000	1.508000	1.054000
22	8	4.438000	-0.509000	0.481000
23	7	-0.013000	-2.179000	-1.678000
24	8	-0.066000	-3.091000	-0.853000
25	8	-0.475000	-2.232000	-2.812000
26	7	-2.960000	1.069000	-0.160000
27	8	-3.976000	0.787000	0.460000
28	8	-2.914000	1.490000	-1.316000
29	1	0.856000	2.794000	1.746000
30	1	0.534000	3.584000	-2.075000
31	1	1.048000	-1.943000	2.851000
32	1	-0.074000	-2.621000	1.680000
33	1	2.492000	2.393000	-0.722000
34	1	1.833000	-2.936000	0.435000
35	1	2.760000	-1.738000	1.321000
36	1	-0.693000	0.146000	-2.538000
37	1	-0.865000	2.588000	-2.490000
38	1	-0.227000	4.001000	0.068000
39	1	1.483000	0.648000	2.709000
40	1	-1.788000	3.554000	-0.618000

Table A.8 Continued

Octanitro PCP ZPVE= 768.985321

Center Number	Atomic Number	Coordinates (Angstroms)		
		X	Y	Z
1	6	0.164000	0.783000	-2.817000
2	6	-0.164000	-0.783000	-2.817000
3	6	0.082000	1.408000	-1.433000
4	6	-0.082000	1.408000	1.433000
5	6	1.218000	1.639000	-0.635000
6	6	-1.132000	1.617000	-0.758000
7	6	-1.218000	1.639000	0.635000
8	6	1.132000	1.617000	0.758000
9	6	-0.082000	-1.408000	-1.433000
10	6	0.082000	-1.408000	1.433000
11	6	-1.218000	-1.639000	-0.635000
12	6	1.132000	-1.617000	-0.758000
13	6	1.218000	-1.639000	0.635000
14	6	-1.132000	-1.617000	0.758000
15	6	-0.164000	0.783000	2.817000
16	6	0.164000	-0.783000	2.817000
17	7	2.343000	1.851000	1.582000
18	8	2.869000	2.943000	1.444000
19	8	2.671000	0.971000	2.371000
20	7	-2.542000	1.835000	1.279000
21	8	-3.510000	1.305000	0.753000
22	8	-2.550000	2.538000	2.283000
23	7	-2.343000	1.851000	-1.582000
24	8	-2.671000	0.971000	-2.371000
25	8	-2.869000	2.943000	-1.444000
26	7	2.542000	1.835000	-1.279000
27	8	2.550000	2.538000	-2.283000
28	8	3.510000	1.305000	-0.753000
29	7	-2.343000	-1.851000	1.582000
30	8	-2.869000	-2.943000	1.444000
31	8	-2.671000	-0.971000	2.371000
32	7	2.542000	-1.835000	1.279000
33	8	2.550000	-2.538000	2.283000
34	8	3.510000	-1.305000	0.753000
35	7	2.343000	-1.851000	-1.582000
36	8	2.671000	-0.971000	-2.371000
37	8	2.869000	-2.943000	-1.444000
38	7	-2.542000	-1.835000	-1.279000
39	8	-3.510000	-1.305000	-0.753000
40	8	-2.550000	-2.538000	-2.283000
41	1	-1.164000	-0.932000	-3.211000
42	1	1.164000	-0.932000	3.211000
43	1	-1.164000	0.932000	3.211000
44	1	0.541000	1.256000	3.503000
45	1	-0.541000	-1.256000	3.503000
46	1	-0.541000	1.256000	-3.503000
47	1	1.164000	0.932000	-3.211000
48	1	0.541000	-1.256000	-3.503000

Table A.9 Cartesian coordinates of the optimized geometries of mono and poly nitro-1, 3-oxazetidines (1-13) at UB3LYP/6-311 + G (d, p).

1 ZPVE=204.9241014

Center Number	Atomic Number	Coordinates (Angstroms) X	Y	Z
1	6	-1.100000	-0.036000	1.027000
2	8	-2.056000	0.280000	0.000000
3	7	-0.167000	-0.546000	0.000000
4	6	-1.100000	-0.036000	-1.027000
5	7	1.151000	-0.100000	0.000000
6	8	1.672000	0.051000	1.095000
7	8	1.672000	0.051000	-1.095000
8	1	-1.464000	-0.796000	-1.719000
9	1	-1.464000	-0.796000	1.719000
10	1	-0.714000	0.839000	1.559000
11	1	-0.714000	0.839000	-1.559000

2 ZPVE=205.1645612

Center Number	Atomic Number	Coordinates (Angstroms) X	Y	Z
1	8	-0.996000	-0.989000	0.471000
2	6	-0.269000	-0.406000	-0.573000
3	6	-1.847000	0.194000	0.488000
4	7	-1.192000	0.675000	-0.744000
5	7	1.154000	0.048000	-0.027000
6	8	2.022000	-0.801000	-0.054000
7	8	1.261000	1.186000	0.402000
8	1	-0.773000	1.598000	-0.692000
9	1	-1.685000	0.803000	1.382000
10	1	-0.019000	-1.068000	-1.403000
11	1	-2.897000	-0.076000	0.367000

Table A.9 Continued

3 ZPVE=205.378258

Center Number	Atomic Number	X	Y	Z
1	6	1.972000	-0.271000	-0.238000
2	8	1.081000	-0.563000	0.871000
3	7	1.044000	0.773000	-0.720000
4	6	0.246000	0.466000	0.440000
5	7	-1.166000	-0.068000	0.007000
6	8	-1.249000	-1.204000	-0.406000
7	8	-2.067000	0.753000	0.086000
8	1	1.403000	1.718000	-0.759000
9	1	2.075000	-1.125000	-0.909000
10	1	0.008000	1.245000	1.168000
11	1	2.946000	0.085000	0.109000

4 ZPVE=211.0446623

Center Number	Atomic Number	X	Y	Z
1	7	-0.044000	-0.493000	0.944000
2	6	0.834000	0.507000	0.394000
3	6	-0.770000	-0.416000	-0.303000
4	8	0.026000	0.661000	-0.758000
5	7	-2.238000	0.025000	-0.066000
6	8	-2.445000	1.177000	0.242000
7	8	-3.056000	-0.873000	-0.177000
8	7	2.233000	-0.039000	-0.039000
9	8	3.073000	0.806000	-0.270000
10	8	2.358000	-1.249000	-0.138000
11	1	1.042000	1.422000	0.946000
12	1	-0.831000	-1.282000	-0.961000
13	1	0.373000	-1.388000	1.178000

Table A.9 Continued

```
                         5 ZPVE=210.6708289
---------------------------------------------------------------------
 Center     Atomic              Coordinates (Angstroms)
 Number     Number             X              Y              Z
---------------------------------------------------------------------
    1          6           0.255000    0.830000   -0.986000
    2          8           1.184000    0.429000    0.000000
    3          7          -0.776000    1.056000    0.000000
    4          6           0.255000    0.830000    0.986000
    5          7          -0.124000   -0.285000   -1.984000
    6          8           0.446000   -1.349000   -1.928000
    7          8          -0.996000    0.057000   -2.767000
    8          7          -0.124000   -0.285000    1.984000
    9          8           0.446000   -1.349000    1.928000
   10          8          -0.996000    0.057000    2.767000
   11          1           0.584000    1.661000   -1.614000
   12          1          -1.283000    1.931000    0.000000
   13          1           0.584000    1.661000    1.614000
---------------------------------------------------------------------
                         6 ZPVE=210.2273504
---------------------------------------------------------------------
 Center     Atomic              Coordinates (Angstroms)
 Number     Number             X              Y              Z
---------------------------------------------------------------------
    1          6          -0.542000   -0.155000   -0.602000
    2          8          -0.580000   -1.543000   -0.768000
    3          7           0.585000   -0.242000    0.310000
    4          6           0.587000   -1.704000    0.080000
    5          7           1.745000    0.515000    0.050000
    6          8           1.566000    1.638000   -0.379000
    7          8           2.797000   -0.025000    0.333000
    8          7          -1.822000    0.356000    0.124000
    9          8          -2.342000    1.345000   -0.358000
   10          8          -2.183000   -0.271000    1.098000
   11          1          -0.441000    0.462000   -1.495000
   12          1           1.462000   -2.064000   -0.462000
   13          1           0.372000   -2.288000    0.973000
---------------------------------------------------------------------
```

Table A.9 Continued

7 ZPVE=210.6958444

Center Number	Atomic Number	Coordinates (Angstroms)		
		X	Y	Z
1	6	0.627000	-1.775000	0.290000
2	8	-0.759000	-1.861000	-0.149000
3	7	0.751000	-0.578000	-0.563000
4	6	-0.688000	-0.590000	-0.726000
5	7	-1.436000	0.451000	0.183000
6	8	-1.022000	0.570000	1.321000
7	8	-2.392000	1.004000	-0.320000
8	7	1.477000	0.560000	-0.180000
9	8	2.448000	0.350000	0.519000
10	8	1.087000	1.615000	-0.641000
11	1	0.723000	-1.573000	1.357000
12	1	1.213000	-2.630000	-0.042000
13	1	-1.121000	-0.473000	-1.717000

8 ZPVE=214.6648272

Center Number	Atomic Number	Coordinates (Angstroms)		
		X	Y	Z
1	6	0.690000	0.147000	-1.006000
2	8	1.222000	1.005000	0.000000
3	7	-0.002000	-0.624000	0.000000
4	6	0.690000	0.147000	1.006000
5	7	0.030000	-2.043000	0.000000
6	8	0.025000	-2.562000	1.095000
7	8	0.025000	-2.562000	-1.095000
8	7	-0.217000	0.927000	-1.974000
9	8	0.393000	1.719000	-2.668000
10	8	-1.403000	0.691000	-1.971000
11	7	-0.217000	0.927000	1.974000
12	8	0.393000	1.719000	2.668000
13	8	-1.403000	0.691000	1.971000
14	1	1.431000	-0.364000	-1.622000
15	1	1.431000	-0.364000	1.622000

Table A.9 Continued

9 ZPVE=215.067639

Center Number	Atomic Number	Coordinates (Angstroms) X	Y	Z
1	6	0.697000	-0.809000	-0.614000
2	8	-0.250000	-1.544000	0.132000
3	7	-0.111000	0.383000	-0.443000
4	6	-0.936000	-0.351000	0.488000
5	7	-2.416000	-0.438000	0.047000
6	8	-3.231000	-0.228000	0.925000
7	8	-2.626000	-0.716000	-1.114000
8	7	0.403000	1.679000	-0.181000
9	8	-0.296000	2.379000	0.515000
10	8	1.449000	1.937000	-0.734000
11	7	2.047000	-0.770000	0.163000
12	8	2.003000	-0.317000	1.290000
13	8	3.005000	-1.229000	-0.421000
14	1	0.918000	-1.169000	-1.616000
15	1	-0.926000	-0.074000	1.541000

10 ZPVE=213.9788184

Center Number	Atomic Number	Coordinates (Angstroms) X	Y	Z
1	8	0.322000	-0.687000	0.884000
2	6	1.222000	-0.923000	-0.208000
3	6	-0.577000	-0.162000	-0.039000
4	7	0.249000	-0.443000	-1.161000
5	7	-0.947000	1.314000	0.247000
6	8	-1.452000	1.517000	1.329000
7	8	-0.674000	2.115000	-0.623000
8	7	2.491000	-0.058000	-0.051000
9	8	3.271000	-0.452000	0.790000
10	8	2.597000	0.919000	-0.769000
11	7	-1.938000	-0.928000	-0.073000
12	8	-1.939000	-2.041000	0.396000
13	8	-2.839000	-0.342000	-0.636000
14	1	1.561000	-1.955000	-0.279000
15	1	0.499000	0.341000	-1.762000

Table A.9 Continued

11 ZPVE=216.5251223

Center Number	Atomic Number	Coordinates (Angstroms)		
		X	Y	Z
1	6	0.044000	0.053000	-0.972000
2	7	1.087000	0.056000	0.000000
3	8	-0.963000	0.177000	0.000000
4	6	0.044000	0.053000	0.972000
5	7	-0.133000	-1.228000	1.831000
6	8	0.698000	-2.097000	1.671000
7	8	-1.103000	-1.227000	2.553000
8	7	0.106000	1.219000	1.985000
9	8	0.969000	1.073000	2.828000
10	8	-0.652000	2.141000	1.823000
11	7	-0.133000	-1.228000	-1.831000
12	8	0.698000	-2.097000	-1.671000
13	8	-1.103000	-1.227000	-2.553000
14	7	0.106000	1.219000	-1.985000
15	8	0.969000	1.073000	-2.828000
16	8	-0.652000	2.141000	-1.823000
17	1	1.768000	-0.702000	0.000000

12 ZPVE=216.9017337

Center Number	Atomic Number	Coordinates (Angstroms)		
		X	Y	Z
1	8	0.061000	1.128000	1.079000
2	6	1.079000	0.117000	1.133000
3	6	-0.720000	0.330000	0.240000
4	7	0.205000	-0.746000	0.390000
5	7	-0.964000	0.947000	-1.179000
6	8	-0.271000	1.888000	-1.474000
7	8	-1.820000	0.391000	-1.831000
8	7	2.335000	0.611000	0.375000
9	8	3.190000	1.090000	1.090000
10	8	2.335000	0.501000	-0.832000
11	7	-2.132000	0.093000	0.839000
12	8	-2.812000	1.094000	0.902000
13	8	-2.389000	-1.027000	1.212000
14	7	0.556000	-1.853000	-0.434000
15	8	1.598000	-2.377000	-0.115000
16	8	-0.233000	-2.142000	-1.294000
17	1	1.397000	-0.170000	2.132000

Table A.9 Continued

13 ZPVE=217.241663

Center Number	Atomic Number	Coordinates (Angstroms)		
		X	Y	Z
1	6	-0.368000	0.153000	-0.983000
2	7	0.214000	-0.724000	0.000000
3	8	-1.067000	0.869000	0.000000
4	6	-0.368000	0.153000	0.983000
5	7	-1.328000	-0.536000	1.994000
6	8	-1.349000	-1.740000	2.006000
7	8	-1.971000	0.253000	2.655000
8	7	0.577000	1.022000	1.860000
9	8	1.177000	0.367000	2.691000
10	8	0.626000	2.200000	1.633000
11	7	-1.328000	-0.536000	-1.994000
12	8	-1.349000	-1.740000	-2.006000
13	8	-1.971000	0.253000	-2.655000
14	7	0.577000	1.022000	-1.860000
15	8	1.177000	0.367000	-2.691000
16	8	0.626000	2.200000	-1.633000
17	7	1.734000	-1.064000	0.000000
18	8	2.467000	-0.112000	0.000000
19	8	1.950000	-2.230000	0.000000

CURRICULUM VITAE

Surname: Atalar
Name: Taner
Date and place of birth: April 11th 1979, Göksun/Kahramanmaraş.
Email address: taneratalar@gmail.com

Education:

Ph.D.: Middle East Technical University Faculty of Arts and Sciences Department of Chemistry 2004 – 2009.
Thesis: Molecular Design of Some Potential Explosives.
Supervisor: Prof. Dr. Lemi Türker

M.S.: Middle East Technical University Faculty of Arts and Sciences Department of Chemistry 2002 – 2004.
Thesis: Synthetic Strategy Directed Towards the Synthesis of Bicyclo[3.3.0]octa-3,5,8-triene-2,7-dione.
Supervisor: Prof. Dr. Metin Balcı

B.S.: Middle East Technical University Faculty of Arts and Sciences Department of Chemistry 1998 – 2002. *In 7 semesters, the BS was completed as an honor student. Normal period of BS is 8 semesters.*

Awards and Degrees:

2004-2005 METU Graduate Courses Performance Award,
Graduate School of Natural and Applied Sciences, METU
11th NTREM (New Trends in Research of Energetic Materials) 2008 Poster
Presentation Award (Czech Republic).

Publications:

1. Türker, L., Atalar, T., *Ab initio* and DFT study on 1,4-dinitroglycoluril configurational isomers: *cis*-DINGU and *trans*-DINGU, Journal of Hazardous Materials A137 (2006) 47–56.
2. Türker, L., Atalar, T., Quantum chemical study on 5-nitro-2,4-dihydro-3H-1,2,4-triazol-3-one (NTO) and some of its constitutional isomers, Journal of Hazardous Materials A137 (2006) 1333–1344.
3. Türker, L., Atalar, T., Positional effect of phenylene moiety on a certain perylenechromophore: a semiemprical treatment, Polycyclic Aromatic Compounds 27 (2007) 1-14.
4. Türker, L., Gümüş, S., Atalar, T., Çamur Y., "Theoretical Treatment of some Novel Nitropyrimidines", in New Research on Hazardous Materials, Nova Publishers, 2007.
5. Türker, L., Atalar, T., Quantum chemical treatment of cyanogen azide and its univalent and divalent ionic forms, Journal of Hazardous Materials A153 (2008) 966–974.
6. Türker, L., Atalar, T., Ab initio and Density Functional Theory Studies on nitrosoketene tautomers, Acta Chim. Slov. 55 (2008) 146-153.
7. Türker, L., Gümüş, S., Atalar, T., Atlanel, S., A theoretical study on nitrourea and its tautomers, Journal of Energetic Materials 26 (2008) 1-16.

8. Türker, L., Atalar, T., Computational studies on nitratoethylnitramine (NENA), its tautomers and charged forms}, Journal of Hazardous Materials, 162 (1) (2009) 193-2003
9. Turker, L., Atalar, T., Gumus, S., Camur, Y., A DFT Study on nitrotriazine, Journal of Hazardous Materials, accepted for pubilaction.